

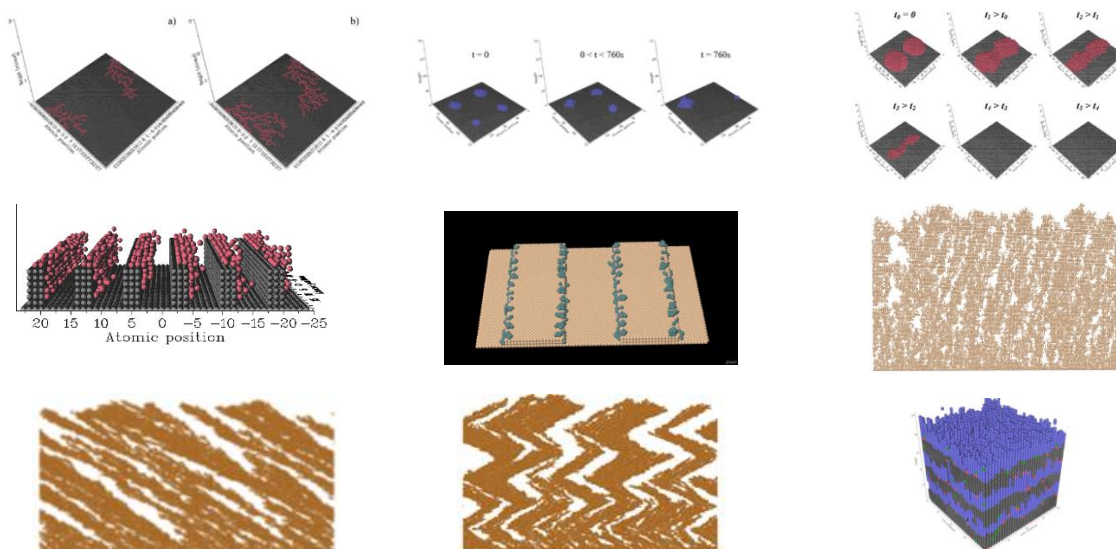
# VIRTUAL COATER™

## NASCAM™ (NanoSCALE Modeling)

**Kinetic Monte Carlo code for the simulation of deposition, diffusion, nucleation and growth of a film on a substrate.**

### Description of examples for version 4.8

S. Lucas, P. Moskovkin, J. Müller



University of Namur (UNamur)

Namur Institute for Structured Materials (NISM)

Laboratoire d'Analyses par Réactions Nucléaires (LARN)

Innovative Coating Solutions (ICS)

<https://www.incosol4u.com/nascam-general>

## Table of contents

<b>Introduction.....</b>	<b>4</b>
<b>1 NASCAM input file description .....</b>	<b>5</b>
<b>2 Basic of JMOL.....</b>	<b>7</b>
<b>3 Example 1: Aggregation Limited by Diffusion (DLA) - fractal growth during deposition. ....</b>	<b>8</b>
<b>4 Example 2: Ostwald ripening. ....</b>	<b>9</b>
<b>5 Example 3: Incident particle energy effect on nucleation. ....</b>	<b>11</b>
<b>6 Example 4: Successive deposition at two different angles .....</b>	<b>15</b>
<b>7 Example 5: Deposition with experimental energy and angular data. ....</b>	<b>17</b>
<b>8 Example 6: Dissolution and dissolution with evaporation .....</b>	<b>18</b>
<b>9 Example 7: Multilayer deposition.....</b>	<b>24</b>
<b>10 Example 8: Ge cluster formation .....</b>	<b>26</b>
<b>11 Example 9: Deposition with a tilted magnetron source. ....</b>	<b>29</b>
<b>12 Example 10: Sample movement .....</b>	<b>31</b>
<b>12.1 Deposition on a rotating substrate through a mask .....</b>	<b>31</b>
<b>12.2 Deposition on a rotating substrate with an initial tilt through a mask .....</b>	<b>33</b>
<b>13 Example 11: Glancing Angle Deposition (GLAD). ....</b>	<b>34</b>
<b>13.1 Simulation parameters.....</b>	<b>34</b>
<b>13.2 Analysis with Porosity plugin.....</b>	<b>36</b>
<b>14 Example 12: Bragg mirrors .....</b>	<b>43</b>
<b>14.1 EUV filters .....</b>	<b>43</b>
<b>14.2 Visible filters .....</b>	<b>45</b>
<b>15 Example 13: Optical incoherent layer .....</b>	<b>49</b>
<b>16 Example 14: SEM cross-section substrate .....</b>	<b>53</b>
<b>17 Example 15: Thermal conductivity.....</b>	<b>56</b>

<b>18</b>	<b><i>Example 16: Mesh substrate from step file.....</i></b>	<b><i>60</i></b>
<b>19</b>	<b><i>Example 17: Dual Magnetron.....</i></b>	<b><i>64</i></b>
<b>20</b>	<b><i>Example 18 Make Process .....</i></b>	<b><i>70</i></b>
20.1	Batchcoater.....	70
20.2	Cluster .....	73
20.3	Linear coater .....	75
<b>21</b>	<b><i>Example 19. Columns .....</i></b>	<b><i>78</i></b>
<b>22</b>	<b><i>Bibliography.....</i></b>	<b><i>80</i></b>

## Introduction

Virtual-Coater is developed by the University of Namur, LARN laboratory under the supervision of Prof. S. Lucas.

Several researchers have participated to this development. Among them, one can cite three major contributors: Dr. P. Moskovkin, Dr. A. Fauroux and Dr. J. Müller.

One can find the original version at:

<https://www.unamur.be/sciences/physique/larn/logiciels/nascam>

Since version 4.7.X, Virtual-Coater is distributed by the company ICS.

The package NASCAM of Virtual-Coater is used to simulate the time evolution of atoms deposited on a substrate (so called adatoms). It is based on the kinetic Monte Carlo (kMC) method.

It is provided with several plugins that allow the user to evaluate the morphology, compute the optical, electrical or thermal properties of the deposited coatings.

Deposition processes demonstrations have been made for magnetron sputtering (metal or reactive) and evaporation (thermal or e-beam).

Product development demonstration have been made for optical EUV reflectors, Porous TiO<sub>2</sub>, Heat Reflectors, ...

The input conditions of the species condensing on the substrates (e.g. energy and angular distribution) can be either measured (mass-spec, RFA, ...) or estimated by the use of software like SIMTRA or DSCM or PIC-MC. Contact ICS for more informations, and possible computation of these for your coater geometry and your process.

This manual describes some examples developed for NASCAM. Here, we give a flavor of the final results. Nevertheless, more detailed analysis can be done by digging into the results of all the examples, to better understand film nucleation and growth within your coater. All of that with a nice GUI.

# 1 NASCAM input file description

Within this manual, we refer to some important parameters of the input file. That file is managed by the GUI, but here is a short description.

*input.txt*: contains the current simulation parameters. The total number of lines is fixed. It must match the number mentioned in the manual. According to some command line switches, some lines are not read BUT have to be present. Table 1 contains a short description.

**Table 1. Short description of input.txt file content.**

<b>Names of fields in input.txt file</b>	<b>Typical values for corresponding variables</b>	<b>Short description</b>
Simulation_options	12 1 0	output a line in csv file every 12 deposited atoms, diffusion & island density computation switches (0-Not/1-Yes)
Substrate_type	0	0 = cubic; 1 = hexagonal
Dimensions	3 3 10 2000 0	$NX_{max}$ , $NY_{max}$ , $NZ_{max}$ - system dimensions in lattice parameter units, $NDep$ - no. of atoms to deposit, $Tmax$ - annealing time(s)
Deposition_rate,(ML/s)	0.05	in Mono-Layer/Seconds (ML/s)
Prefactor_correction	1.0	1 for atoms, lower values for nanoparticles
Masked_deposition	0	0 = no mask, 1 = there is a mask; leave it at 0 to start with
Pattern_name	LARN.txt	the name of the file containing the mask definition
Source_linear_movement	0 0.0	1 <sup>st</sup> no. is a switch: 0 = not move, 1 = move; 2 <sup>nd</sup> no. is a speed in lattice parameters/sec
Ea_diff, ...(eV)		Activation energies. If you have no clue, leave them to default values and go for RT deposition without diffusion (see Run NASCAM below)
Specie: Metal_X	1.0 Co 63.546  1 0.029 E_Metal_1.txt	Fraction of mobile particles in the total flow: 1.0 nature and atomic mass of the depositing particle: (Co 63.546) Energy switch (metal & gas): 0 $\Rightarrow$ read energy distribution from a data file (e.g. E_Metal_1.txt) 1 $\Rightarrow$ use the given energy mean value $E_0$ (e.g. $E_0 = 0.029\text{eV}$ ). 2 $\Rightarrow$ compute energy using the analytical function $f = \exp(-E/E_0) / E_0$ .  angle switch: 0 $\Rightarrow$ read angular distribution from a data file (e.g. A_Metal_1.txt) 1 $\Rightarrow$ use the given values for $\theta_0$ , $\varphi_0$ and $\Delta\theta$

	1 80.0 0.0 1.0 A_Metal_1.txt	<i>theta angle <math>\theta_0</math>: 80.0° phi angle <math>\varphi_0</math>: 0.0° delta theta <math>\Delta\theta</math>: 1.0°</i>
Specie:Reactive_X	0.0 O 15.99 1 0.5 E_Reactive_1.txt 1 0.0 0.0 0.0 A_Reactive_1.txt	<i>Idem as above</i>
Specie:Neutral	0.0 Ar 39.948 1 0.029 E_Neutral.txt 1 0.0 0.0 0.0 A_Neutral.txt	<i>Idem as above</i>

Names of fields in input.txt file	Typical values for corresponding variables	Short description
Specie:Substrate	Fe 28.085	<i>substrate nature &amp; atomic mass</i>
Temp,(eV)	0.035	<i>deposition temperature: 75 °C = 0.03 eV</i>
Save_data	1 10000	<i>1<sup>st</sup> no. is a switch: 0 = do not save, 1 = save intermediate results every 10000 deposited atoms</i>
Surface_binding_energy_of_the_substrate,(eV)	4.34	<i>e.g. TRIM values (heat of sublimation): Fe = 4.34; Al = 3.36; Si = 4.7; Ti = 4.89; Cr = 4.12; Cu = 3.52 ...</i>
Surface_binding_energy_of_the_film,(eV)	3.0	
Sputtering_Thresh/Yield	0.0 0.0	
w_rot(1/s);init_tilt(deg); A_osc(deg);w_osc(1/s)	0.0 0.0 0.0 0.0	<i>substrate rotation speed, initial tilt angle, oscillation amplitude and oscillation frequency</i>
Forced_deposition	1.0E15	<i>a limit for the number of diffusion events that can happen between two successive deposition events</i>

substrate.xyz: contains a geometrical and chemical description of the substrate. If the *substrate.xyz* file is not present in the current folder or if it is empty, the substrate is considered flat, with the physical size and chemical composition as defined in the *input.txt* file.

## 2 Basic of JMOL

The GUI includes structure display through the interface JMOL (<http://jmol.sourceforge.net/>). It needs JAVA and therefore the more powerful computer the better (RAM and CPU).

You can use the mouse to zoom in, zoom out, select data set to plot, select the radius of the atoms, do some measurements, ...

For mouse manipulation, look at: [http://wiki.jmol.org/index.php/Mouse\\_Manual](http://wiki.jmol.org/index.php/Mouse_Manual)

Everytime you have a structure display in the 3D window, this one may contain several datasets.

It is therefore a good idea to right click on the drawing to display the menu and look at the “model” menu (third from the top). There may be several datasets to display. To display them in sequence, like a movie, select either “Tools Animate Once” or “Tools Animate Loop” in the menu.

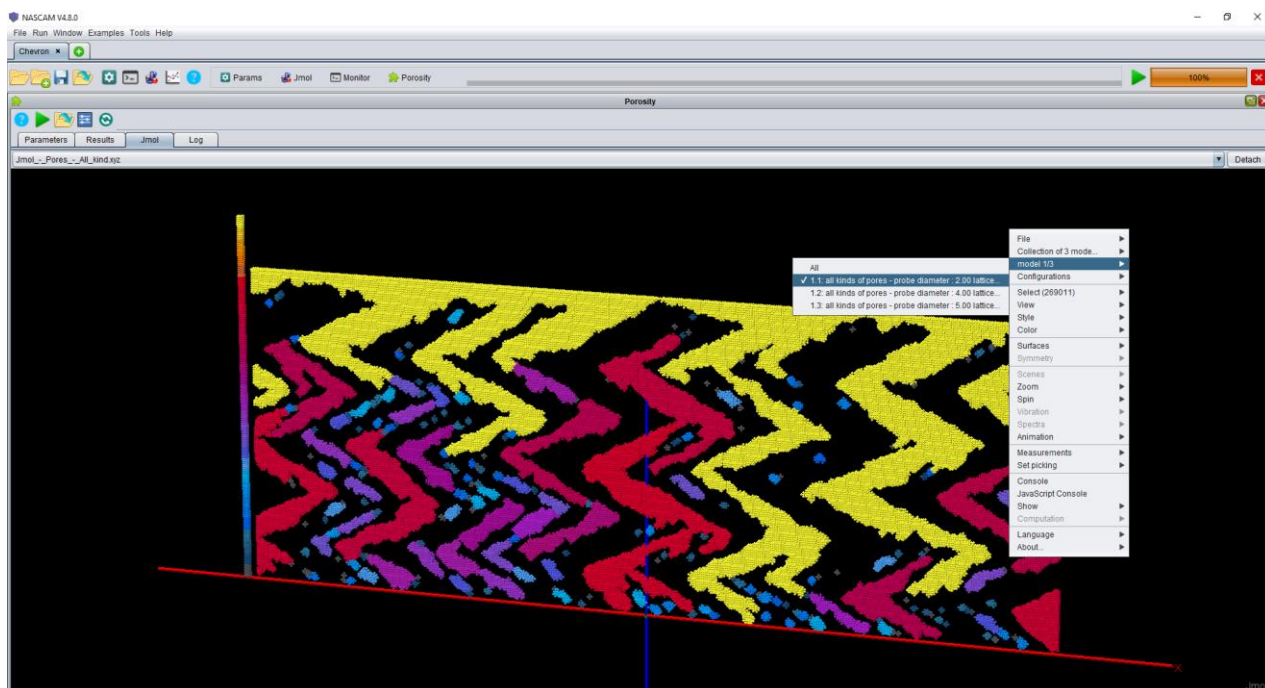


Figure 1: JMOL GUI.

### 3 Example 1: Aggregation Limited by Diffusion (DLA) - fractal growth during deposition.

During a deposition at a low deposition rate, and only taking into account free particle diffusion (see the [NASCAM manual](#) for definition), a growth of fractal structures on the surface appears. Only taking into account free particle diffusion is equivalent to setting the activation barriers for all the other processes at large enough values such as, at the simulation temperature, the occurrence probabilities for these processes are close to zero. Under such simulation conditions, once attached, the atoms cannot move anymore. As a result, the growth of a fractal cluster can be observed.

The values of the relevant parameters leading to the structures shown in Figure 2 are given below:

Simulation_options	1 1 1
Dimensions	108 108 5 1000 0.0
Deposition_rate(ML/s)	0.003
Ea_diff(eV)	0.5
Ea_nn_inc(eV), Ea_nn_dec(eV), Ea_detach(eV), Ea_up(eV), Ea_down(eV), Ea_detrap(eV), Ea_sub_evap(eV), Ea_lay_evap(eV)	> 1.9
Specie:Metal_1	1.0 Al 26.982 ...
Specie:Reactive_X	0.0 O 15.999 ...
Specie:Neutral	0.0 Ar 39.948 ...
Specie:Substrate	Cu 63.54
Temp(eV)	0.03
Save_data	1 500

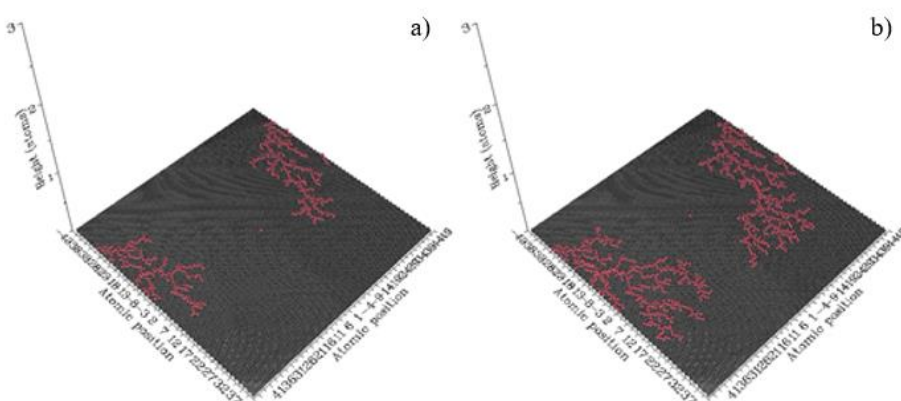
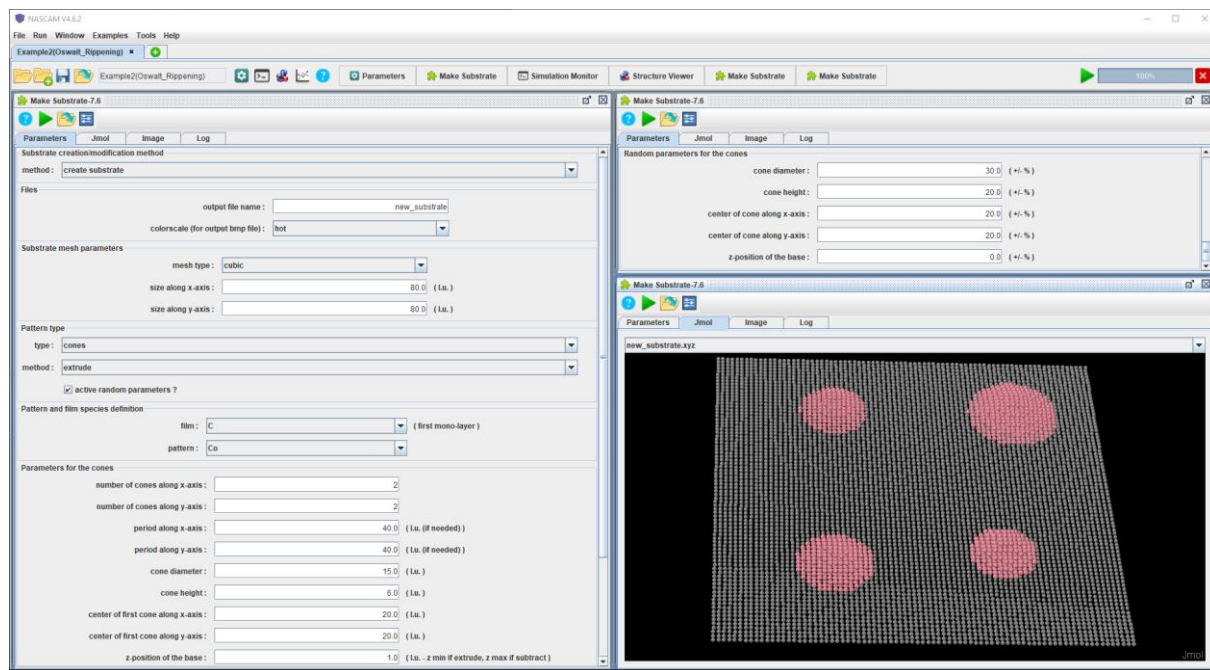


Figure 2: Snapshots of the surface structures (in red) taken after deposition of 500 (a) and 1000 (b) atoms.

## 4 Example 2: Ostwald ripening.

Ostwald ripening describes the continuous growth of a large island incorporating particles detached from smaller islands, in such a way that the smaller islands disappear and the larger survive.

To illustrate such an effect, the first thing to do is to create a substrate containing several islands of different sizes, as shown in Figure 3. This is done with the *Make\_Substrate* plugin (do not forget to activate the random option).



**Figure 3: Creation of the substrate (xyz file) containing four conical islands (in red) by using the *Make\_Substrate* plugin.**

Figure 4 shows the effect on such an initial structure consisting of four islands, with different dimensions. Before launching the NASCAM simulation, you have to load the created substrate in the *Parameters* window (Substrate Definition tab).

This file is usually stored in the “Example2 (Oswalt\_Ripening) \plugins\Make Substrate\save\substrate\_name.xyz” folder. In this example, there is no deposition but only annealing and the values of all the other relevant parameters leading to the (successive) structures shown in Figure 4 are given in the table below:

Simulation_options	1 1 0
Dimensions	80 80 10 0 500.0
Deposition_rate(ML/s)	0.002
Ea_diff(eV)	1.2
Ea_nn_inc(eV)	1.45
Ea_nn_dec(eV)	1.7
Ea_detach(eV)	1.7
Ea_up(eV)	2.0
Ea_down(eV)	1.9
Ea_detrap(eV), Ea_sub_evap(eV), Ea_lay_evap(eV)	4.5
Specie:Metal_1	1.0 Co 58.933 ...
Specie:Reactive_X	0.0 O 15.999 ...
Specie:Neutral	0.0 Ar 39.948 ...
Specie:Substrate	C 12.0
Save_data	1 50
Temp(eV)	0.0646

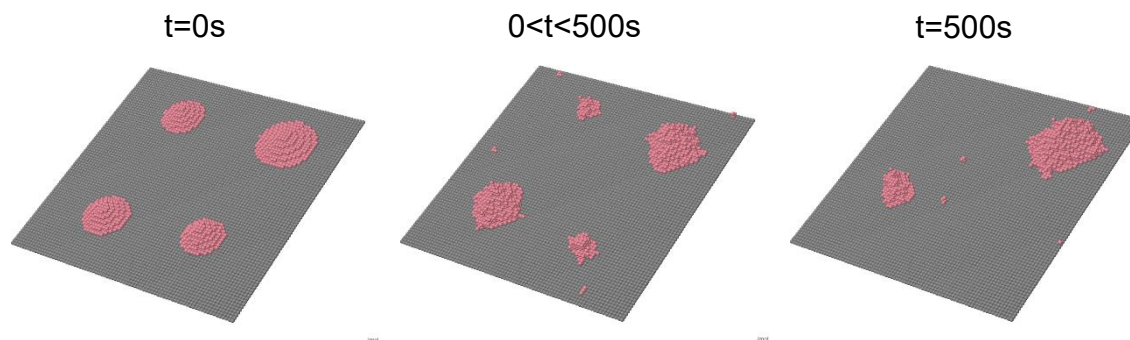


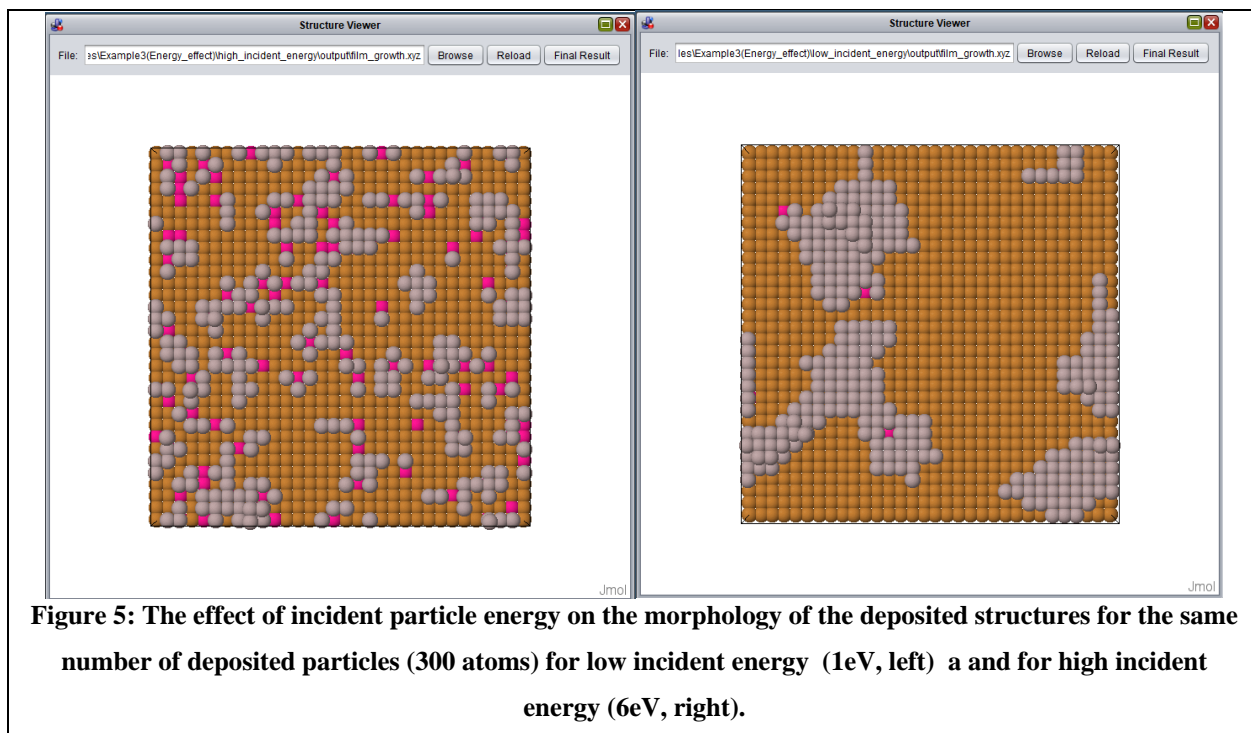
Figure 4: Ostwald ripening illustration. In all snapshots, t stands for time.

## 5 Example 3: Incident particle energy effect on nucleation.

These examples show the effects of incident particles energy on the growing film morphology. When colliding with a substrate, an atom can produce a surface defect if its energy is higher than the surface binding energy. The higher the average energy of incident atoms in the depositing flux, the higher the probability to create a surface defect. Consequently, the density of surface defects is higher in the case of higher energy flux. A defect acts as a nucleation center for the incoming particles, meaning a higher value of the mean incident particle energy leads to a higher number of islands. Supposing the same number of particles is deposited, the average island size is smaller for high incident energy than for low incident energy. Figure 5 shows these effects, comparing the deposited structures obtained after the deposition of the same number of particles (~0.25 ML) using two different values for average incident particle energy.

All the relevant parameters for both deposition conditions are given below:

	<u>Low incident energy</u> (1 eV)	<u>High incident energy</u> (6 eV)
Dimensions	32 32 10 250 0.0	32 32 10 250 0.0
Deposition_rate(ML/s)	0.002	0.002
Ea_diff(eV)	0.6	0.6
Ea_nn_inc(eV)	0.8	0.8
Ea_nn_dec(eV)	1.0	1.0
Ea_detach(eV)	1.4	1.4
Ea_up(eV)	2.3	2.3
Ea_down(eV)	1.7	1.7
Ea_detrap(eV), Ea_sub_evap(eV), Ea_lay_evap(eV)	4.5	4.5
Specie:Metal_1	1.0 Al 26.982 2 <b>1.0</b> ...	1.0 Al 26.982 2 <b>6.0</b> ...
Specie:Reactive_X	0.0 O 15.999 ...	0.0 O 15.999 ...
Specie:Neutral	0.0 Ar 39.948 ...	0.0 Ar 39.948 ...
Specie:Substrate	Cu 63.546	Cu 63.546
Temp(eV)	0.03	0.03
Surface_binding_energy_of_substrate(eV)	3.52	3.52



One can clearly see the influence of the defect creation on the substrate that impedes the diffusion: larger islands are observed when atoms may diffuse.

Then it could be interesting to study the influence of the energy of deposited atoms and the coating thickness on the electrical conductivity of this coating. However, there is not enough matter to observe conductivity. To solve that, go to “Simulation setup” panel, increase the total number of deposited atoms to 3000 and check the box “Save intermediate 3D structures”. Put a reasonable number into the field “Save intermediate 3D structure every”, like 100.

Relaunch the NASCAM computation (it has to be done for the two examples: low and high incident energy if you want to compare). That may take a little bit of time because simulations involve diffusion.

Then, launch the *Electrical* plugin. Do not forget to tick the boxes “Loop on the intermediate 3D structures” in the section *Coating to Study*. That will allow you to check the electrical properties versus number of deposited atoms. Also, tick “save structure (JMOL Display)” in the section *output files* to observe the evolution of 3D electrical parameters as atoms are deposited.

First, it is possible to observe the evolution of the electrical resistivity of the two cases.

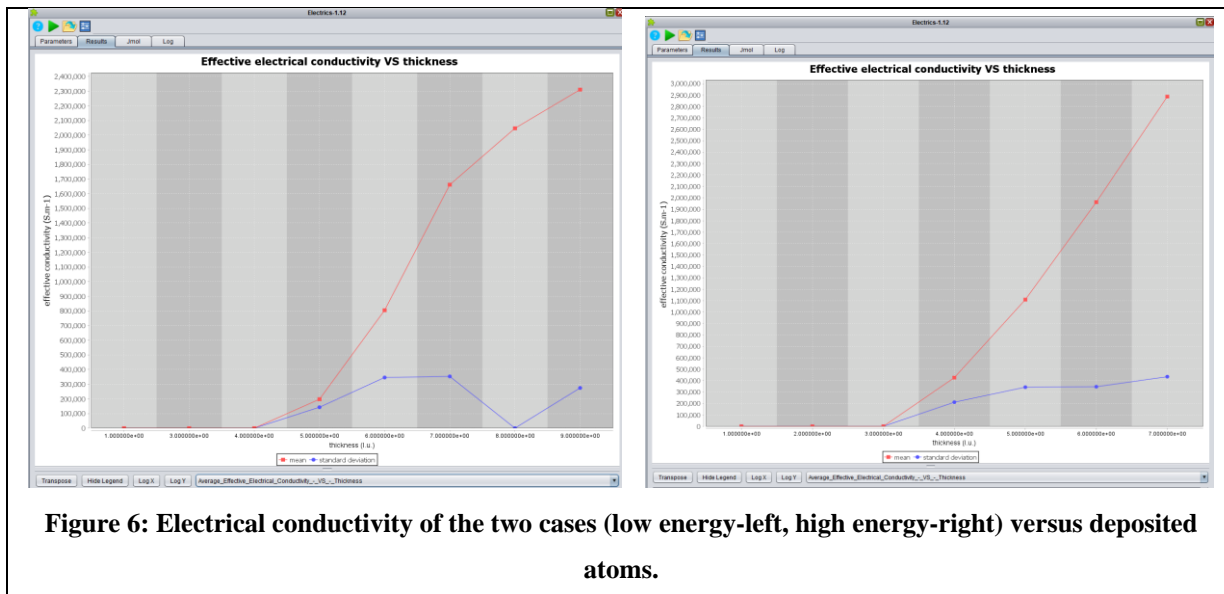


**Figure 6: Electrical conductivity of the two cases (low energy-left, high energy-right) versus deposited atoms.**

The higher the energy of the deposited atoms, the lower the diffusion, the higher the number of islands, the sooner the layer becomes conductive by connection between islands, and the higher is the electrical conductivity for a large number of deposited atoms.

The figure below shows the current flow for a not yet conductive layer (low energy, 400 deposited atoms) and a conductive layer (low energy, 1000 deposited atoms).

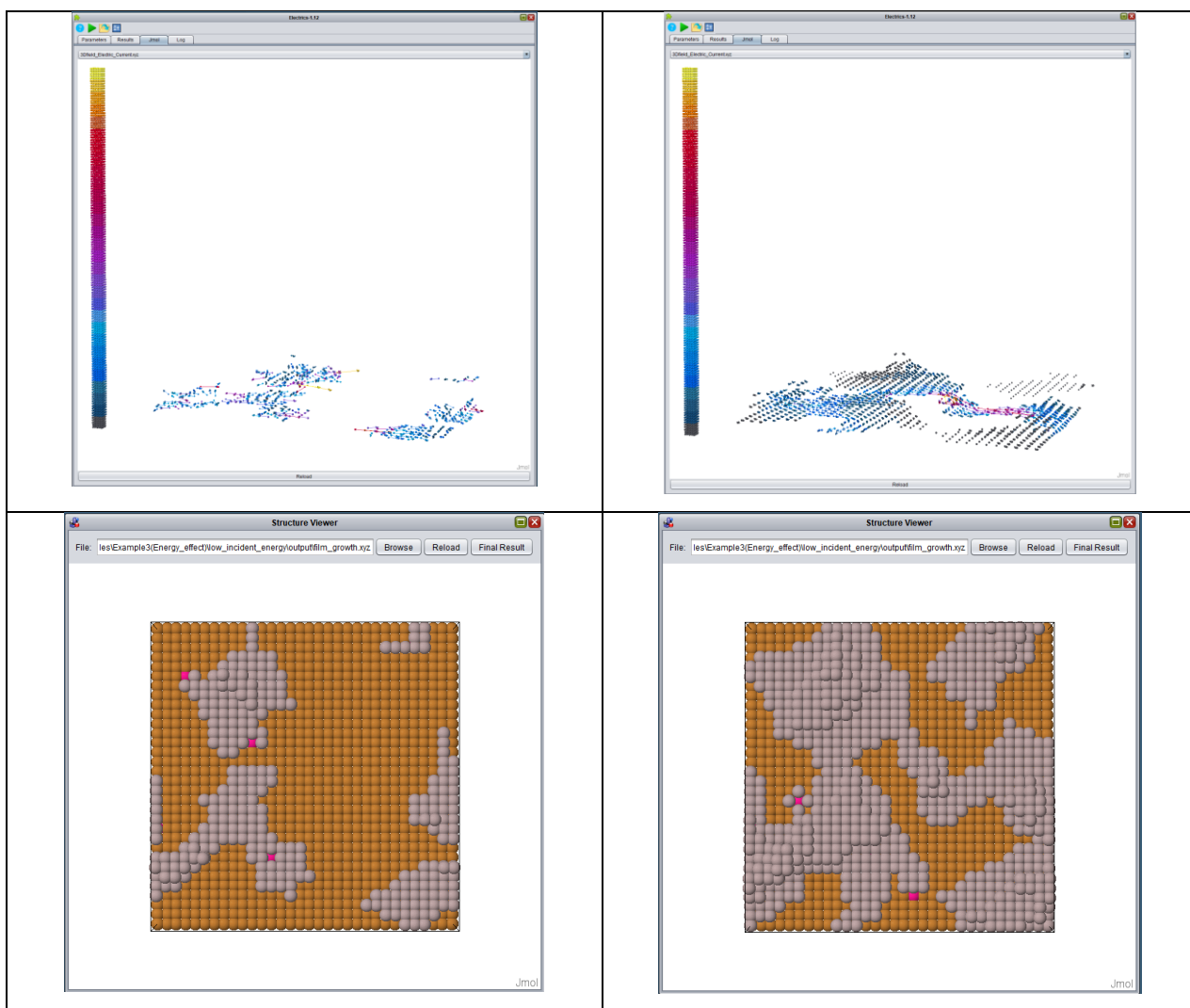


**Figure 7: Upper part: 3D-top view of the Electrical field current for 400 atoms deposited at low energy (left) and 1000 atoms deposited at high low energy (right). The corresponding atomic top 3D atom maps are also shown (lower part).**

## 6 Example 4: Successive deposition at two different angles

The goal of this example is to see the influence of the incoming particles incident angles on a pre-patterned substrate. Such a substrate, composed of rectangular rows, can be created with the *Make\_Substrate* plugin, as shown in the figure below. The created file is stored in the “plugins\Make Substrate\output\substrate\_name.xyz” folder. Do not forget to load it before running the simulation.

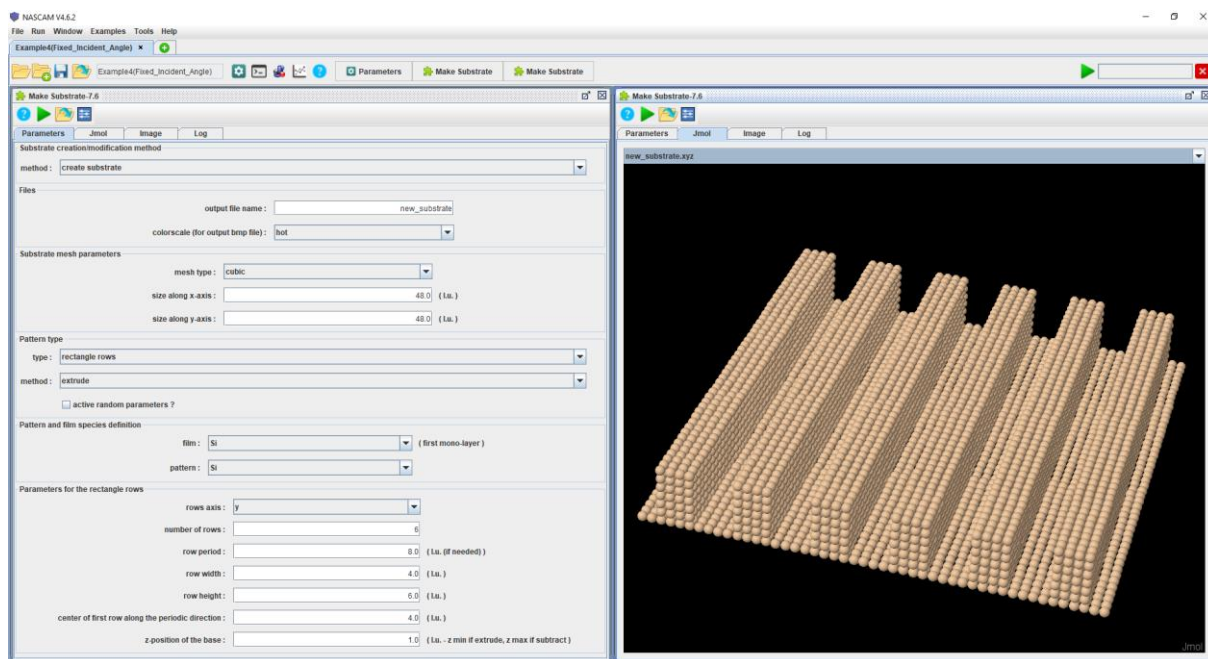


Figure 8: Creation of the substrate (xyz file) composed of rectangle rows by using the Make\_Substrate plugin.

The figure below shows the results of two successive simulations, corresponding to two different incoming particles incident angles.

At each simulation step, 500 particles were deposited. Thermal activated processes were taken into account. In both cases,  $\theta_0 = 45^\circ$  and  $\Delta\theta = 0^\circ$ , while  $\varphi_0 = 0^\circ$  for the first step and  $\varphi_0 = 180^\circ$  for the second one. For the first simulation step, the *substrate.xyz* file contains a pre-patterned substrate. When the first deposition step was finished, its *coating.xyz* output file was renamed to *substrate.xyz* and was used as an input file for the second deposition step.

All the relevant parameters for both simulation steps are given below:

	<u>First simulation step</u> ( $\varphi_0 = 0^\circ$ )	<u>Second simulation step</u> ( $\varphi_0 = 180^\circ$ )
Simulation_options	1 0 0	1 0 0
Dimensions	48 48 11 500 0.0	48 48 11 500 0.0
Deposition_rate(ML/s)	1.0	1.0

Specie: Metal_1	1.0 Al ... histo.txt 1 45 0 0 a_dst.txt	1.0 Al ... histo.txt 1 45 <b>180</b> 0 a_dst.txt
Specie: Reactive_X	0.0 O 15.999 ...	0.0 O 15.999 ...
Specie: Neutral	0.0 Ar 39.948 ...	0.0 Ar 39.948 ...
Specie: Substrate	Si 28.0	Si 28.0

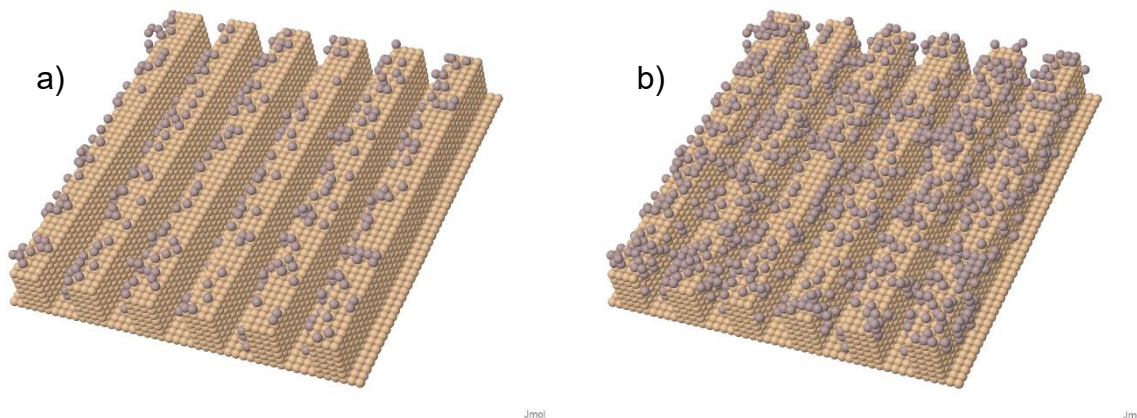


**Figure 9: Lateral views of the simulation box:**

**after the first simulation step corresponding to  $\theta_0 = 45^\circ$ ,  $\varphi_0 = 0^\circ$ ,  $\Delta\theta = 0^\circ$**

**after the second simulation step corresponding to  $\theta_0 = 45^\circ$ ,  $\varphi_0 = 180^\circ$ ,  $\Delta\theta = 0^\circ$ .**

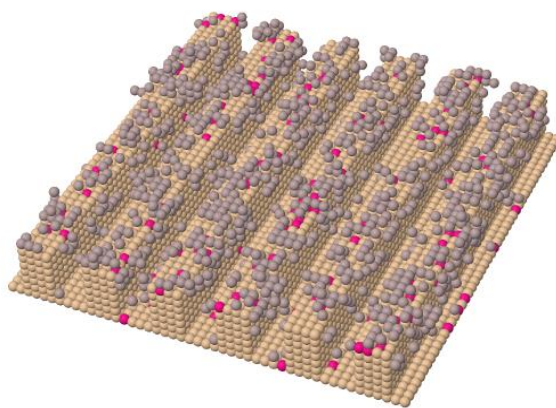
**The deposited particles are represented in grey and the structure in a) was used as substrate for the second simulation step.**

## 7 Example 5: Deposition with experimental energy and angular data.

This example is similar to example 4, but with the energy and angular distributions given in specific input files: **energy\_file\_dst.txt** for energy distribution and **angle\_file\_dst.txt** for angular distribution. These can originate either from experimental measurements or from simulation output from SIMTRA (see plugins manual). The simulation box contains a pre-patterned surface similar to the one used in the first simulation step of example 4 and the simulation result is shown below.

All the relevant parameters for this example are given below:

Simulation_options	1 0 0
Dimensions	48 48 9 1000 0.0
Deposition_rate(ML/s)	1.0
Specie: Metal_1	1.0 Al 26.982 0 1.0 <b>energy_file_dst.txt</b> 0 45 0 0 <b>angle_file_dst.txt</b>
Specie: Reactive_X	0.0 O 15.999 ...
Specie: Neutral	0.0 Ar 39.948 ...
Specie: Substrate	Si 28.0



Jmol

**Figure 5. Lateral view of the structure deposited according to the “experimental” energy and angular distributions read from the corresponding data files.**

## 8 Example 6: Dissolution and dissolution with evaporation

This is an example where two pre-existing elongated hemispheres are «dissolved» or «dissolved and evaporated» during an annealing process. The two hemispheres are created by *Make\_Substrate* plugin (note: the elongation is done by periodically repeating the semi-spheres in the y direction with a period of one lu). The created file is usually stored in the “plugins\Make Substrate\output\substrate\_name.xyz” folder.

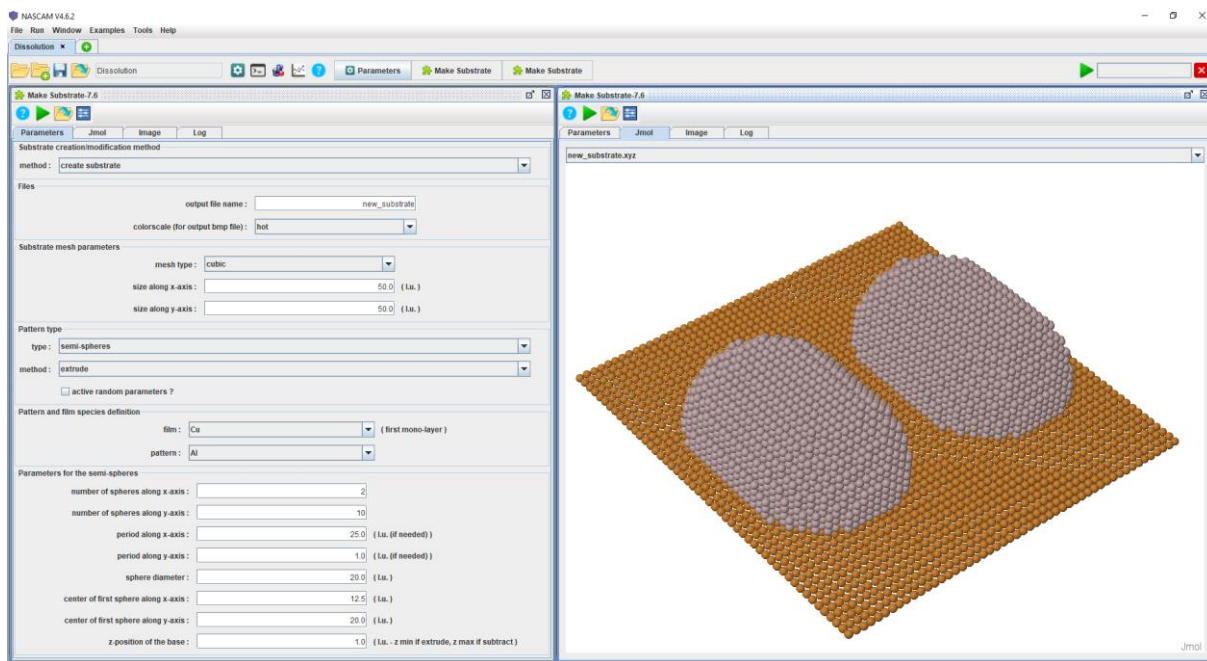


**Figure 10: Creation of the substrate (xyz file) composed of elongated semi-spheres by using the *Make\_Substrate* plugin.**

All the relevant parameters for both NASCAM simulations are given below:

	<u>Dissolution</u>	<u>Dissolution with evaporation</u>
Simulation_options	1 1 1	1 1 1
Dimensions	50 50 15 0 0.005	50 50 15 0 0.004
Deposition_rate(ML/s)	1.0	1.0
Ea_diff(eV)	1.0	1.0
Ea_nn_inc(eV)	1.3	1.3
Ea_nn_dec(eV)	1.4	1.4
Ea_detach(eV)	1.4	1.4
Ea_up(eV)	1.75	1.75
Ea_down(eV)	1.45	1.45
Ea_detrap(eV)	3.85	3.85
Ea_sub_evap(eV)	<b>3.85</b>	<b>1.1</b>
Ea_lay_evap(eV)	<b>3.85</b>	<b>1.95</b>
Specie: Metal_1	1.0 Al 26.982 ...	1.0 Al 26.982 ...

Specie:Reactive_X	0.0 O 15.999 ...	0.0 O 15.999 ...
Specie:Neutral	0.0 Ar 39.948 ...	0.0 Ar 39.948 ...
Specie:Substrate	Cu 63.54	Cu 63.54
Temp(eV)	0.075	0.075

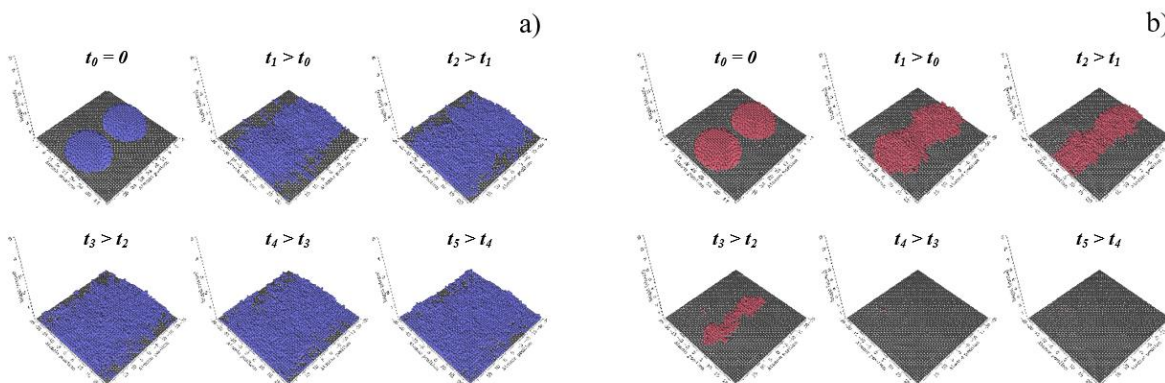


**Figure 11: Snapshots of the evolution of the two domes versus time under dissolution conditions in a) and dissolution and evaporation conditions in b). In both series, all snapshots, except the first one (initial structure), were at the same time interval of about (annealing time)/5 (~0.001s).**

Beside the qualitative information given in figure above some quantitative information is given in this case as well. All the following images were generated by using the graphics facilities available in GUI, which uses statistic information collected during the annealing processes corresponding to the studied phenomena, dissolution and dissolution with evaporation.

In the beginning and in both cases, things seem to happen in a similar way: due to the activation energy values, there is a net downward particle diffusion current. Therefore, the number of particles in the lower layers increases and the substrate coverage increases, leading to the two initial islands/domes coalescence. Of course, the dome heights decrease and so does the roughness.

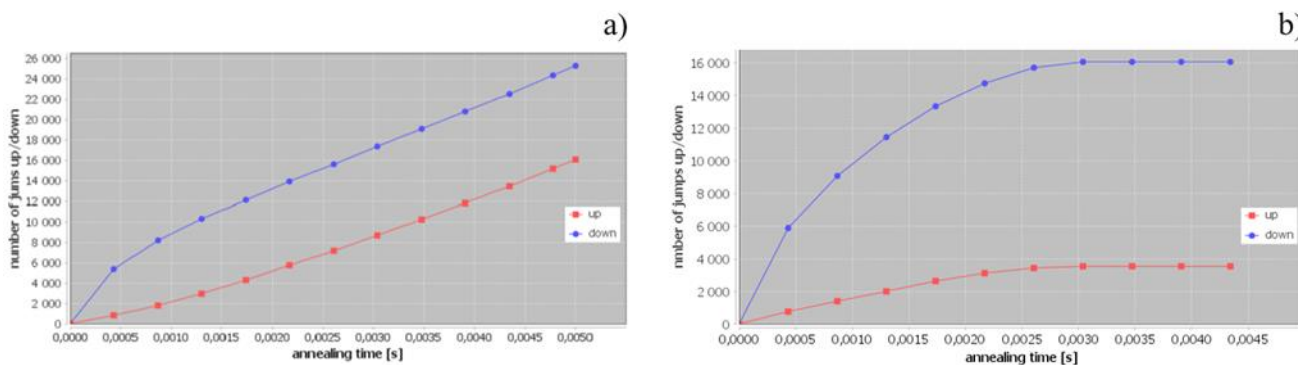


**Figure 12: The numbers of jump up (in red) and jump down (in blue) diffusion events during the annealing processes: a) dissolution without evaporation; b) dissolution with evaporation**

Without considering the evaporation event, the substrate coverage increases continuously to 1 while the roughness decreases continuously to an equilibrium value. For the sake of simplicity, both are shown below. The substrate coverage is a dimensionless coefficient varying from 0 to 1, while the surface roughness is given in lattice parameter units (lpu or lu).

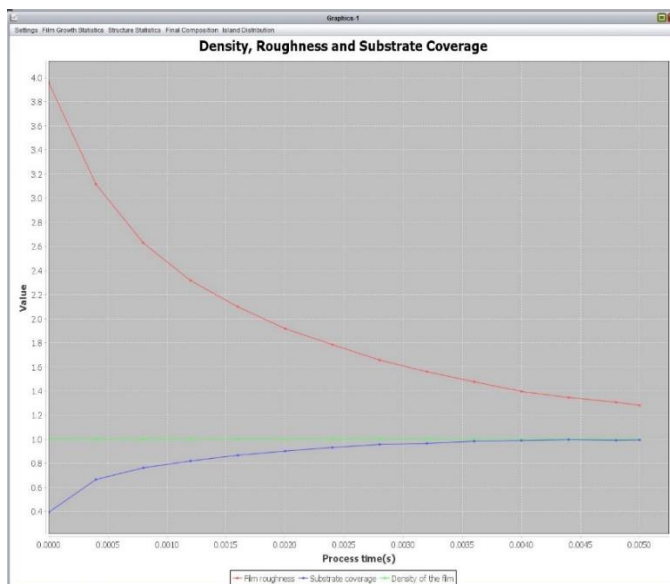


Figure 13: The surface roughness in lattice units, and the substrate coverage coefficient as well as the density for dissolution without evaporation simulation.

The numbers of atoms in the first four layers also reach some stationary values: lower layer number larger than the particle number within figure below.

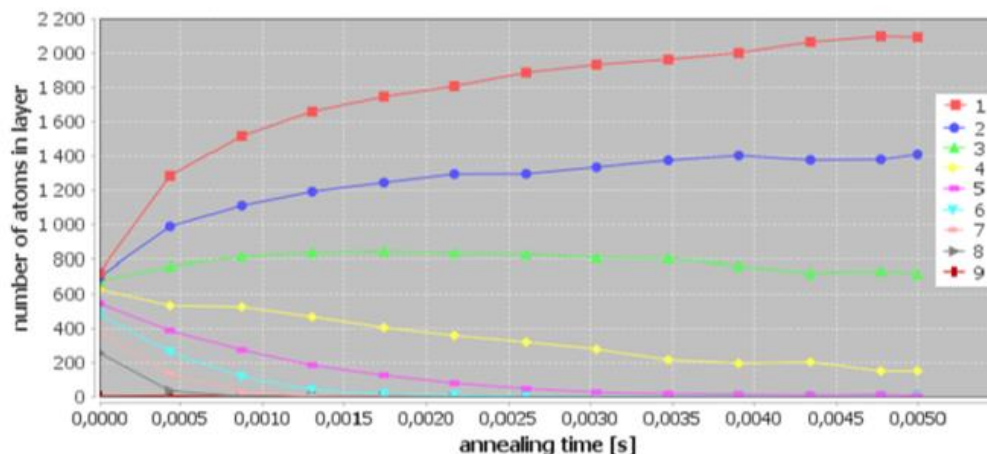


Figure 14: Time dependence of the number of atoms in each layer during the simulation corresponding to dissolution without evaporation.

In the end, there is only one large island covering almost the whole surface of the substrate. This is in agreement with the result for the surface coverage value. There are also some isolated particles, most probably belonging to layers 2 to 4 than to the first layer...



**Figure 15: Time evolution of the number of free atoms, dimers and trimers, and islands during the simulation corresponding to dissolution without evaporation.**

Taking into account evaporation, according to the results shown in Figure a (see below), the number of particles in the system decreases at a constant rate. After about  $3 \cdot 10^{-3}$ s from the beginning of the simulation, there are no particles in the system. Therefore, the number of evaporated particles stops to increase, as shown in Figure b (see below).

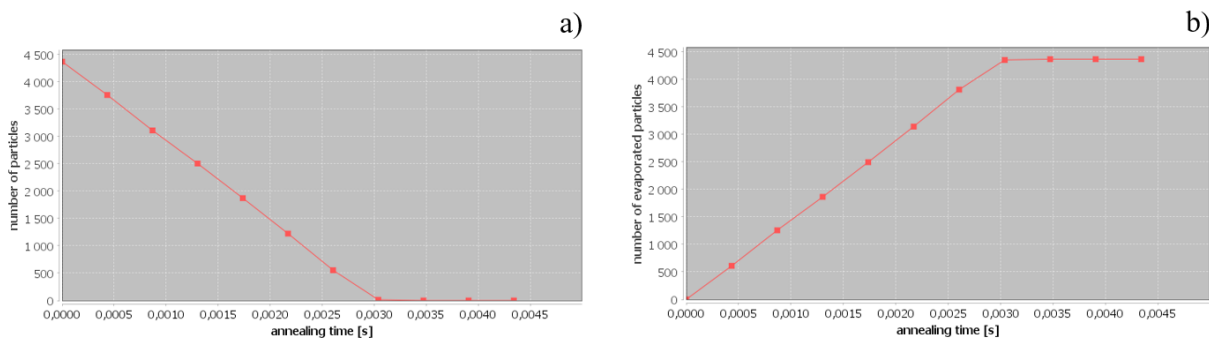


**Figure 16: Time dependence of the number of particles in the system (a) and the number of evaporation events (b) during the dissolution with evaporation simulation.**

With evaporation, the downward diffusion current is larger than it was when we did not take it into account. This is because the number of particles able to jump up decreases: once detached at the first level and after a few diffusion jumps as a free particle, a particle will evaporate instead of re-

attaching to a step edge and eventually jump up later. After  $3 \cdot 10^{-3}$ s from the beginning of the simulation, the slope of the jump up/down curves equals 0.

As shown in the figure below, after an initial small increase, the substrate coverage and the number of atoms in the lower layers decreases continuously to 0, reaching this value after  $3 \cdot 10^{-3}$ s from the beginning of the simulation. The roughness, decreasing continuously, reaches 0 (flat surface – the substrate) simultaneously.

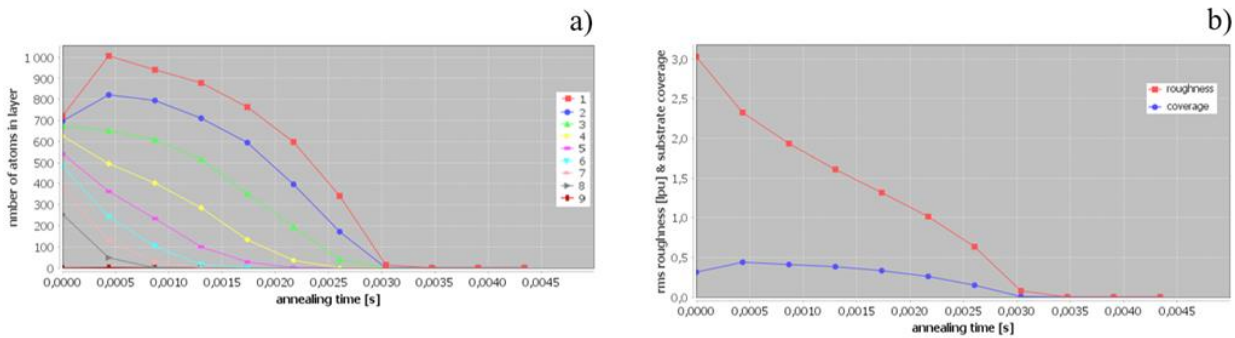


**Figure 17: Time dependence of the number of atoms in each layer (a) and the surface roughness and substrate coverage coefficient (b) during the simulation corresponding to dissolution with evaporation. In b) the roughness, in lattice parameter units (lpu), is plotted in red while the substrate coverage coefficient is plotted in blue.**

The number of islands is almost constant, with a small value (varies from 1 to 2) during the whole simulation time. This means that a nucleation event is quite improbable: the particles on the substrate evaporate soon after becoming free particles, before they meet and stick together. This is in agreement with the free particles time dependence.

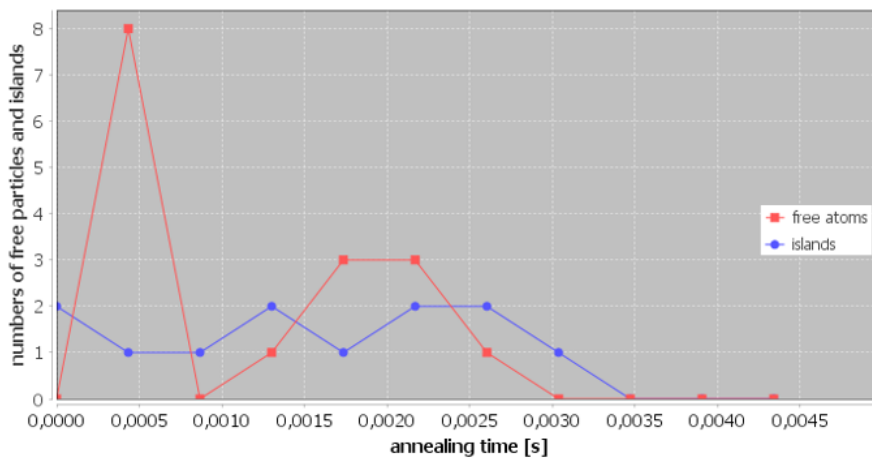


**Figure 18: Time dependence of the number of free particles (in red) and islands (in blue) when evaporation is considered.**

For both simulations (dissolution and dissolution with evaporation), the curves of the free particle mean diffusion path have the same evolution: they reach a stationary value soon after the beginning of each simulation, as can be seen below. However, a slightly higher stationary value is observed for dissolution without evaporation.

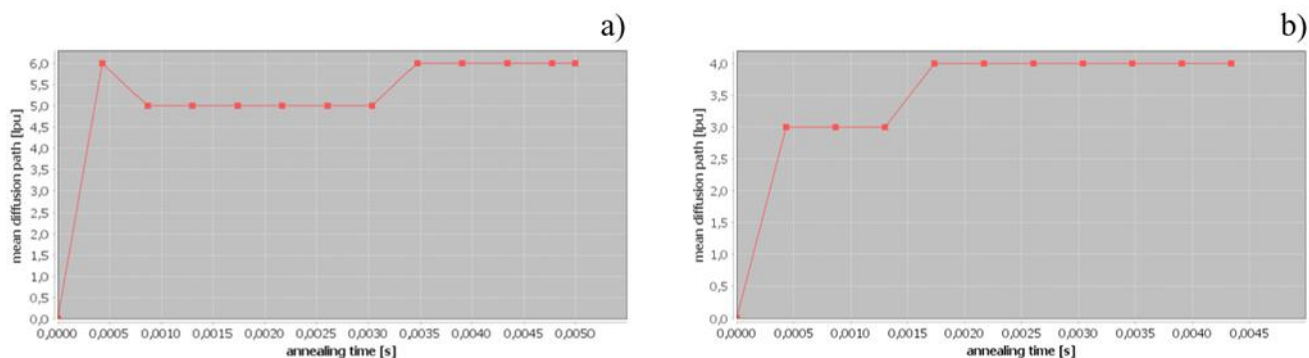


**Figure 19: The mean diffusion path of free particles, in lattice parameter units (lpu), corresponding to the dissolution (a) and dissolution with evaporation (b) simulations.**

## 9 Example 7: Multilayer deposition

This is an example of multilayer deposition with energetic neutral gas particles co-bombardment (Ar particles with a 20 eV energy), a gas - substrate collision leading to a defect creation. This is also an example on how to run NASCAM in a multilayer mode (Co/Cu/Co/Cu/Co/Cu) - this is done automatically in GUI (see the [GUI manual](#)). All relevant parameters for both kinds of deposited particles are given below:

	Cu – the initial substrate and 2 <sup>nd</sup> , 4 <sup>th</sup> and 6 <sup>th</sup> deposited element	Co – 1 <sup>st</sup> , 3 <sup>rd</sup> and 5 <sup>th</sup> deposited element
Dimensions	32 32 50 5600 0.0	32 32 50 5600 0.0
Deposition_rate(ML/s)	1.0	1.0
Specie:Metal_1	1.0 Cu 63.546 2 1 histo.txt 1 0 0 15 ang_dstr.txt	1.0 Co 58.933 2 1 histo.txt 1 0 0 15 ang_dstr.txt
Specie:Reactive_X	0.0 O 15.999 ...	0.0 O 15.999 ...
Specie:Neutral	0.1 Ar 39.948 1 20 histo_gas.txt 1 0 0 15 ang_dstr_gas.tx	0.1 Ar 39.948 1 20 histo_gas.txt 1 0 0 15 ang_dstr_gas.tx
Specie:Substrate	Co 59.0	Cu 63.54
Surface_binding_energy_of _the_substrate(eV)	3.52	3.52
Surface_binding_energy_of _the_film(eV)	4.43	4.43

Figure below shows the final structure and the number of atoms of each specie versus the structure height – Xx stands for a defect. In each deposition step, the same amount of particles was deposited (5600 particles/deposition step).

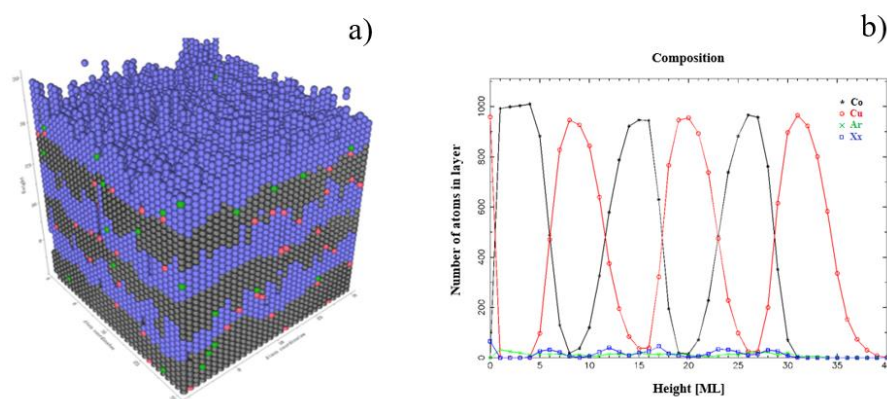


**Figure 20: Final morphology of multilayer deposition in a), and the number of atoms in each layer in b).**

**The colours in a) and b) do not correspond to the same kind of atom:**

**in a - Co = black, Cu = blue, Ar = green and Xx = red**

**in b - Co = black, Cu = red, Ar = green and Xx = blue**

Figure 21 shows the dependence of the number of deposited atoms on time. To understand this plot, remember that only the current depositing metal specie is taken into account. For the time intervals from 0 s to 6 s, 12 s to 18 s, and 24 s to 30 s, atoms of Co were deposited. Atoms of Cu were deposited from 6 s to 12 s, 18 s to 24 s, and 30 s to 36 s. Thus, for the time intervals (0, 6), (12, 18), (24, 30), you can see a successive increase of the number of Co atoms, and for the time intervals (6, 12), (18, 24), (30, 36), a successive increase of the number of Cu atoms.

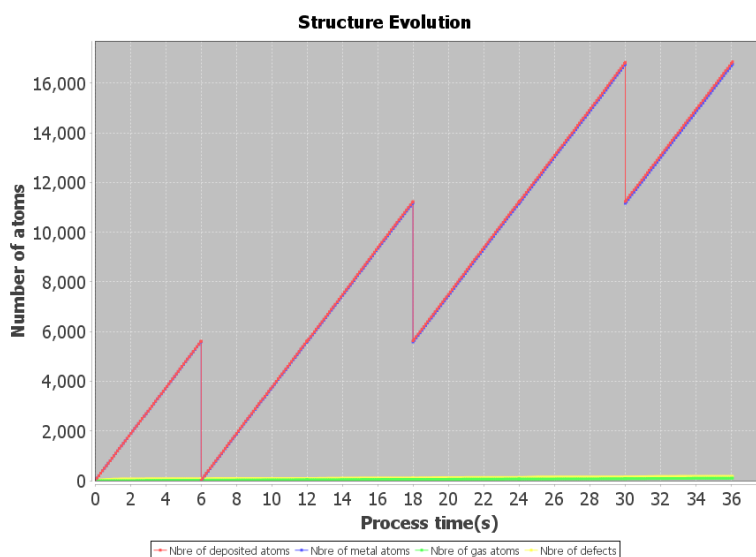


**Figure 21: Structure evolution: the dependence of the number of deposited atoms on time.**

## 10 Example 8: Ge cluster formation

This is an example taken from a 2013 publication of P. Moskovkin and S. Lucas [1]. In this work, they investigated the growth of the first atomic layer of Ge on stepped Si substrate.

The first step consists in creating the substrate, as shown in 2 next figures.

First, the main pattern is created.

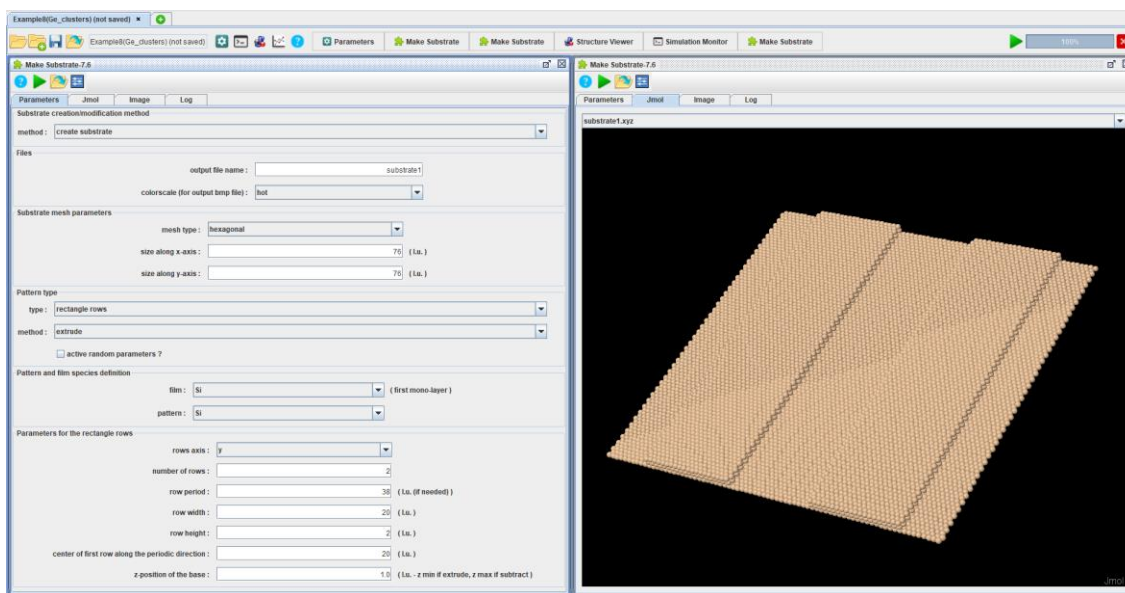


Figure 22: Creation of the substrate (xyz file). Step 1: rectangular rows.

In a second step, defects/site (artificial matter, that appears red in JMOL) of no diffusion will be created along the edges of the rectangular rows. These defects will act as nucleation centers (trap) for the growth of Ge quantum dots.

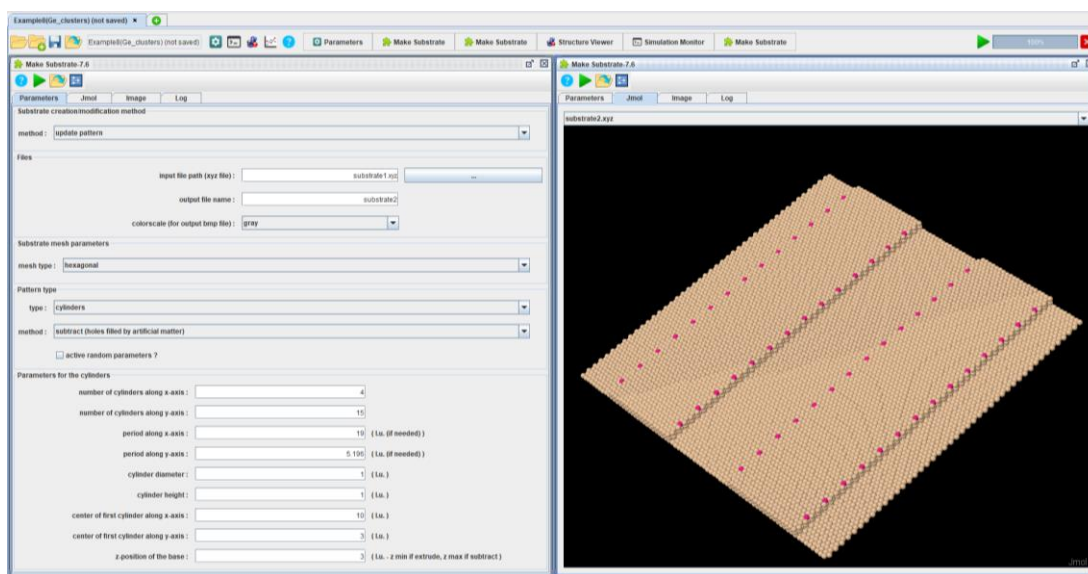


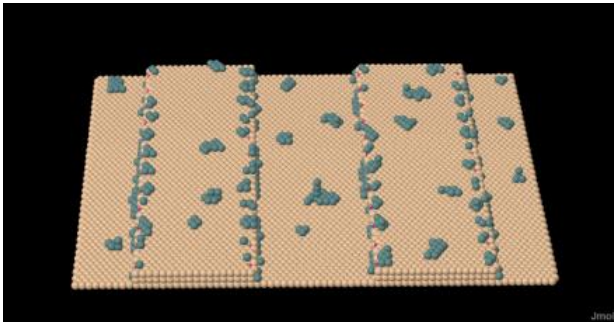
Figure 23: Creation of the substrate (xyz file). Step 2: “trap” printing.

To see these defects (red) in the JMOL window, change the atom size (right click/Style/Atoms/25 % van der Waals).

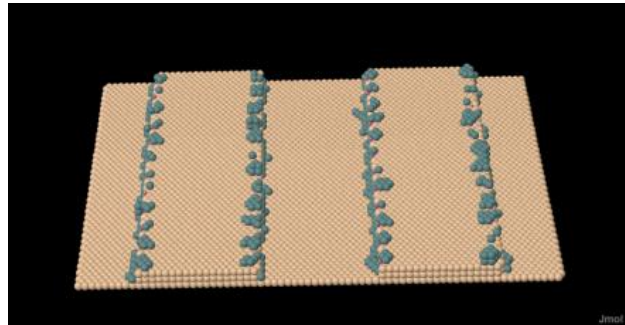
Then, load the last substrate (obtained after the last step “trap printing”) and launch NASCAM simulations at 75°C, 250°C, 300°C (run 3 different simulations). As you can see in next figure, deposition occurring at these temperatures are followed by annealing during several minutes at the same temperature. There is a transition from cluster formation in the middle of the steps to the formation at step edges. There are three temperature regimes: formation of Ge clusters on the terrace for low temperatures ( $\ll 150^\circ\text{C}$ ), at the step edges for intermediate temperatures ( $\geq 150^\circ\text{C}$ ), and at the bottom of the steps at high temperatures ( $\geq 300^\circ\text{C}$ ). In addition, the formation of Ge clusters also depends on the deposition rate and terrace width. For more details, see the publication. All the relevant NASCAM parameters for this example are given below:

Substrate_type	1
Dimensions	76 88 15 400 100.0
Deposition_rate(ML/s)	0.003
Pattern_name	pattern.txt
Ea_diff(eV)	0.8
Ea_nn_inc(eV)	0.928
Ea_nn_dec(eV)	1.024
Ea_detach(eV)	3.8
Ea_up(eV)	1.056
Ea_down(eV)	1.056
Ea_detrapp(eV)	1.52
Ea_sub_evap(eV)	2.7
Ea_lay_evap(eV)	2.7
Specie:Metal_1	1.0 Ge 72.64 1 0 histo.txt 1 0 0 0 ang_dstr.txt
Specie:Reactive_X	0.0 O 15.999 ...
Specie:Neutral	0.0 Ar 39.948 ...
Specie:Substrate	Si 28.0
Temp(eV)	<b>To be set</b>

Figure 24 below shows the results corresponding to three simulation temperatures.



T = 75°C



T = 250°C

**Figure 24: Cluster formation at deposition and annealing temperature of 75°C, 250°C.**

## 11 Example 9: Deposition with a tilted magnetron source.

This example shows how to predict the film morphology in a system where a magnetron source is tilted, with respect to the sample substrate, and samples (Z1 and Z2), which are placed at two different places (zones) on the sample holder. Based on this work, a paper was published in 2014 by G. Vanda et al [2]. Next figure, taken from the cited paper, shows the experimental setup:

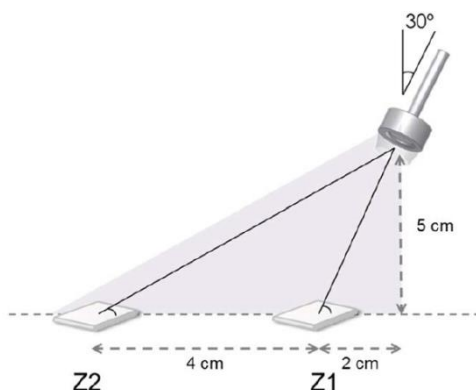


Figure 25: Experimental setup (Figure 1 in ref. 2).

First, a SIMTRA simulation (Simulation of Metal TRANsport, available at <http://www.draft.ugent.be/>) is performed in order to derive the angular and energy distribution of the species sputtered from the magnetron and reaching the samples. Then the SIMTRA file (ParticleData) is converted to a format compatible with NASCAM (see the *SIMTRA TO NASCAM* plugin). Next Figure shows the angular and energy distributions together with the simulation resulting structures corresponding to each zone. The deposition conditions correspond to Si magnetron sputtering at an Ar pressure of about 5 mbar and are given below:

	<u>Zone Z1</u>	<u>Zone Z2</u>
Simulation_options	100 0 0	100 0 0
Substrate_type	1	1
Dimensions	200 4 100 50000 0	200 4 100 50000 0
Deposition_rate(ML/s)	9	5
Specie: Metal_1	1.0 Si 28.0 1 0.0 ../input/e_dst_Z1.csv 0 0.0 0.0 0.0 ../input/a_dst_Z1.csv	1.0 Si 28.0 0 0.0 ../input/e_dst_Z2.csv 0 0.0 0.0 0.0 ../input/a_dst_Z2.csv
Specie: Reactive_X	0.0 O 15.999 ...	0.0 O 15.999 ...
Specie: Neutral	0.0 Ar 40 ...	0.0 Ar 40 ...
Specie: Substrate	Si 28.1	Si 28.1

Regarding energy distributions, the distance the atoms have to travel from the magnetron to the sample location is larger for zone 2 compared to zone 1. Consequently, the atoms have more collisions and the probability to have atoms with low energy is higher for zone 2.

The angular distribution varies substantially from zone 1 to zone 2 leading to a tilted columnar structure morphology in zone 2. In addition, the porosity is different.

In both cases, the structure is not dense because of the low average energy (lower than the lattice binding energy) of the species impinging the film.

Deposition is performed at low temperature and therefore no diffusion takes place.

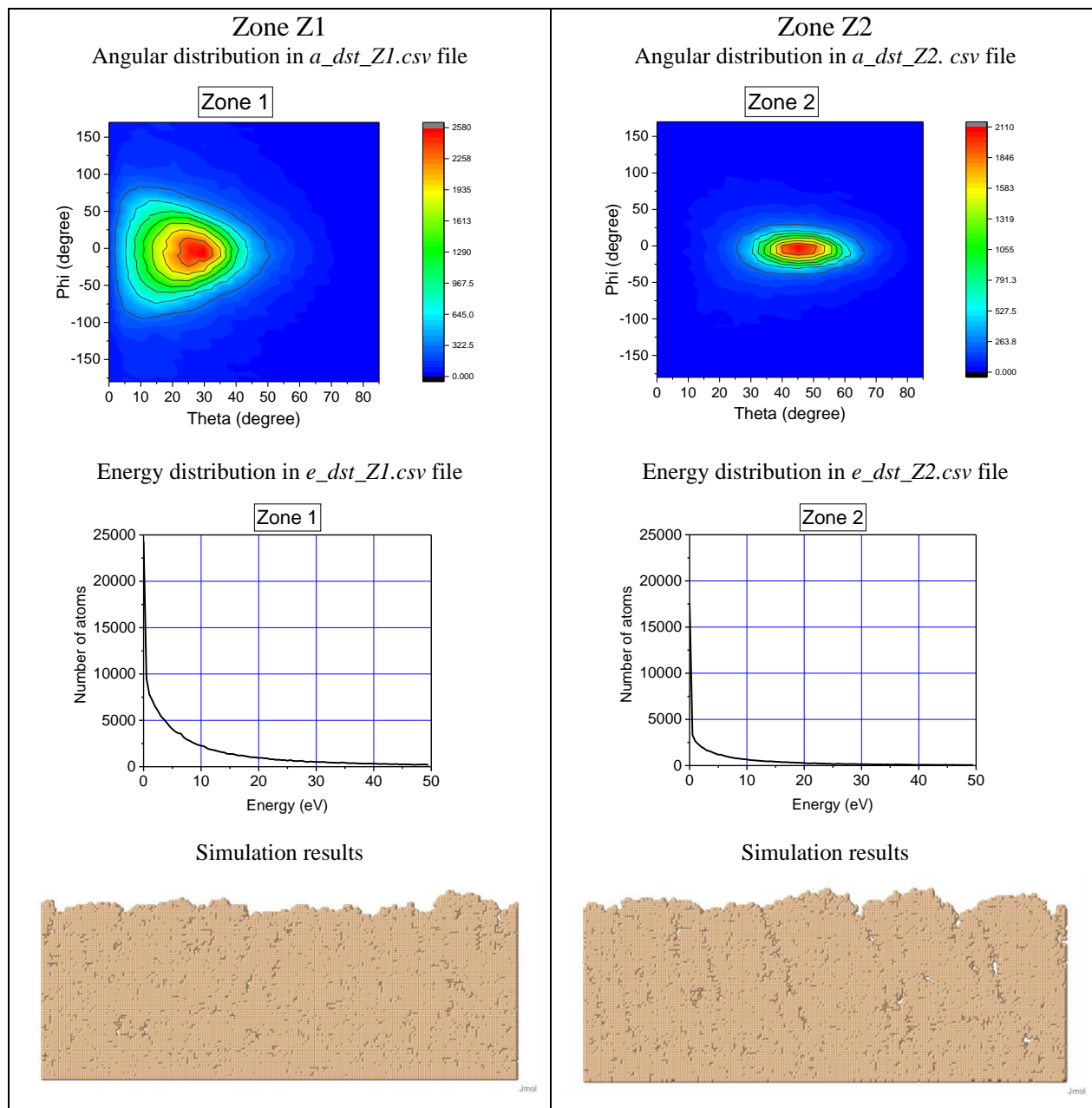


**Figure 26: The angular and energy distributions and the simulation resulting structures corresponding to each zone Z1 and Z2.**

## 12 Example 10: Sample movement

### 12.1 Deposition on a rotating substrate through a mask

This example demonstrates deposition at a glancing angle (80°) on a rotating substrate through a mask. This technique enables to grow spiral columnar structures. The columns morphology depends on a number of parameters: deposition angle, deposition rate, rotation rate, chamber base pressure (i.e. the energy of depositing atoms). Thus, it is quite helpful to perform simulations before doing the real deposition in order to adjust these parameters. The simulations are done at a low temperature; diffusion is not taken into account.

Simulation_options	1000 0 0
Substrate_type	0
Dimensions	90 30 20 40000 0.0
Deposition_rate(ML/s)	<b>1.0</b>
Masked_deposition	<b>1</b>
Pattern_name	<b>pattern.txt</b>
Specie:Metal_1	2.0 Ti 47.867 1 <b>10.5</b> E_Metal.txt 1 <b>80.0</b> 0.0 0.0 A_Metal.txt
Specie:Reactive_X	0.0 O 15.999 ...
Specie:Neutral	0.0 Ar 39.948 ...
Specie:Substrate	Si 28.0
Temp(eV)	0.0366
Surface_binding_energy_of_the_substrate,(eV)	3.52
Surface_binding_energy_of_the_film,(eV)	4.89
w_rot(1/s);init_tilt(deg);A_osc(deg);w_osc(1/s)	<b>0.01</b> 0.0 0.0 0.0

The substrate includes two circular features, and the deposition is happening only on the features through a mask. The mask has been drawn with NASCAM GUI:

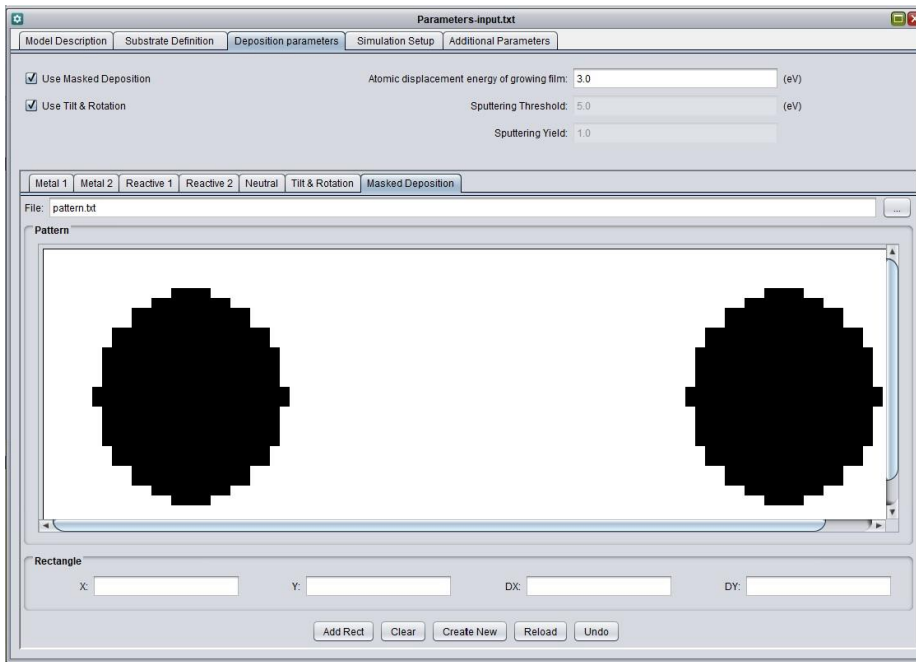


Figure 27: Mask as defined for this example : atoms can only go through the black area.

Please make sure that the mask has the same size as the substrate.

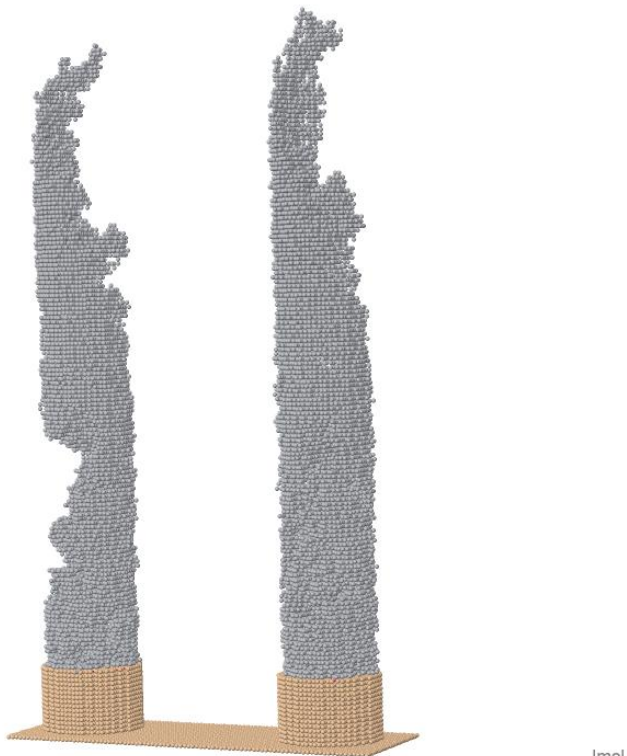


Figure 28: Illustration of deposition on a substrate through a mask.

## 12.2 Deposition on a rotating substrate with an initial tilt through a mask

This example demonstrates deposition on a substrate at variable deposition angle (tilting angle depends on time) through a mask. Again the final morphology depends on deposition rate, maximum deposition angle, frequency of the substrate oscillation, the energy of depositing atoms.

Simulation_options	500 0 0
Substrate_type	0
Dimensions	500 4 20 300000 0.0
Deposition_rate(ML/s)	<b>1.0</b>
Masked_deposition	<b>1</b>
Pattern_name	<b>pattern.txt</b>
Specie:Metal	2.0 Ti 47.867 1 1.5 E_Metal.txt 1 0.0 0.0 0.0 ...
Specie:Gas	0.0 Ar 39.948 ...
Specie:Substrate	Si 28.0
Temp(eV)	0.0366
Surface_binding_energy_of_the_film,(eV)	4.89
w_rot(1/s);init_tilt(deg);A_osc(deg);w_osc(1/s)	0.0 0.0 <b>85.0 0.004</b>

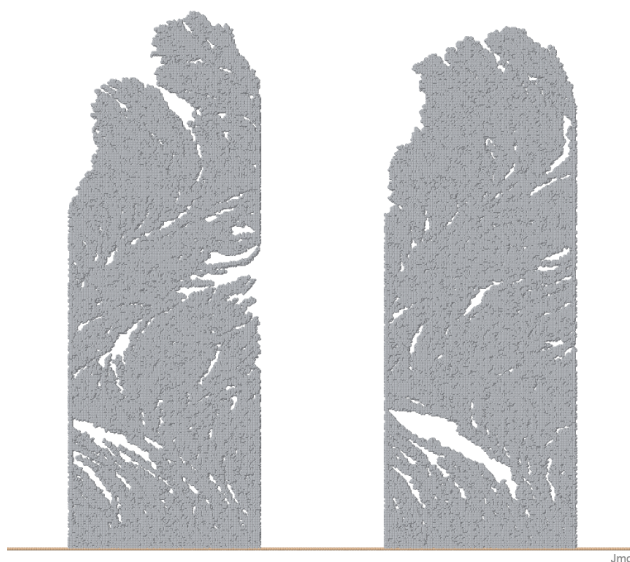


Figure 29: Illustration of a slice cut (plugin slice) of the example of glancing angle deposition on a rotating substrate.

## 13 Example 11: Glancing Angle Deposition (GLAD).

### 13.1 Simulation parameters

In the following examples, we simulate “*slanted post*”, “*vertical post*”, and “*chevron-like*” structures. For more information, look at Figure 13.4 from “*Glancing Angle Deposition*” by Michael T. Taschuket et all. [3].

The angle  $\alpha$  in the reference 3 is equivalent to  $\theta$  in NASCAM. For these examples, we will use the analytical function for the angular distribution. Theta is fixed ( $80^\circ$ ) and  $\varphi$  varies.

The slanted case corresponds to a deposition using  $\theta = 80^\circ$ ,  $\Delta\theta = 1^\circ$  and  $\varphi = 0^\circ$ .

The chevron case corresponds to a deposition using  $\theta = 80^\circ$ ,  $\Delta\theta = 1^\circ$  and choosing alternatively  $\varphi = 0^\circ$  and  $\varphi = 180^\circ$  (three times each).

The vertical post case corresponds to a continuous rotation with  $0.1 \text{ s}^{-1}$  around the z-axis, and to a deposition using  $\theta = 80^\circ$ ,  $\Delta\theta = 1^\circ$  and  $\varphi = 0^\circ$ .

	<u>Chevron</u> ( $\varphi_0 = 0^\circ$ & $\varphi_0 = 180^\circ$ )	<u>Slanted post</u> ( $\varphi_0 = 0^\circ$ )	<u>Vertical post</u> ( $\varphi_0 = 0^\circ$ )
Simulation_options	1 0 0	1 0 0	1000 0 0
Substrate_type	0	0	0
Dimensions	400 4 10 2000 0	400 4 40 100000 0	200 60 200 500000 0
Deposition_rate(ML/s)	0.05	0.05	0.5
Specie:Metal_1	1 Cu 63.546 1 0.029 eDst.txt 1 80.0 $\varphi_0$ 1 aDst.txt	1 Cu 63.546 1 0.029 eDst.txt 1 80.0 $\varphi_0$ 1 aDst.txt	1 Cu 63.546 1 0.029 eDst.txt 1 80.0 $\varphi_0$ 0 aDst.txt
Specie:Reactive_X	0.0 O 15.999 ...	0.0 O 15.999 ...	0.0 O 15.999 ...
Specie:Neutral	0 Ar 39.948 ...	0 Ar 39.948 ...	0 Ar 39.948 ...
Specie:Substrate	Cu 63.546	Cu 63.546	Cu 63.546
w_rot(1/s);init_tilt(deg); A_osc(deg);w_osc(1/s)	0 0 0 0	0 0 0 0	<b>0.1</b> 0 0 0

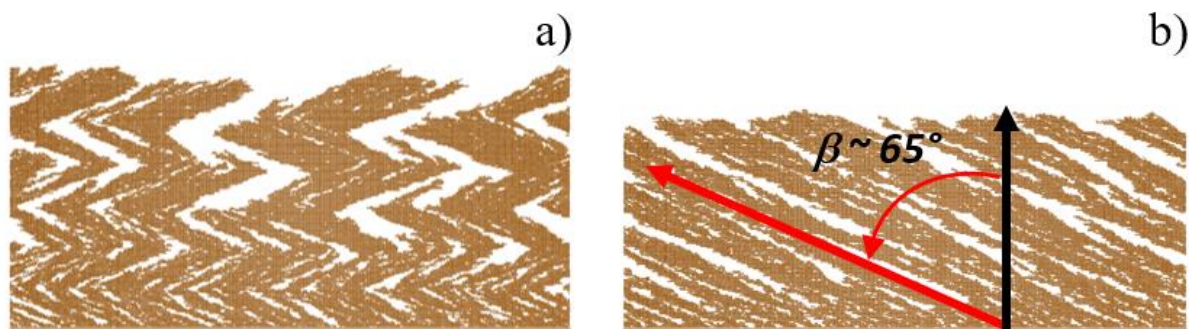
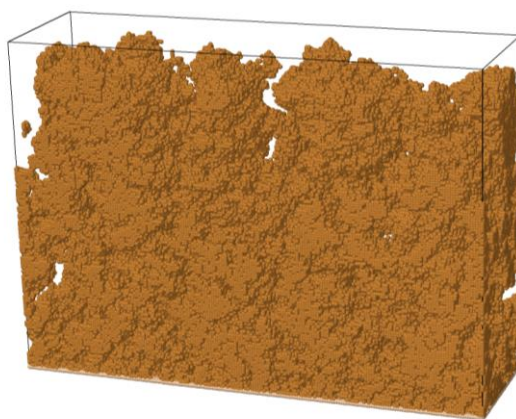


Figure 30: Two different kinds of GLAD structures:

- a) A “chevron-like” deposited structure: a succession of six deposition steps each corresponding to the same angle  $\theta_0 = 80^\circ$  but alternatively to  $\varphi_0 = 0^\circ$  and  $\varphi_0 = 180^\circ$  (see [example 7](#))
- b) A “slanted post” deposited structure obtained using  $\theta_0 = 80^\circ$  and  $\varphi_0 = 0^\circ$ ; note the broadening of the columns, and the tilt angle  $\beta \sim 65^\circ$

In both cases, a small narrow beam,  $\Delta\theta = 1^\circ$ , was used (collimated vapor beam).

Keeping constant both polar and azimuthal deposition angles ( $\theta_0 = 80^\circ$  and  $\varphi_0 = 0^\circ$ ), but adding a slow rotation to the substrate ( $w_{rot} = 0.1s^{-1}$ ), a vertical post is obtained. In fact the rotation movement is equivalent to a continuous variation of the azimuthal angle  $\varphi_0$ . By attentively looking at the structures in Figure 30a, we can see that the substrate rotation combined with vertical film growth results in the development of “screw-like” structures. The pitch of these “screws” can be controlled by varying the deposition rate and the substrate rotation speed properly. Such deposition conditions lead to a structure with high porosity, its density being about 40.3% the nominal density (see *log\_file.txt* or *stat\_film\_structure.csv* file).



Jmol

Figure 31: Example of vertical post GLAD conditions.

In the following, a pore analysis of this simulation result is performed using the *Porosity* plugin. Indeed, it is rather difficult to decide whether the pores are connected to air or are occluded, just by looking at these simulation outputs.

### 13.2 Analysis with Porosity plugin

*Porosity* is a plugin that allows the characterizing of thin films porosity simulated by NASCAM (and other packages). Results are stored in .csv files for statistical analysis and .xyz files for 3D visualization (JMOL). Here, we illustrate the porosity analysis of the 3D example “GLAD – vertical post”, but obviously, it is possible to do it for 2D structures.

After loading the plugin, select the scanning probe diameter from range 6 to 16, step of 2 lattice units (lu). Run the plugin and then display the results in JMOL (JMOL tab). For each probe diameter, you can select a 3D view of open pores, connected pores and occluded pores (right click, model...). Connected pores are the pores in between two layers and do not exist in this case because there is only one layer.

#### 13.2.1 3D display

##### 1) Air connected pores.

The figure below shows the 3D view of air connected pores (open pores) having a diameter larger than 8 and 16 lu.

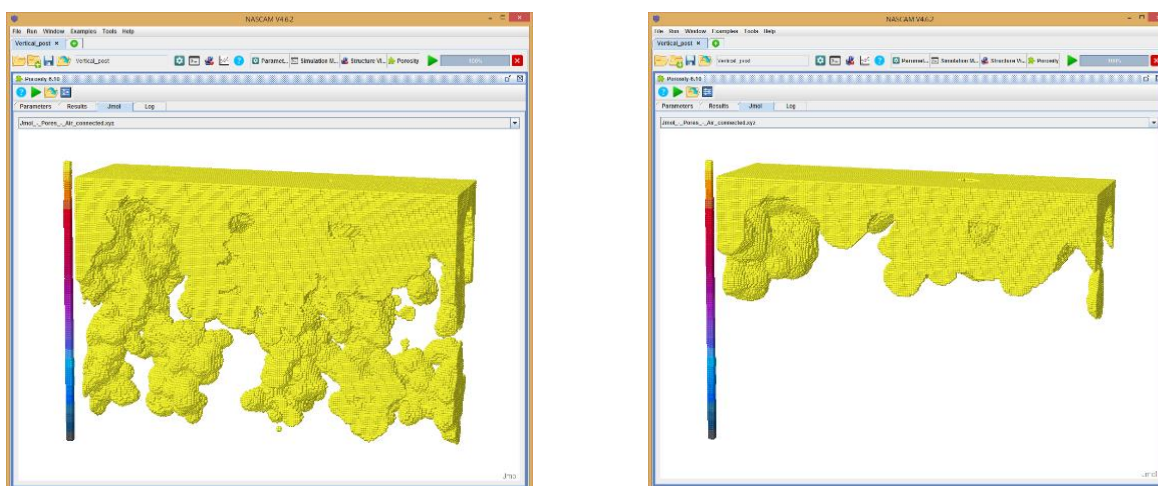
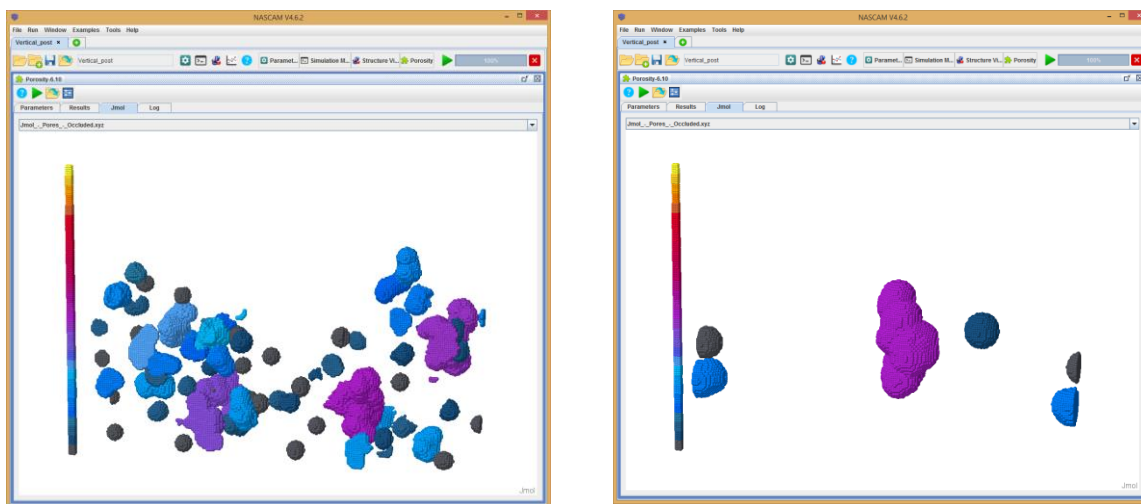


Figure 32: 3D views of air connected pores for a diameter 8 lu probe (left) and a diameter 16 lu probe (right)

2) Occluded pores

Next figure shows the results of the analysis for occluded pores, i.e., pores surrounded only by the substrate or deposited particles (without any “air” contact). The occluded pore dimension is shown in a colour scale. In addition to open pores, the sample contains numerous occluded pores randomly distributed throughout the film.



**Figure 33: 3D views of occluded pores for a diameter 8 lu probe (left) and a diameter 16 lu probe (right).**

3) All kinds of pores.

The figure below shows the results of the analysis for air connected and occluded pores larger than an 8 and a 16 lu probe diameter.

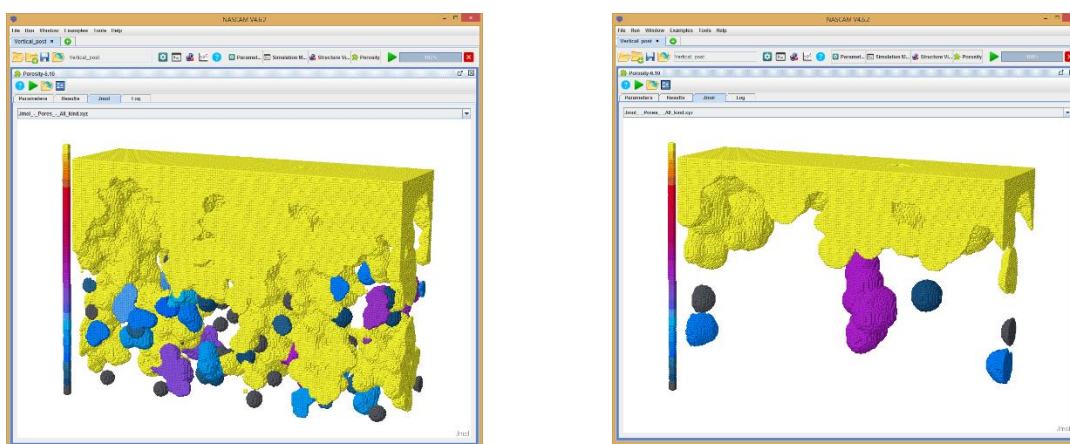


**Figure 34: 3D views of the occluded and air connected pores for a diameter 8 lu probe (left) and a diameter 16 lu probe (right).**

### 13.2.2 Statistical porosity analysis

This procedure is particularly useful if you want to know what the structure accessible porosity with a probe (molecule) of a given size (diameter) is.

Next figure shows the histogram of occluded pores size distribution detected by a diameter 8 lu probe.

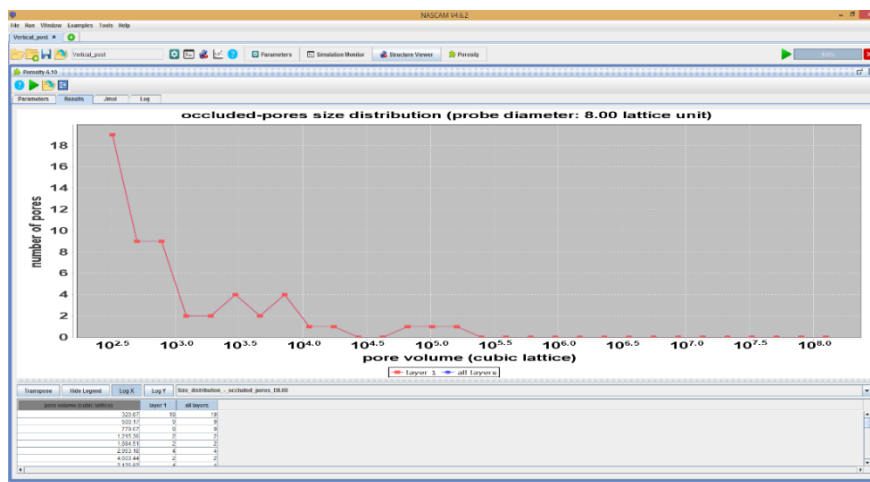


Figure 35: Volume distribution of occluded pores (in lu<sup>3</sup>) detected by a diameter 8 lu probe (the log<sub>10</sub> representation of pores volumes is for convenience, but can be changed by a linear one).

This is a linear-log graph of the number of pores versus their volume.

As shown in Figure 35, 19 pores have a volume V greater than 320 lu<sup>3</sup> and smaller than 500 lu<sup>3</sup>. If

these pores are spherical, the equivalent diameter is  $D_{eq} = 2 \sqrt[3]{\frac{3V}{4\pi}}$  i.e. between 8.4 and 9.7 lu.

Another possible statistical study about the number of occluded pores versus the probe diameter can be found in Figure below:

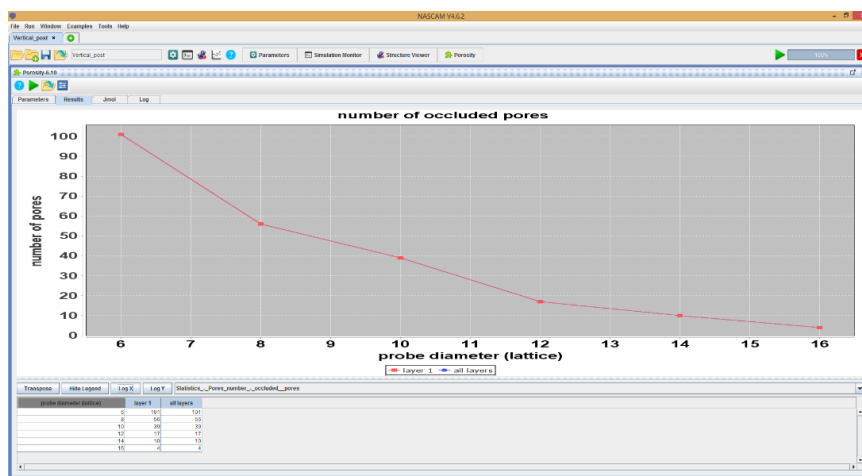


Figure 36: Number of occluded pores vs. probe size.

As shown above, 56 pores can accommodate a diameter 8 lu probe.

If we are interested in the total pore volume, Figure 37 shows that all the occluded pores which are accessible by a diameter 6 lu probe represent a total volume of 48954 lu<sup>3</sup>.

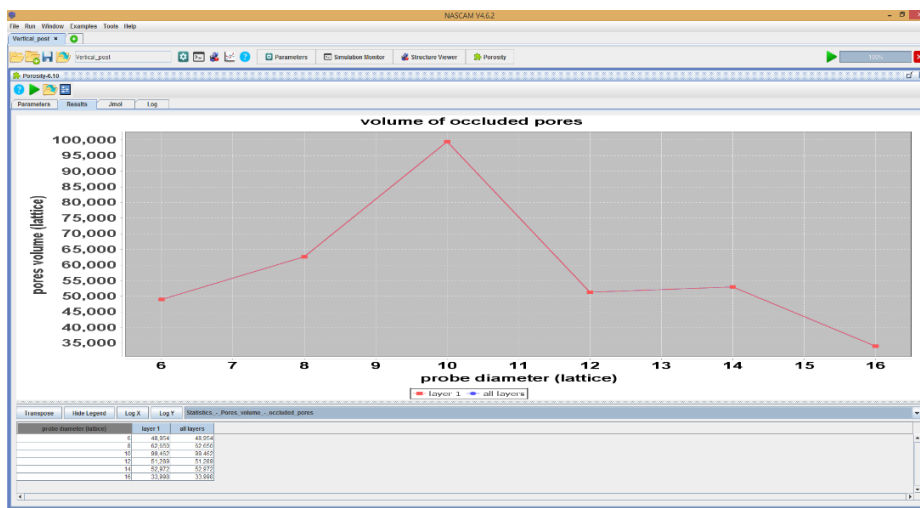


Figure 37: Volume of occluded pores vs. probe size.

Finally, you can also compute the volume ratio (%) of occluded pores (i.e. the total volume of occluded pores divided by the volume of the respective layers (or of the whole structure)) versus the probe diameter, as shown in Figure 38.

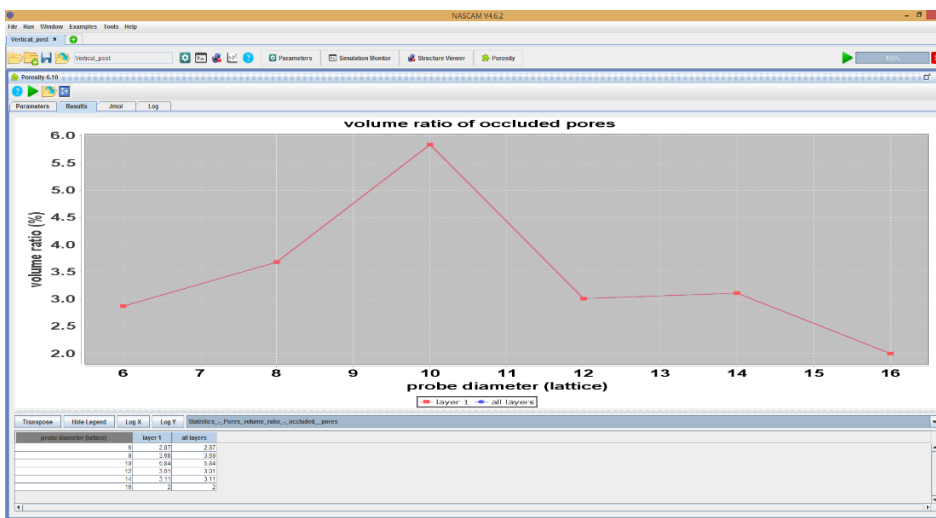


Figure 38: Volume ratio of occluded pores vs. probe size.

In this case, the total volume of occluded pores which can be scanned by a diameter 6 lu probe is about 2.87% of the total structure volume (and of layer 1).

The same study can be done for the volume ratio of all pores (occluded and air-connected) as shown in the Figure 39.

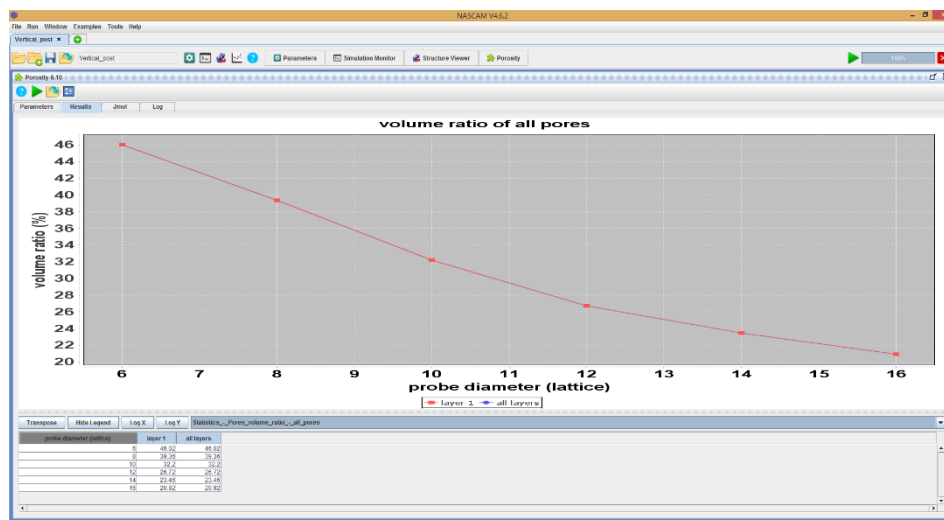
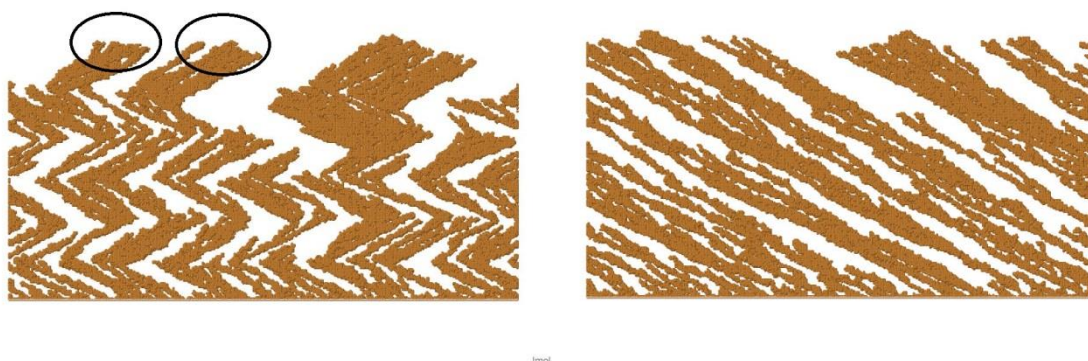


Figure 39: Volume ratio of all kinds of pores (air-connected and occluded) vs. probe size.

The total porosity accessible by a diameter 6 lu probe represents 46% of the structure volume. Finally, to know what the volume ratio (%) of open and occluded porosity is, the plugin has to be run with a 1 lu diameter probe. In accordance with NASCAM on the fly statistical calculation, the result is that the total porosity is 70.7%, among which 69.4% is air-connected and only 1.3% is occluded. The structure is mainly open.

### 13.2.3 Surface roughness

Use the *Roughness* plugin in order to analyze surface morphology. In this section, we apply the plugin to the surfaces obtained in the *Chevron* and *Slanted* post examples. Results of the simulations are shown in Figure 40.



**Figure 40** Film columnar structure for the *Chevron* (left) and the *Slanted* (right) posts. The number of deposited atoms is equal to  $1.2 \cdot 10^5$  for both cases. Some of the surface features are marked for the *Chevron*.

The *Roughness* plugin can analyze these surfaces (see Figure 41). The film roughness is lower for the *Slanted* post. In addition, you can use a surface correlation function,  $G(R)$ ,

$$G(r) = \langle (h(x + R, y) - h(x, y))^2 \rangle,$$

where  $h(x, y)$  is the local thickness of the film. The function is used to estimate the characteristic size of surface structures. For details, see the Plugin manual.

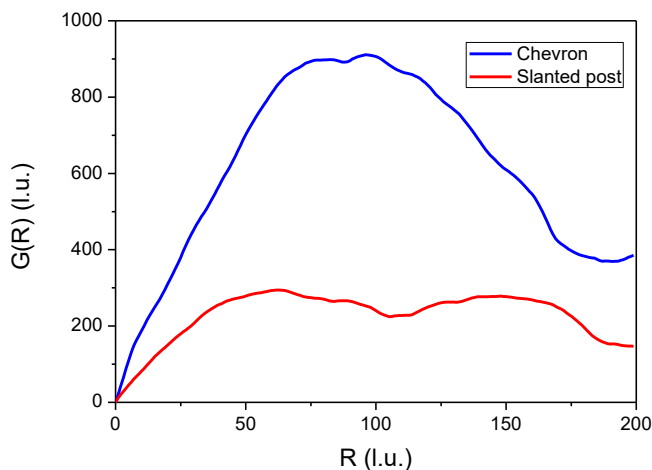


**Figure 41:** Surface correlation functions for in *Chevron* and *Slanted* post coatings.

Figure 41 shows that

- The ratio of the maximum  $G(R)$  values for these examples is about 3, i.e. equal to the square of the coatings roughness ratio. This is in agreement with the analysis given in the Plugins manual.

- Characteristic sizes of the surface structure are close and equal to about 60 and 80 lattice units for *Chevron* and *Slanted* post coatings respectively. We determine the characteristic size from the plot of  $G(R)$  as a range when the function reaches its maximum. There are more surface features on the *Slanted* post and their sizes are smaller, in agreement with the analysis.

Results may differ when you run the simulation several times because it is Monte-Carlo.

## 14 Example 12: Bragg mirrors

### 14.1 EUV filters

This example was inspired by the paper of S. Braun et al. [4]. In this work, the cited authors studied different types of Mo/Si multilayers in the extreme ultraviolet (EUV) spectral range. For pure Mo/Si-multilayers prepared by magnetron sputtering deposition (MSD), the deposition parameters were optimized so that a normal incidence reflectivity of  $R_{EUV} = 68.7\%$  could be realized through the Si and Mo alternative deposition of 131 single element layers.

Without taking diffusion into account, we simulated a continuous deposition process consisting of 131 elementary deposition steps. Each deposition step corresponds to a single specie deposition. Si and Mo were deposited alternatively, using the results of SIMTRA simulations for the angular and energy distributions of the deposited particles. These simulations were performed at a pressure of 2mTorr and for a target-substrate distance of 10cm.

All relevant parameters, corresponding to each elementary deposition step (single specie deposition) are given below:

	Specie: Mo	Specie: Si
Simulation_options	100 0 0	100 0 0
Substrate_type	0	0
Dimensions	32 4 20 1458 0.0	32 4 20 2397 0.0
Deposition_rate(ML/s)	1	1
Specie:Metal	1.0 Mo 95.96 0 2.0 Mo_e_dst.txt 0 0 0 15 Mo_a_dst.txt	1.0 Si 28.085 0 2.0 Si_e_dst.txt 0 0 0 15 Si_a_dst.txt
Specie:Neutral	0.0 Ar 39.948 ...	0.0 Ar 39.948 ...
Specie:Substrate	Si 28.085	Mo 95.96
Surface_binding_energy_of_the_substrate(eV)	2.0	2.0
Surface_binding_energy_of_the_film(eV)	0.8	0.8

The figure below shows the composition of the final structure. You can easily see the succession of the Si/Mo layers.

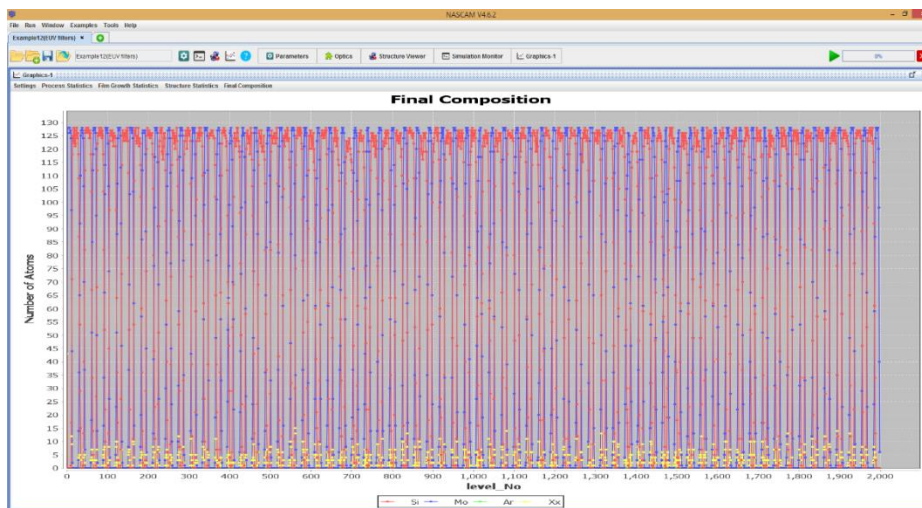


**Figure 42: The final composition of the deposited structure: 131 layers of Si and Mo deposited alternatively.**

After finishing the Monte-Carlo simulation, run the optical plugin called *Optics* with the Maxwell-Garnett model (MG) using the parameters shown below.

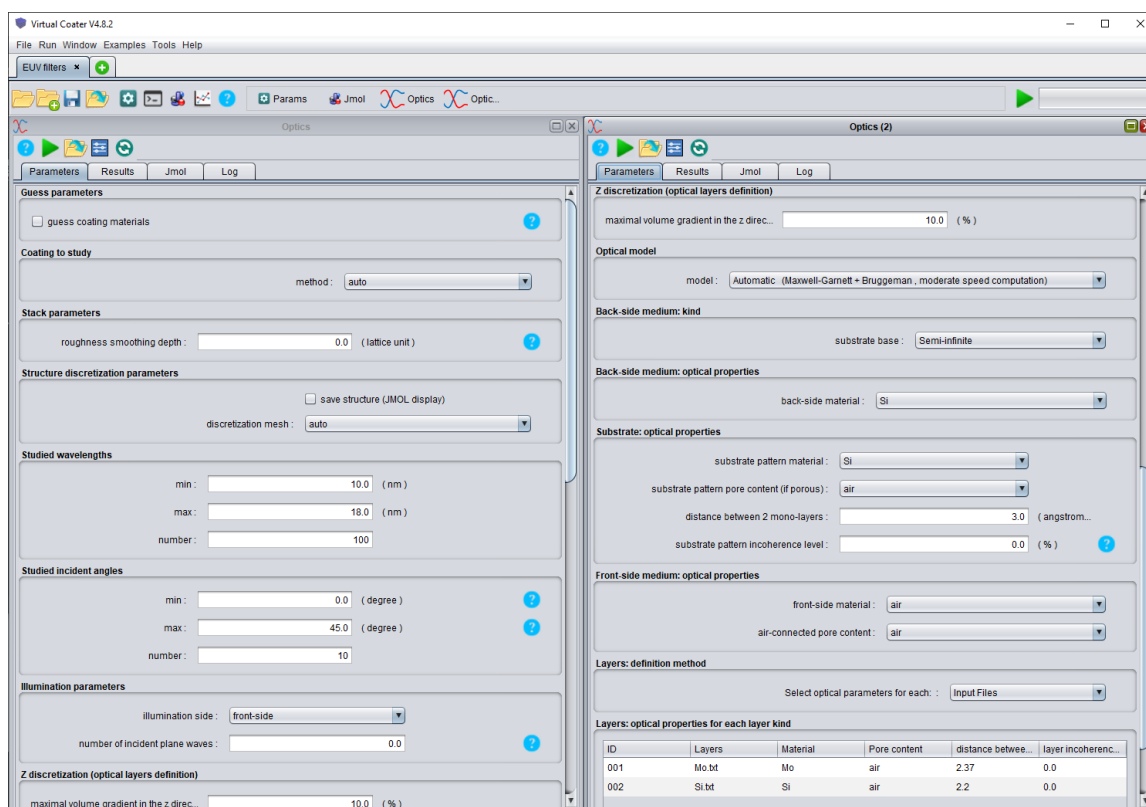


**Figure 43: The parameters frame of the *Optics* plugin.**

Figure 44 shows the experimental results from the cited paper (ref. 4), while the *Optics* plugin results corresponding to the simulated structure are shown in Figure 45.

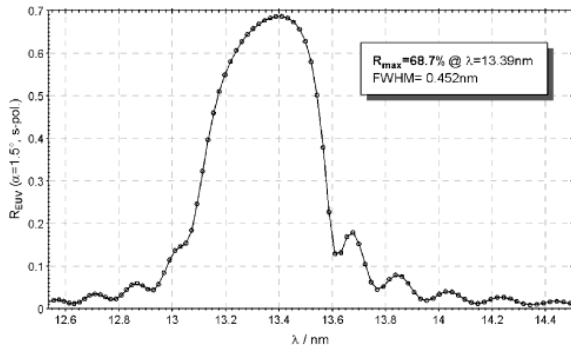


**Figure 44: EUV reflectivity of pure Mo/Si-multilayers (dperiod = 6.82 nm, = dMo/dperiod = 0.39, number of periods N = 65) prepared by MSD (Figure 1 in ref. 4).**

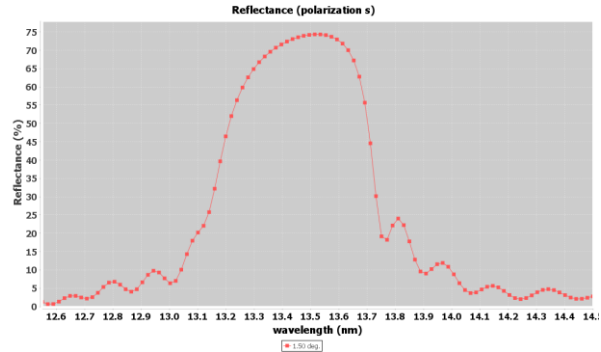


**Figure 45: EUV reflectivity of simulated deposition of Mo/Si-multilayers and computed by the Optics plugin.**

You will notice the very nice agreement between the simulated structure reflectance spectra and the experimental results (see above). There is a shift of about 0.1 nm only, but with a little wider peak. The total reflectance is almost the expected one for the real MSD experiment. The difference may be due to layer and interface thickness variations from experimental data.

### 14.2 Visible filters

In this work, we will study the case of a dielectric Bragg mirror in the visible spectral range composed by a TiO<sub>2</sub>(50nm)/SiO<sub>2</sub>(81nm) 10-layered coating optimized to have a maximal reflectance at a wavelength of 500nm. The mirror will be deposited on a 3mm glass substrate.

We first simulated a continuous deposition process consisting of 10 elementary deposition steps without taking diffusion into account. Each deposition step corresponds to a single metallic specie deposition in an oxygen atmosphere. Si and Ti were deposited alternatively.

All relevant parameters, corresponding to each elementary deposition step are given below:

	Specie: SiO <sub>2</sub>	Specie: TiO <sub>2</sub>
Simulation_options	1000 0 0	1000 0 0
Substrate_type	0	0
Dimensions	20 20 20 107600 0.0	20 20 20 60480 0.0
Deposition_rate(ML/s)	0.1	0.1
Specie: Metal	1.0 Si 28.085 2 0.5 xxx.txt 1 0.0 0.0 20.0 xxx.txt	1.0 Ti 47.867 2 0.5 xxx.txt 1 0.0 0.0 20.0 . xxx.txt

Specie:Reactive	20.0 O 15.999 2 0.03.txt 2 0.0 0.0 0.0 xxx.txt	20.0 O 15.999 2 0.03 xxx.txt 2 0.0 0.0 0.0 xxx.txt
-----------------	--	--

Figure 46 shows the composition of the final structure. You can easily see the succession of the SiO<sub>2</sub>/TiO<sub>2</sub> layers.

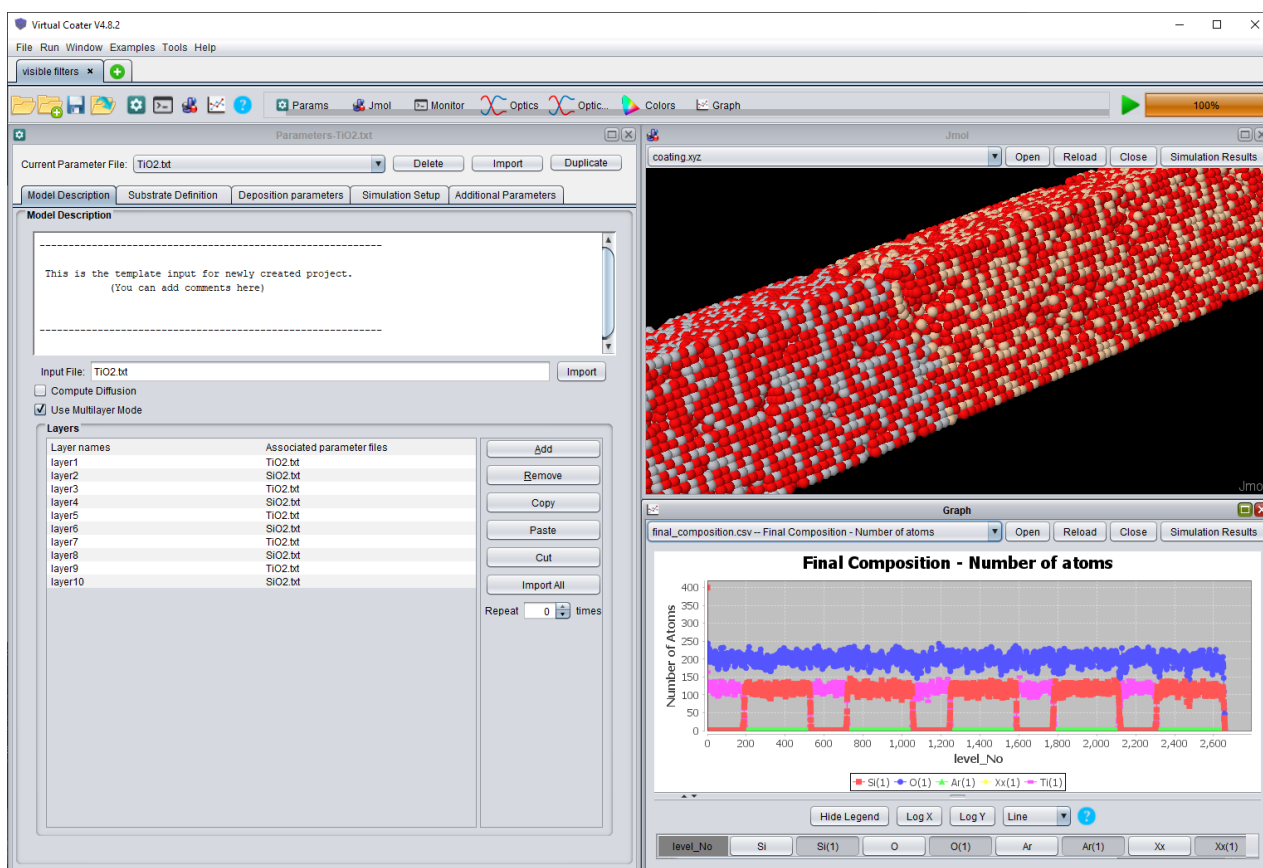


**Figure 46: The final composition of the deposited structure: 10 layers of SiO<sub>2</sub> and TiO<sub>2</sub> deposited alternatively.**

After finishing the Monte-Carlo simulation, run the optical plugin called *Optics* with the Maxwell-Garnett model (MG) using the parameters in Figure 46. Due to the high thickness of the 3mm glass substrate (slab), you will have to consider it as an incoherent layer (set the incoherence level of the slab at 100% and the number of incident planewaves at 25), but the TiO<sub>2</sub> and SiO<sub>2</sub> layers must be modelled as coherent one (incoherence level = 0%)

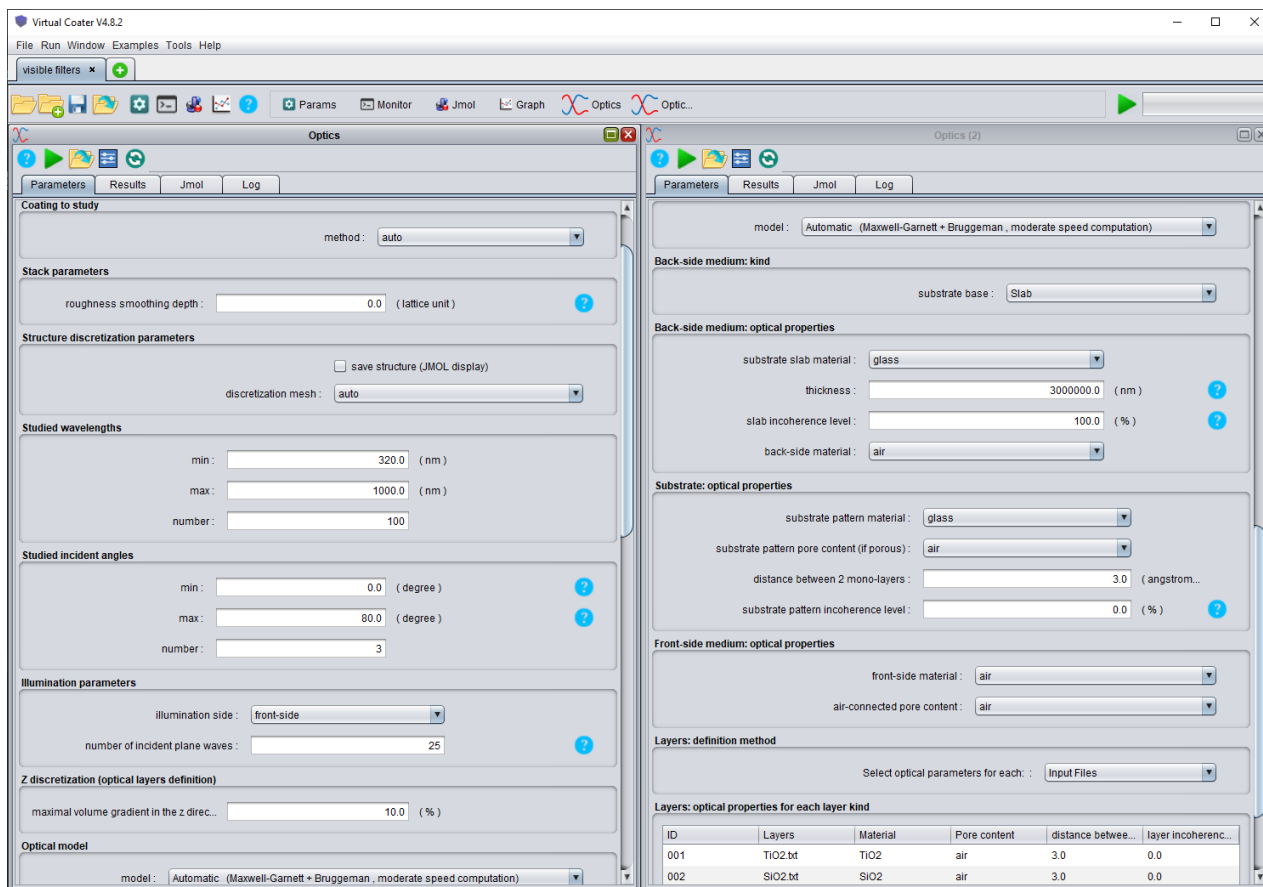


Figure 47: The parameters frame of the *Optics* plugin.

Figure 48 shows the reflectance of the mirror provided by the *Optics* plugin for 3 different incidence angles (0°, 40° and 80°). Two situations are shown here. The first one (left) is obtained while considering the 3mm glass slab below the coating as coherent, which explain the unphysical narrow oscillations. In the second one (right), the glass slab is considered fully incoherent, which allows to solve the error.

Finally, thanks to these reflectance spectra, it is possible to predict the color of such dielectric mirror as shown in Figure 48 (right) for each incidence angle.

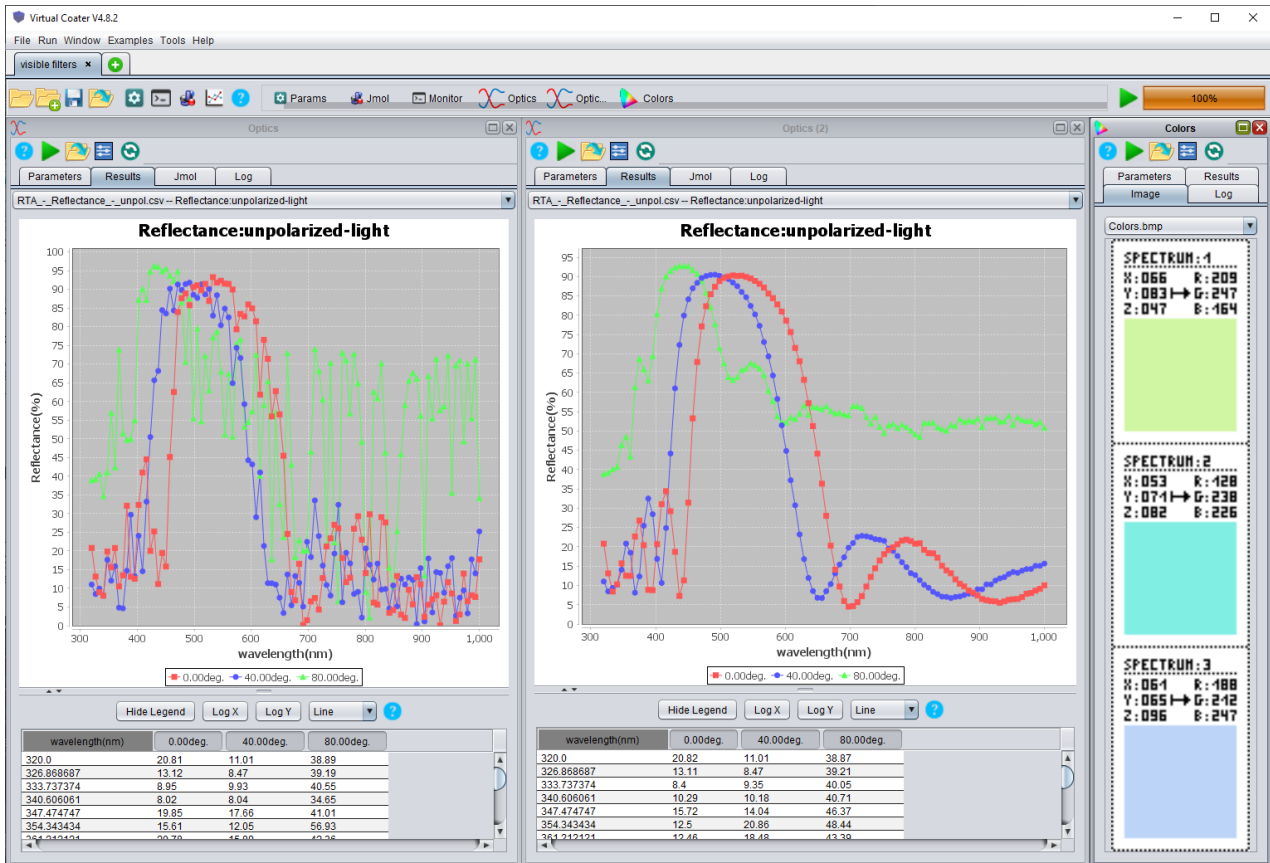


Figure 48: Reflectance for different incident angles of TiO<sub>2</sub>/SiO<sub>2</sub> 10-layers coating on 3mm glass substrate supposed to be coherent (left) or incoherent (right), and corresponding colors.

## 15 Example 13: Optical incoherent layer

This example was inspired by the paper of Troparevsky et al. [5]. In this work, the cited authors studied the influence of light coherence on thick silicon simple layers.

The NASCAM parameters, described in the table below, are set to obtain a highly dense Si layer with a thickness of 150nm approximately.

Specie: Si	
Simulation_options	1000 0 0
Substrate_type	0
Dimensions	40 5 800 128143 0.0
Deposition_rate(ML/s)	1
Specie:Metal	2.0 Si 28.085 2 10.0 E_Metal.txt 1 0 0 20 A_Metal.txt
Specie:Neutral	0.0 Ar 39.948 ...
Specie:Substrate	Si 28.1
Surface_binding_energy_of_the_substrate(eV)	1.0
Surface_binding_energy_of_the_film(eV)	2.0

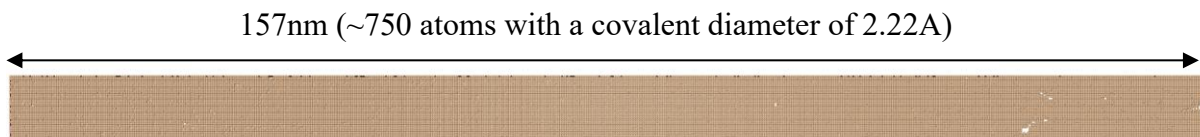


Figure 49: Final structure of the Si deposition (lateral view).

Now, the purpose consists in computing the transmittance of such a structure while considering it as a coherent or incoherent layer. The main difference between the two situations is defined in the "Illumination parameters" and the "layer optical properties" tabs, as shown in Figure 50:

- For a coherent layer: set the incoherence level to 0. Then, just one incident planewave is enough to do the computation.
- For an incoherent layer: set the incoherence level to 100%. Then, several incident plane-waves are needed to mimic an incoherent light (usually about 50).

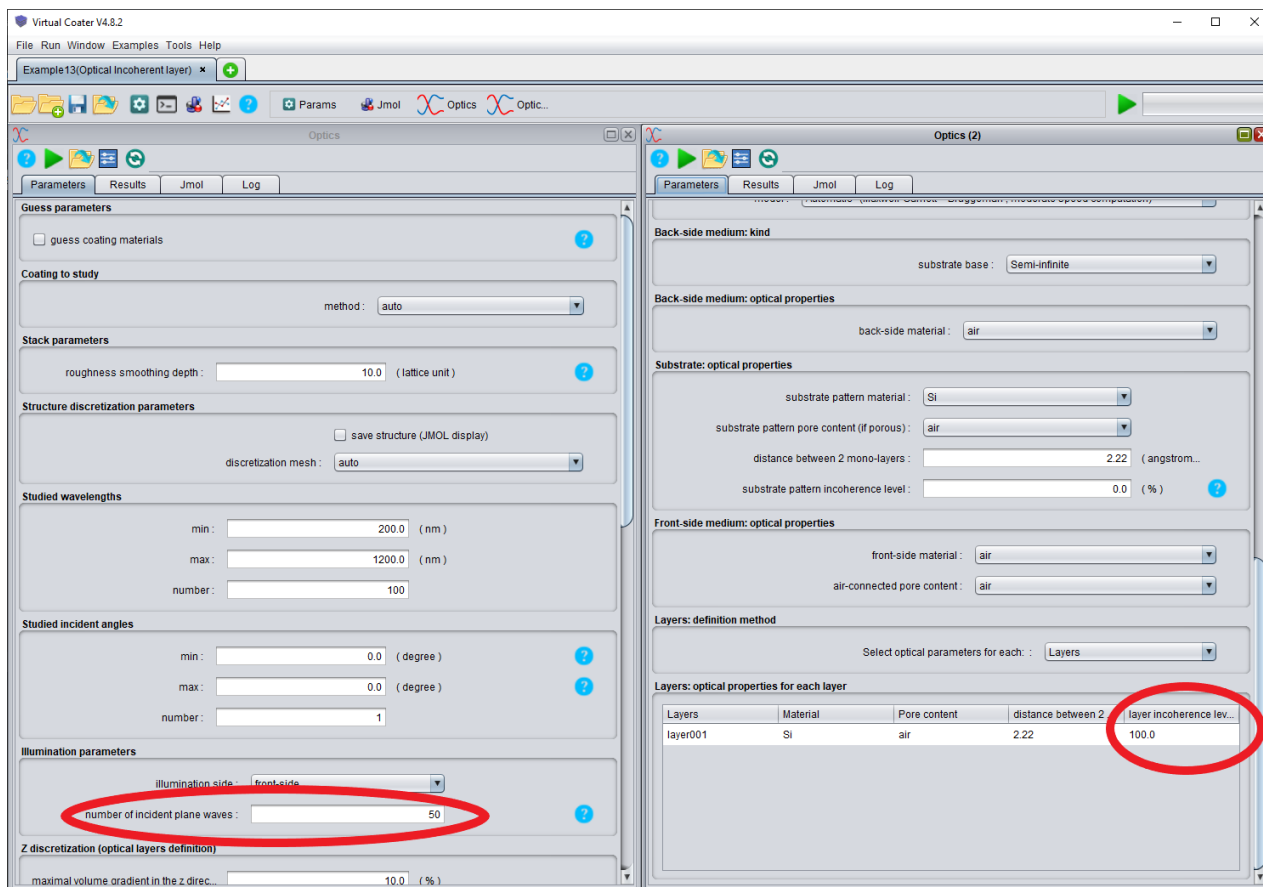


Figure 50: Optics parameters

Figure 51 and Figure 52 shows the comparison of the transmitted light (for coherent and incoherent layers) given by literature [5] and by the *Optics* plugin. For your information, it is possible to display the color of such transmitted light by using the *Colors* plugin (then, load the file “*RTA\_-\_Transmittance\_-\_unpol.csv*” stored in the *Optics* plugin folder).

We can observe a good agreement in the case of a coherent layer. However, for incoherent layer, the transmittance given by the *Optics* plugin seems overestimated (about 15%). This difference is due to the Si layer roughness provided by NASCAM, reducing the reflectance and then increasing the transmittance (given that the Si presents a low absorbance in the visible and IR spectra).

By playing with the “*roughness smoothing depth*” parameter of the *Optics* plugin, it is possible to smoothen the top surface of the Si layer by removing the 10 last monolayers. Then, set this parameter to 10 and relaunch the simulations (for coherent and incoherent layer).

As shown in Figure 53 the match between literature and the NASCAM simulations is almost perfect.

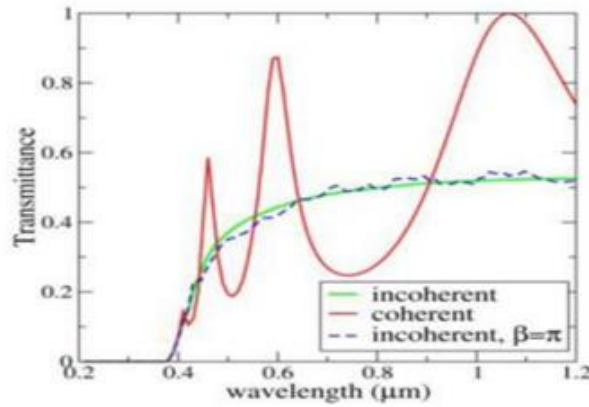


Figure 51: Transmitted light for a Si film of 150 nm thickness: coherent and incoherent transmittance spectra for a perfectly flat and homogenous Si film from [5].

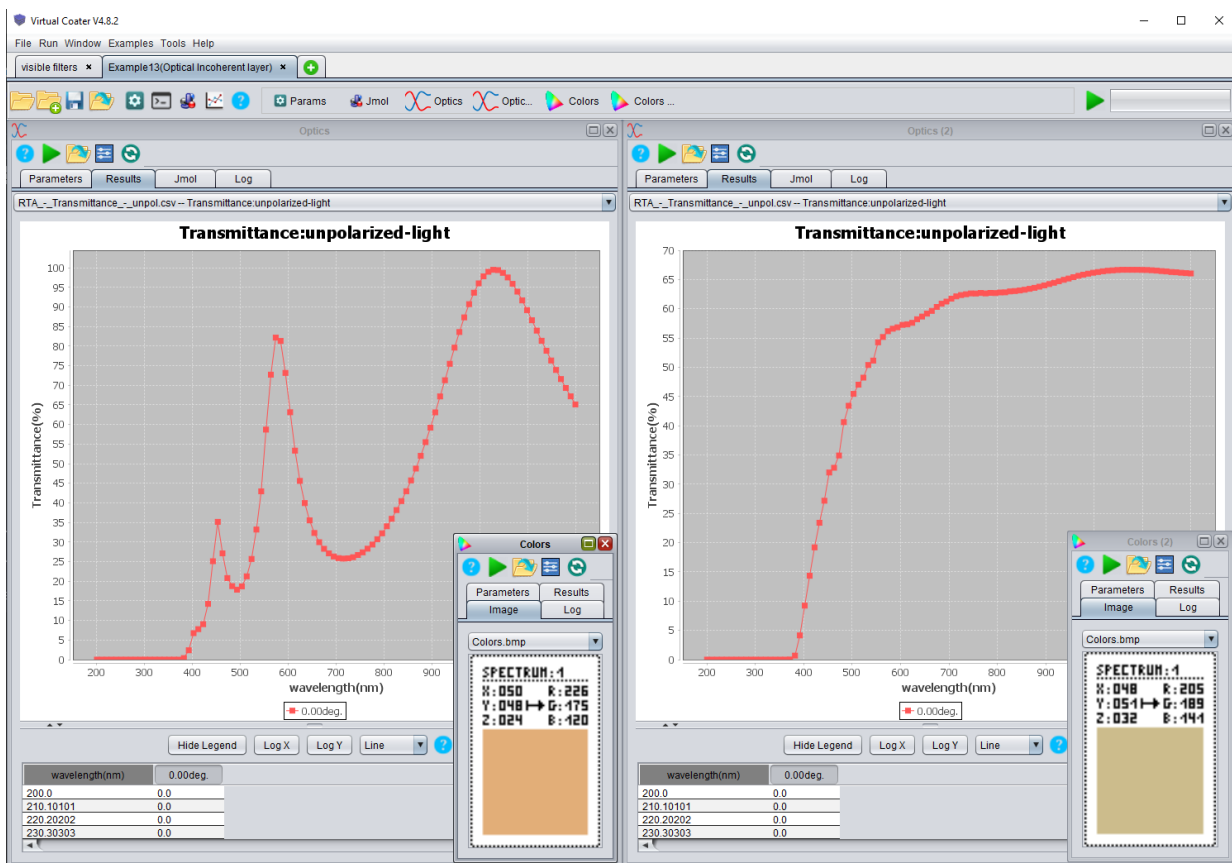
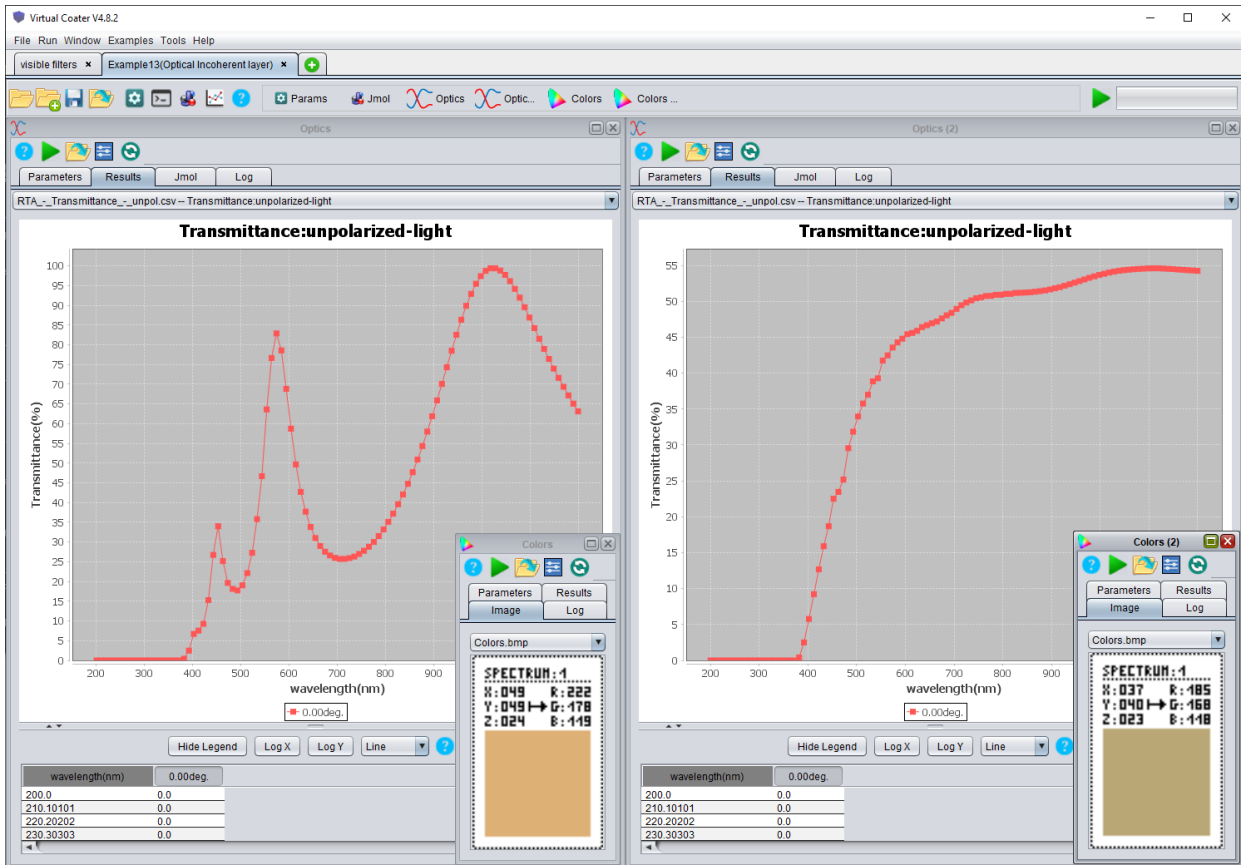


Figure 52: Transmitted light for a Si film of 150 nm thickness. Coherent (left) and incoherent (right) transmittance spectra computed by the *Optics* plugin for a rough Si film, and their corresponding colors (if illuminated by sunlight – D65)



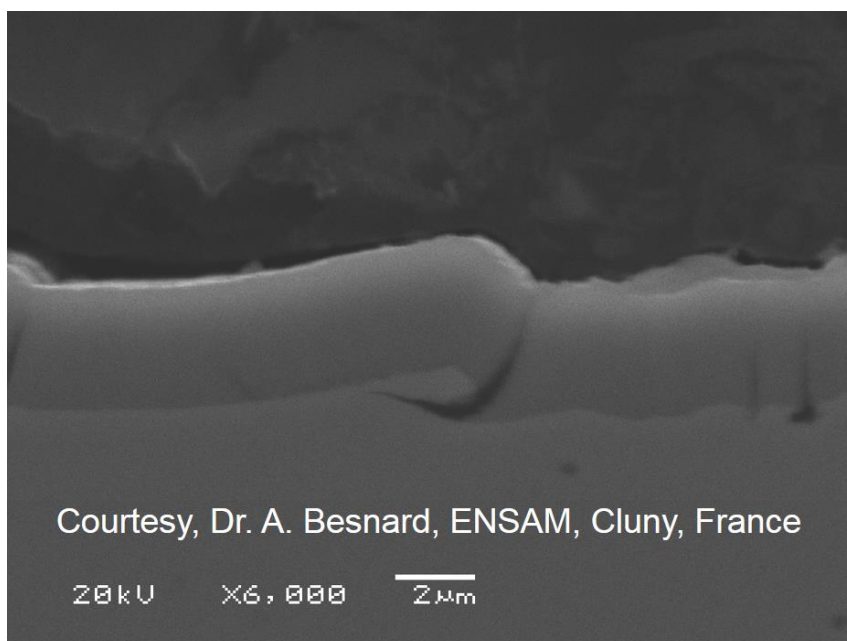
**Figure 53: Transmitted light for a Si film of 150 nm thickness. Coherent (left) and incoherent (right) transmittance spectra computed by the *Optics* plugin for a flat Si film, and their corresponding colors (if illuminated by sunlight – D65)**

## 16 Example 14: SEM cross-section substrate

In this example, we digitalized an SEM cross-section image of a substrate with a particular feature. Cu is deposited on Fe. Others parameters are given in the table below.

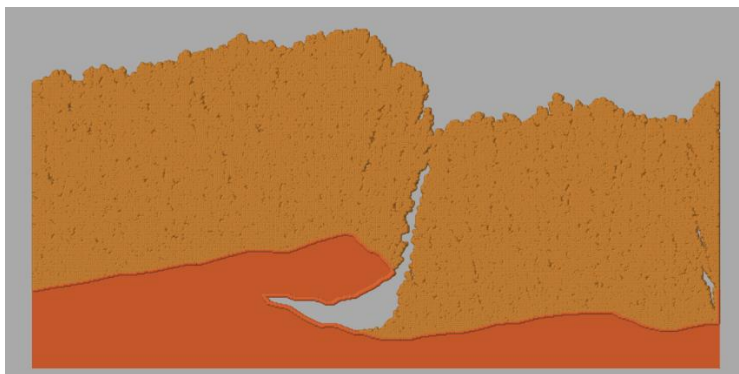
Simulation_options	1000 0 0
Substrate_type	0
Dimensions	620 4 100 350000 0.0
Deposition_rate(ML/s)	0.1
Specie: Metal	2.0 Cu 63.546 2 2.0 E_Metal.txt 1 0.0 0.0 15.0 A_Metal.txt
Specie: Neutral	0.0 Ar 39.948 ...
Specie: Substrate	Fe 55.845
Surface_binding_energy_of_the_film(eV)	1.0

The substrate is generated by the *MakeSubstrate* plugin, which uses a digitalized SEM film image (see Figure 54). The details about how to digitalize the image and to use the plugin are given in the NASCAM Plugins Manual (*Nascam\_plugins.pdf*).



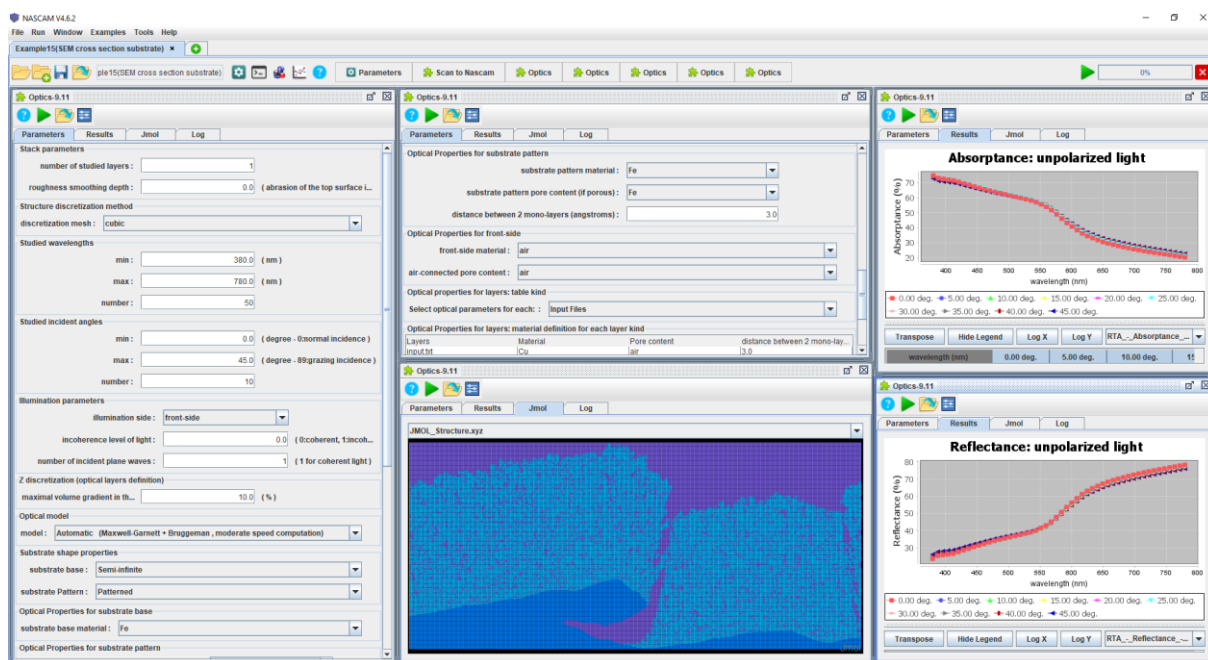
**Figure 54:** A cross-section of a Cu film deposited on a Fe substrate with a particular feature. You can see a crack in the film near the feature.

Figure 55 shows the simulation results.



**Figure 55: Simulation of Cu deposition on a Fe substrate. The substrate was digitalized from a SEM image shown above.**

Then, it can be interesting to study the optical behaviour of such a structure. First, open the *Optics* plugin and launch the computation to obtain the layer reflectance in the visible range (from 380nm to 780nm) for different incidence angles. All the input parameters and the results are shown in Figure 56.



**Figure 56: The *Optics* plugin window: computation of the reflectance, transmittance and absorbance. Left and top-middle: parameters. Bottom-middle: studied structure after reconstruction (artificial species!). Right: absorbance and reflectance of the structure.**

The last step consists in deducing the colour of the structure thanks to the reflectance spectra computed by the *Optics* plugin. For that, open the *Colors* plugin, load the reflectance spectra file (stored in the *Optics* plugin output folder) and launch the simulation. Figure 57 shows the results.

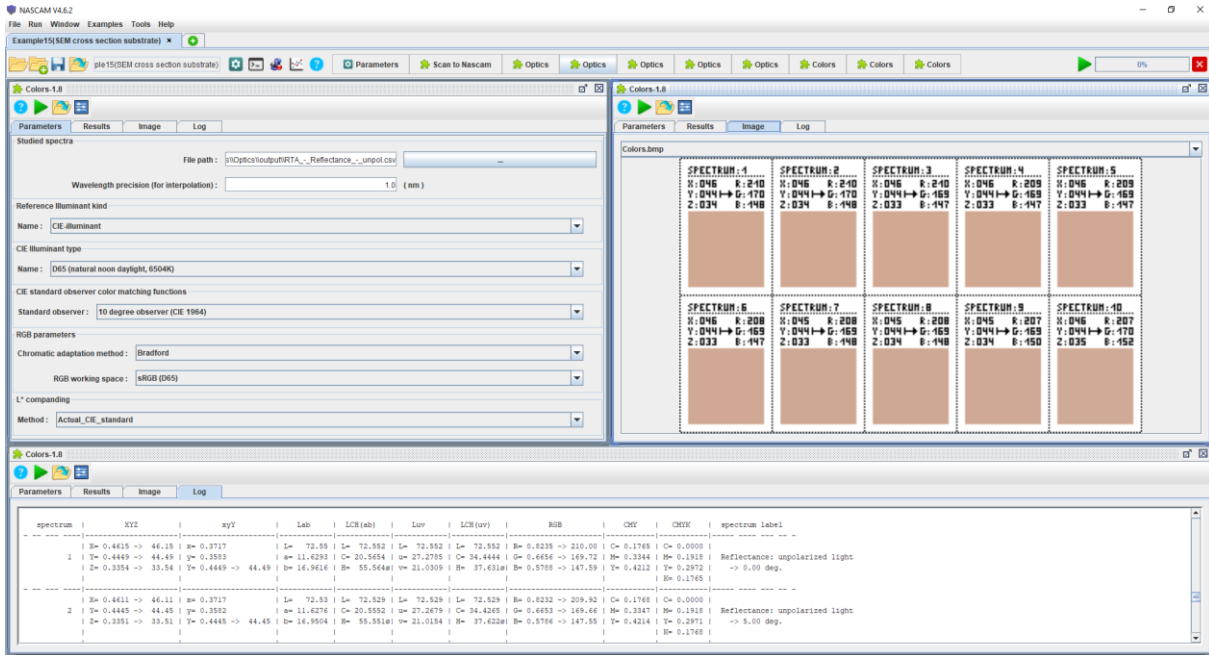


Figure 57: The Colors plugin window: computation of the colour of the light reflected by the structure (see Figure 56) illuminated by sunlight (for several incident angles). Left: input parameters ; Bottom: log display of the computed colour space coordinates ; Right: colour displays.

## 17 Example 15: Thermal conductivity

For the illustration we will give examples of calculations of the thermal conductivity for multi-layer TiN/TiAlN film (experimental details see M.K. Samani et al, Thermal conductivity of titanium nitride/titanium aluminum nitride multilayer coatings deposited by lateral rotating cathode arc, [Thin Solid Films 578 \(2015\) 133–138](#)). Experimental results are given in Figure 58.

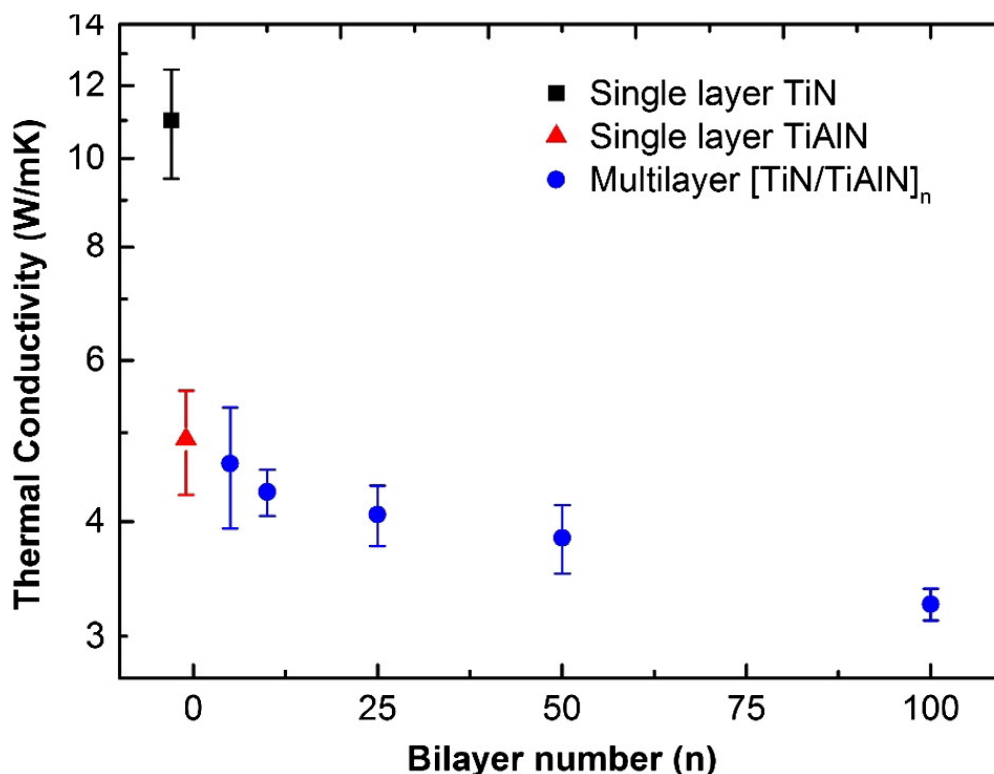


Figure 58: Thermal conductivity of the as-deposited TiN, TiAlN single layers and [TiN/TiAlN]<sub>n</sub> multilayer coatings.

For the examples two cases were chosen, with number of bilayers  $n=5$  and  $n=10$ . Firstly, it is necessary to setup NASCAM simulation for cases of multilayer deposition. To simulate such a film one has to simulate deposition  $N = 4*n-1$  single layers. This number is easy to understand if one takes into account that the structure of the film is as follow:

```
TiN/Interface/TiAlN/interface/
TiN/interface/TiAlN/interface/
.../
TiN/interface/TiAlN/interface/
TiN/interface/TiAlN/
```

Therefore, for each bilayer it is necessary to simulate 4 single layers, except for the last bilayer, where there is no last interface layer. Figure 59 illustrates the simulation setup and results of the simulations for number of bilayers equals to 5.

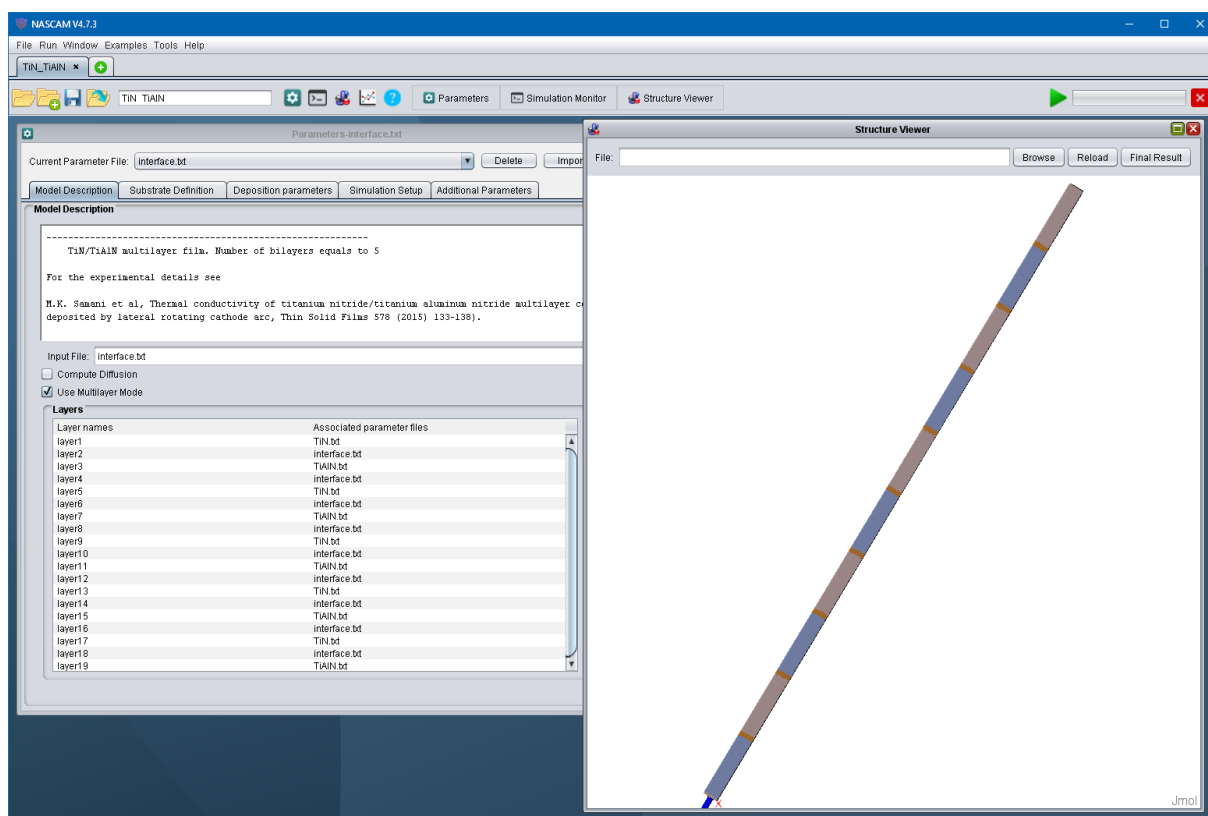


Figure 59: Simulation of deposition of 5 bilayers of TiN/TiAlN.

On completing film growth simulation one can start calculation of the thermal conductivity of the film, see Figure 60.

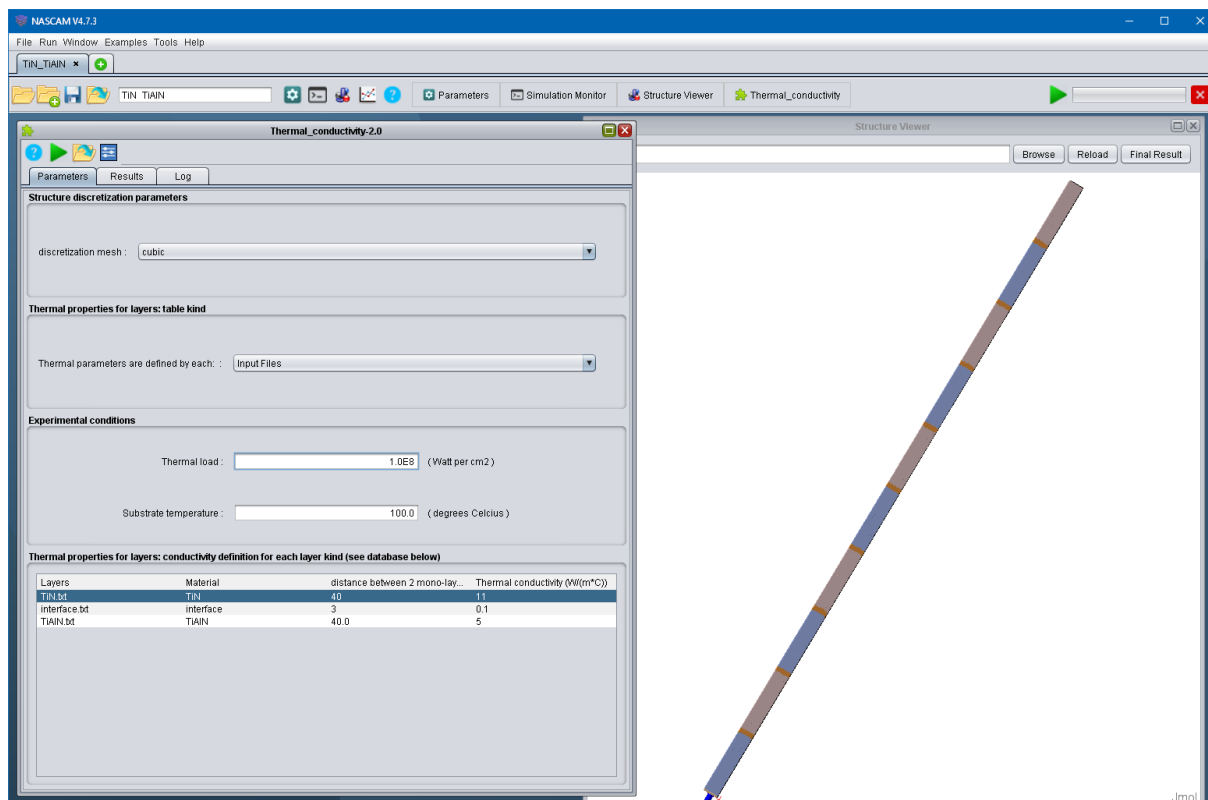
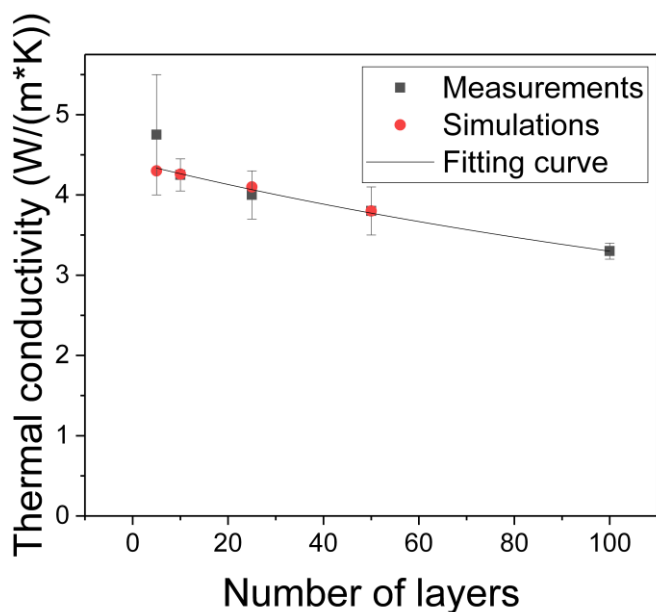


Figure 60: Input parameters for Thermal plugin. Important input parameters are marked by red.

To start the calculations it is necessary to set up thermal conductivity of each layer and thickness of each layer. In addition, to get a temperature profile it is necessary to set the thermal load and substrate temperature.

Although there are 19 deposited layers in the example it is not necessary to set the data for each layer as the data for all TiN layers, TiAlN layers and interface layers are the same. For this reason, one should set up the data only three times, for each kind of deposited layers. Obviously, there are 3 different kind of deposited layers in the example, that’s why there are only three lines in the input table for the thermal properties of the materials.

Setting up of the layer thickness should be done as follow. The idea is to scale up the thickness of a simulated layer to the real thickness of a sample. The scaling is a necessary step as usually the simulation are not capable to reproduce experiment 1:1. Therefore, it is necessary to find the ratio of experimental thickness in nm to simulated thickness, which is expressed in number of deposited monolayers. This value should be used as “distance between two monolayers” for the corresponding simulated deposited layer.



**Figure 61: Experimental values of thermal conductivity of TiN/TiAlN multi layer film and values simulated by Thermal plugin and calculated by Eq. 3**

Equation 3 may be used to estimate thermal resistance of the interfaces. The value of the thermal resistance may be evaluated to get the best fit to the experimental data. This procedure gives  $r = 3.66 \cdot 10^{-4} \text{ m} \cdot \text{K} / \text{W}$ . It is necessary to note that it is the thermal resistance of the interfaces that results into the decrease of the thermal conductivity of the film with the increase of the number of bi-layers TiN/TiAlN. In addition, we have to mention the best agreement to the experimental data was obtained when the values of thermal conductivities of TiN and TiAlN monolayers were taken about 1.5 times less than they were measured. The correction to the experimental values required additional considerations.

## 18 Example 16: Mesh substrate from step file

In this example, the idea is to deposit a thin film of copper on complex shape substrate generated by Gmsh and MakeSubstrate.

First, you have to generate the substrate tanks to the *MakeSubstrate* plugin. It will be done in several steps:

- generate the msh file by using the Gmsh software: here, it will be done by working directly with the step file "step\_file\_example.step" located in the folder "geometry" of this example. For more details about how to use Gmsh, please refer to the NASCAM Plugins Manual (*Nascam\_plugins.pdf*), section MakeSubstrate.

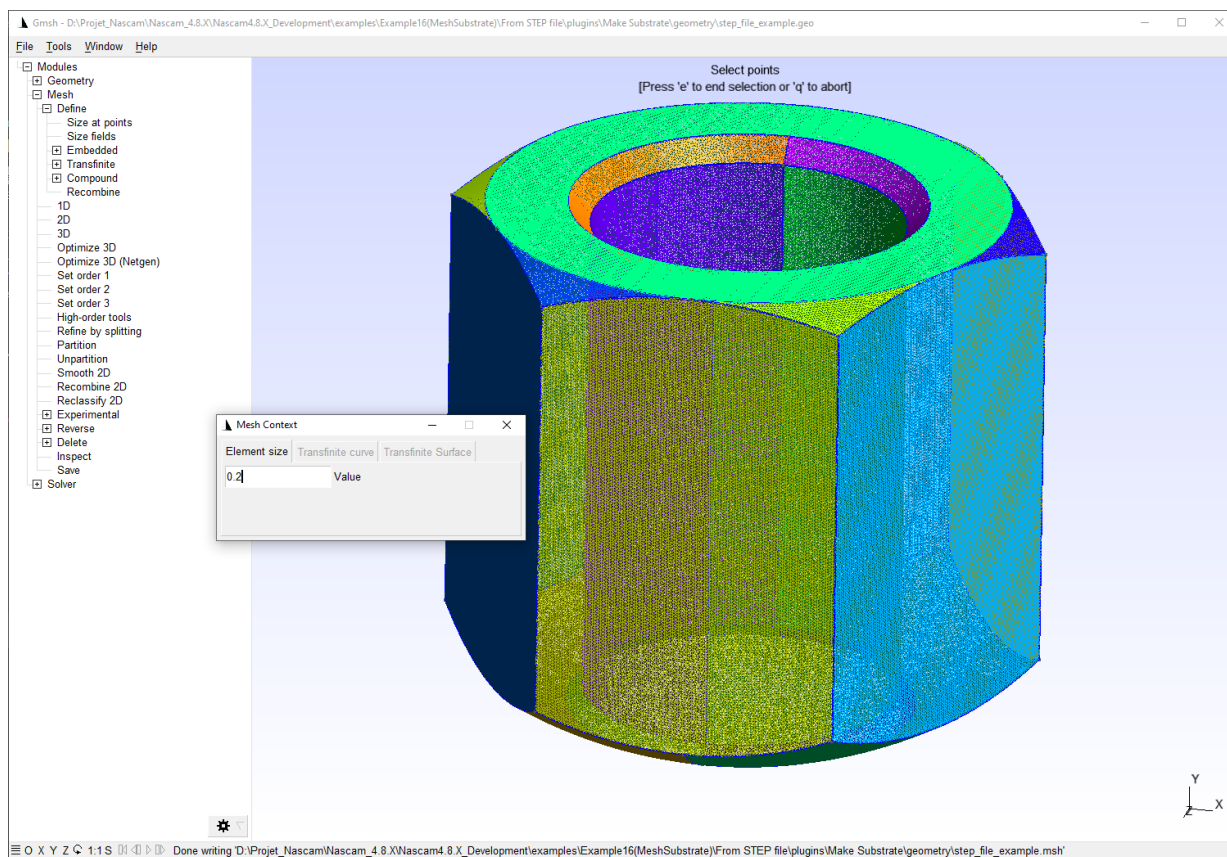


Figure 62: step file to mesh file conversion with Gmsh.

- then, you can convert the msh file to generate a substrate compatible to NASCAM by using the plugin MakeSubstrate

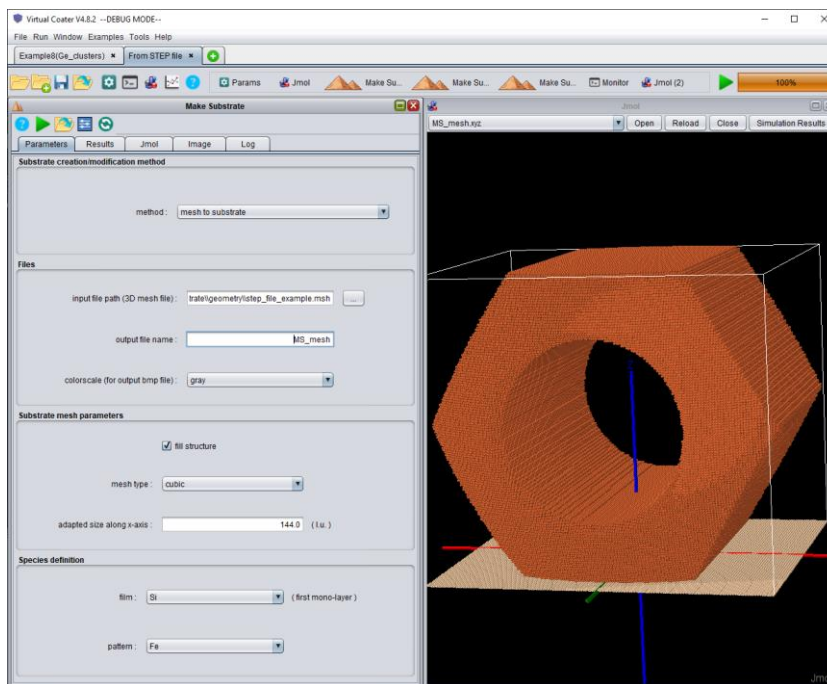


Figure 63: msh to NASCAM substrate conversion.

- if needed, it is possible to rotate the substrate:

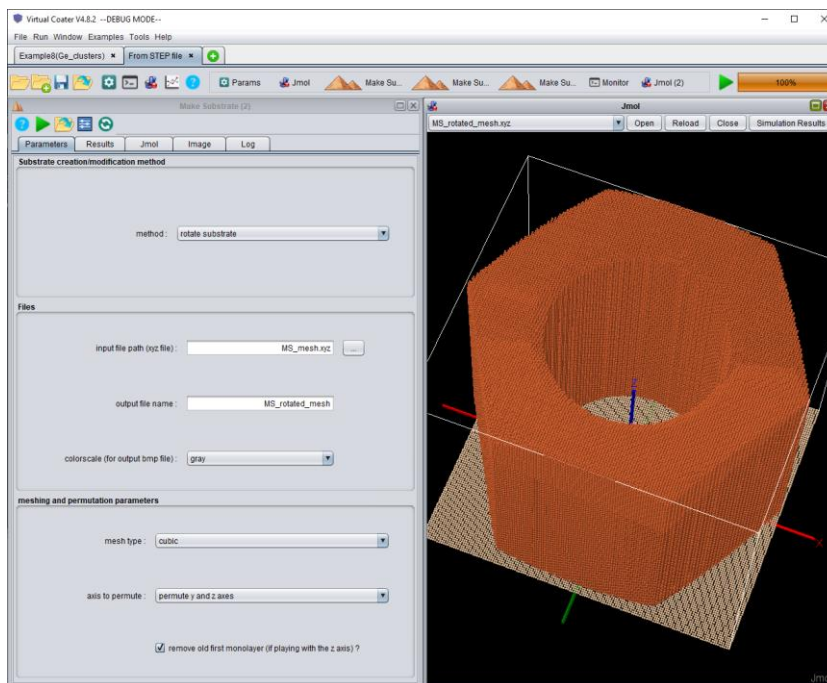


Figure 64: rotation of the substrate.

- if needed, it is possible to extend the substrate in the x and y directions to reduce the influence of the periodic boundary conditions.

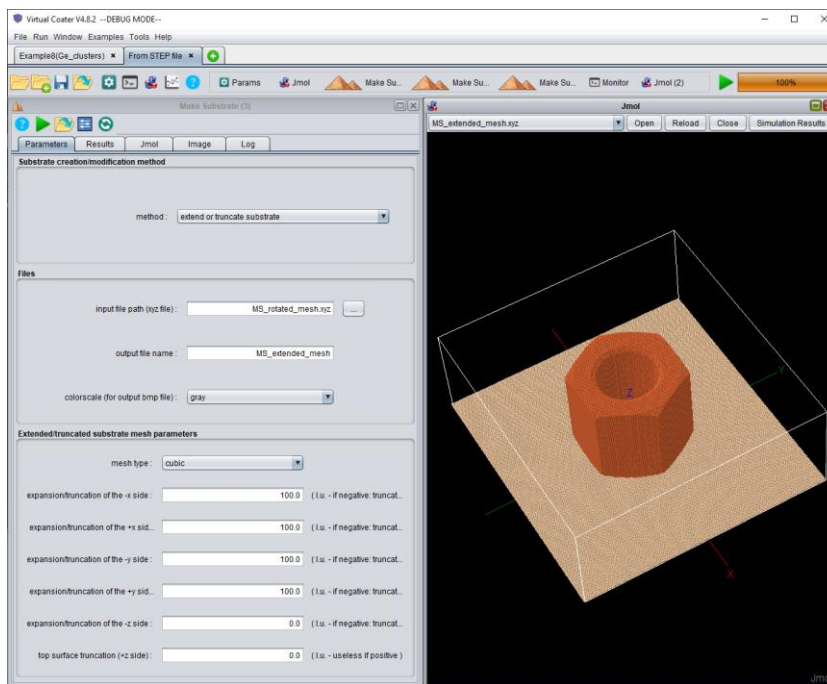


Figure 65: extension of the substrate.

Then, you can load the substrate in the "Substrate Definition" tab of the NASCAM parameters. Other deposition parameters are given in the table below.

Simulation_options	1000 0 0
Substrate_type	0
Dimensions	345 326 132 1000000 0.0
Deposition_rate(ML/s)	0.1
Specie: Metal	1.0 Cu 63.546 2 2.0 E_Metal.txt 1 0.0 0.0 15.0 A_Metal.txt
Specie: Neutral	0.0 Ar 39.948 ...
Specie: Substrate	Fe 55.845
Surface_binding_energy_of_the_film(eV)	1.0

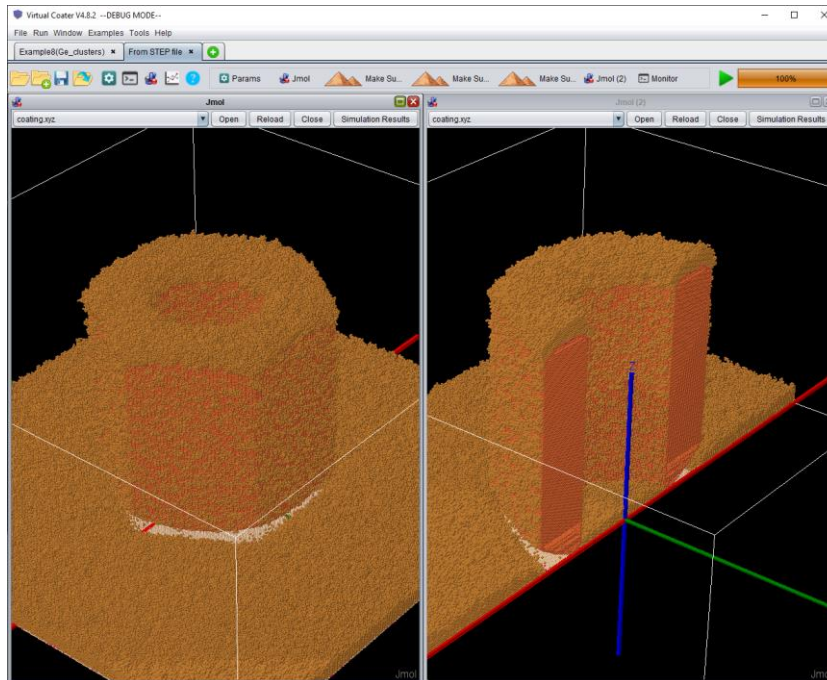
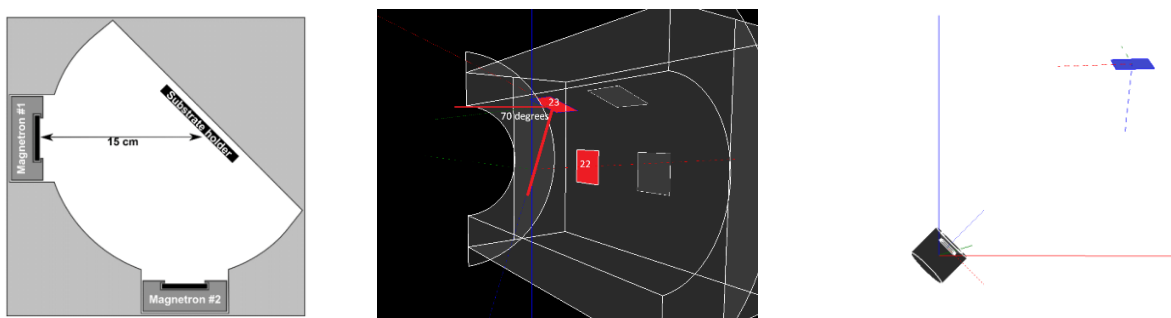


Figure 66: coated object with Cu thin film.

## 19 Example 17: Dual Magnetron

The example demonstrate simulation of TiO<sub>2</sub> film growth by means of reactive sputter deposition in a system with two magnetrons. The magnetrons have Ti targets and fluxes from the targets to a substrate are calculated with a help of **Simulate Magnetron** plug-in, see for details *Plugin Manuals*, chapter 4.

Geometry of the system is shown in Figure 67. Two magnetrons are positioned on the left and on the right from the center of a substrate holder and look at it at the angle of 45 degrees. The substrate of the interest, 23, is additionally tilted at 70 degrees.



**Figure 67: From left to right: mutual positions of magnetrons and substrate holder; substrate holder with positions of several substrates; one of the magnetrons and Substrate 23**

To run the simulation it is necessary to setup the fluxes from both targets as well as an Oxygen flux to the substrate. The fluxes of Ti are calculated by **Simulate Magnetron** plug-in. Input parameters for **Simulate Magnetron** plug-in are shown in Figure 68. The details of the calculations are given in *Plugin Manual*. To setup Oxygen flux one has to set energy of Oxygen and to indicate that the angular distribution of incident Oxygen is uniform.

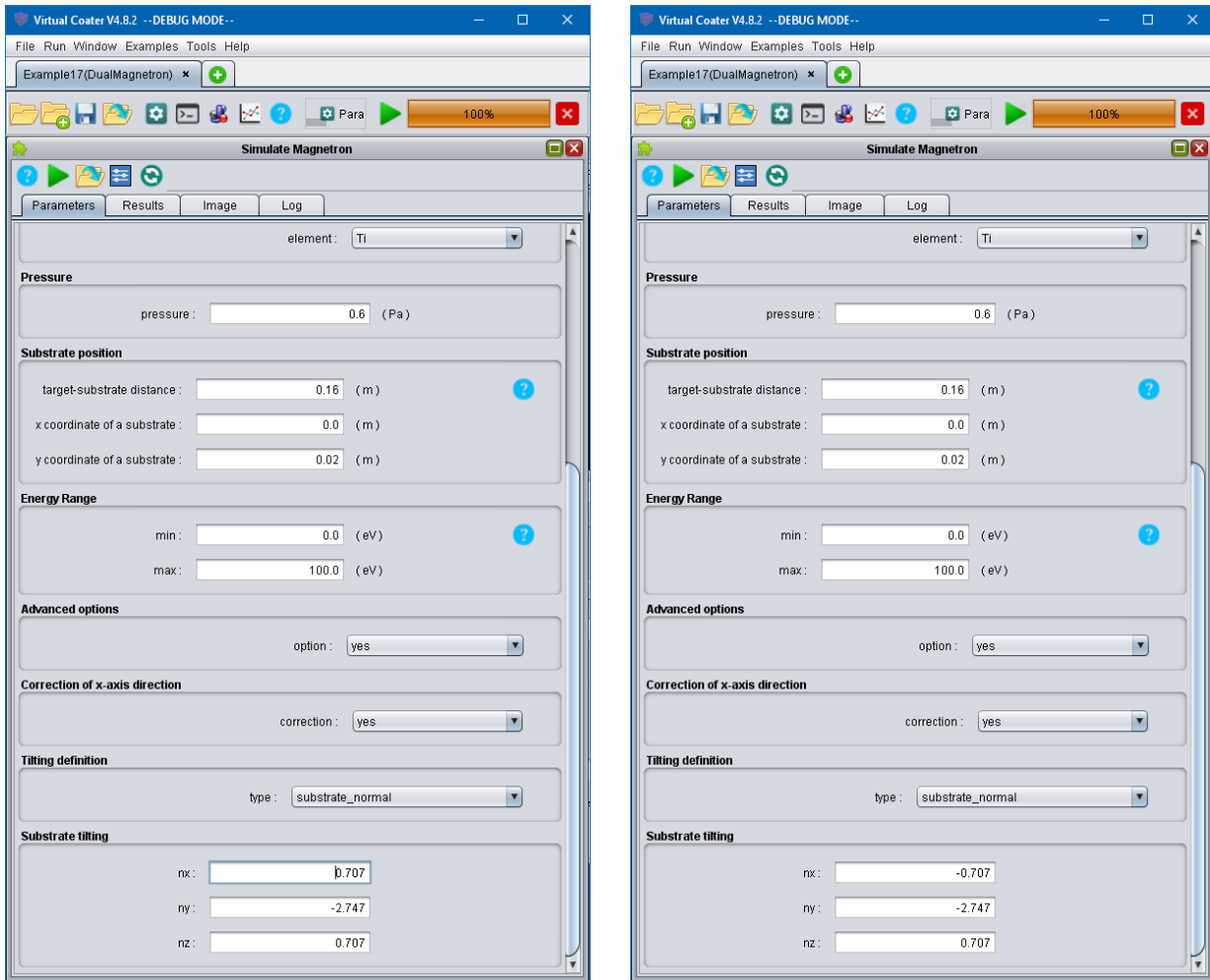
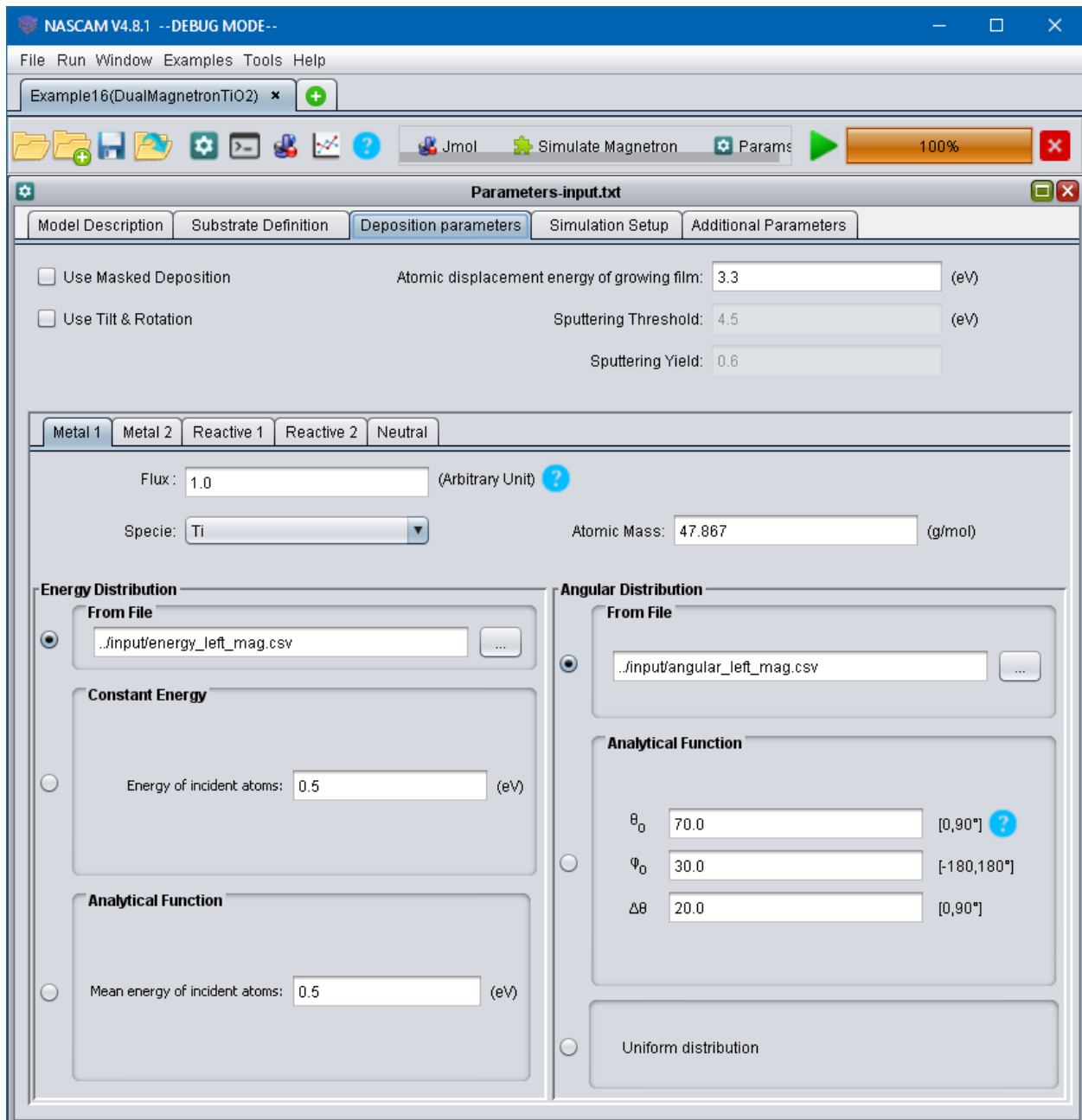


Figure 68: Setup of Magnetron Plug-in for dual magnetron system for each magnetron.

Input parameters for the Ti fluxes from both targets and for Oxygen are shown in Figure 69.



The screenshot shows the NAsCAM V4.8.1 software interface in debug mode. The main window is titled "Parameters-input.txt" and contains several tabs: "Model Description", "Substrate Definition", "Deposition parameters", "Simulation Setup", and "Additional Parameters". The "Deposition parameters" tab is active, showing the following settings:

- Use Masked Deposition
- Use Tilt & Rotation
- Atomic displacement energy of growing film: 3.3 (eV)
- Sputtering Threshold: 4.5 (eV)
- Sputtering Yield: 0.6

Below these are tabs for "Metal 1", "Metal 2", "Reactive 1", "Reactive 2", and "Neutral". The "Reactive 1" tab is selected, showing:

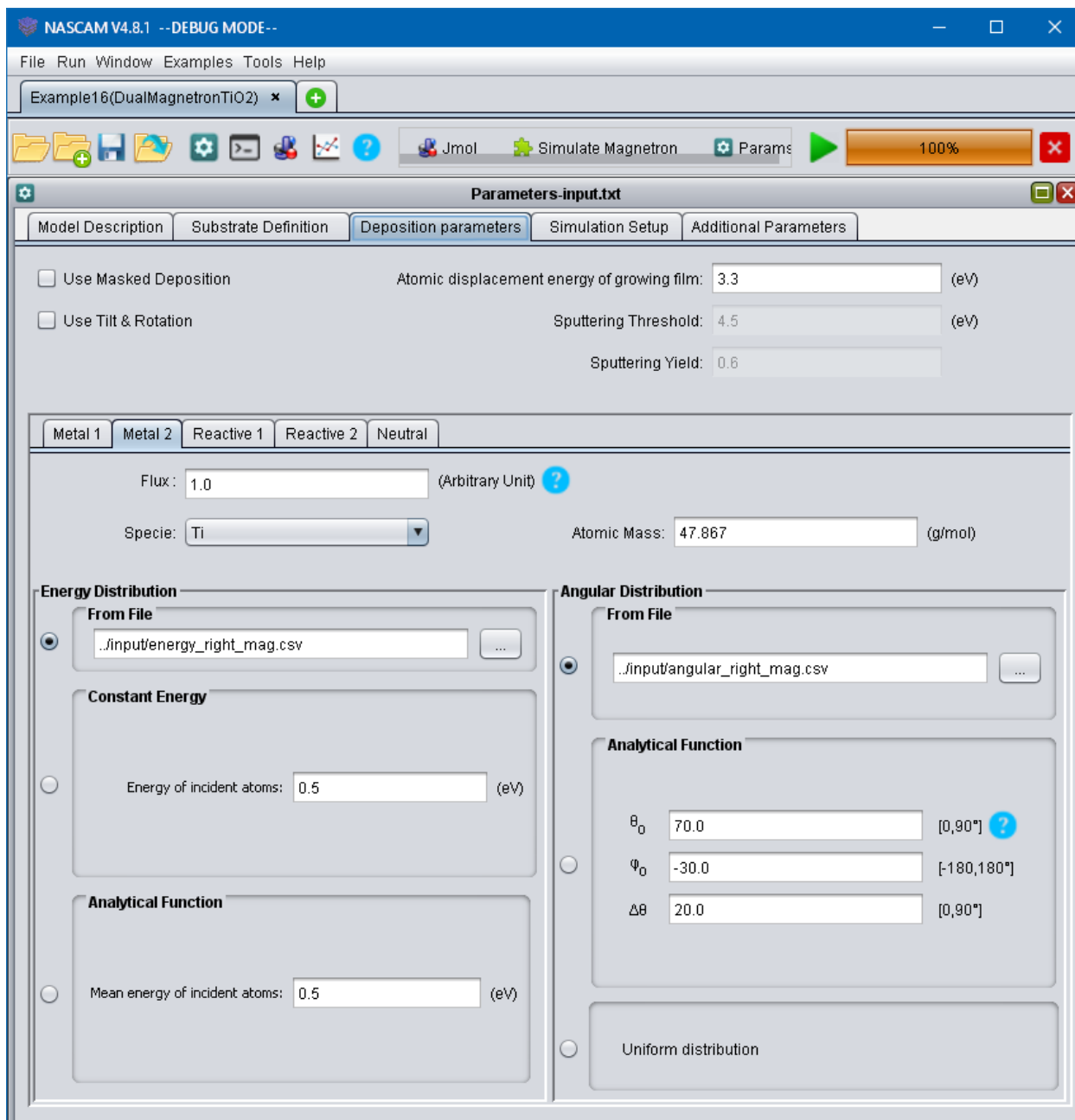
- Flux: 1.0 (Arbitrary Unit)
- Specie: Ti
- Atomic Mass: 47.867 (g/mol)

The "Energy Distribution" section has three options:

- From File: ..input/energy\_left\_mag.csv
- Constant Energy: Energy of incident atoms: 0.5 (eV)
- Analytical Function: Mean energy of incident atoms: 0.5 (eV)

The "Angular Distribution" section has three options:

- From File: ..input/angular\_left\_mag.csv
- Analytical Function:
  - $\theta_0$ : 70.0 [0,90°]
  - $\varphi_0$ : 30.0 [-180,180°]
  - $\Delta\theta$ : 20.0 [0,90°]
- Uniform distribution



The screenshot shows the NAsCAM V4.8.1 software interface in debug mode. The main window is titled "Parameters-input.txt" and contains several tabs: "Model Description", "Substrate Definition", "Deposition parameters", "Simulation Setup", and "Additional Parameters". The "Deposition parameters" tab is active and displays the following settings:

- Use Masked Deposition
- Use Tilt & Rotation
- Atomic displacement energy of growing film: 3.3 (eV)
- Sputtering Threshold: 4.5 (eV)
- Sputtering Yield: 0.6

Below these are tabs for "Metal 1", "Metal 2", "Reactive 1", "Reactive 2", and "Neutral". The "Reactive 1" tab is selected, showing:

- Flux: 1.0 (Arbitrary Unit)
- Specie: Ti
- Atomic Mass: 47.867 (g/mol)

The interface is divided into two main sections: "Energy Distribution" and "Angular Distribution".

**Energy Distribution:**

- From File:** Selected. File path: ..\input\energy\_right\_mag.csv
- Constant Energy:** Energy of incident atoms: 0.5 (eV)
- Analytical Function:** Mean energy of incident atoms: 0.5 (eV)

**Angular Distribution:**

- From File:** Selected. File path: ..\input\angular\_right\_mag.csv
- Analytical Function:**
  - $\theta_0$ : 70.0 [0,90°]
  - $\varphi_0$ : -30.0 [-180,180°]
  - $\Delta\theta$ : 20.0 [0,90°]
- Uniform distribution:** Unselected.

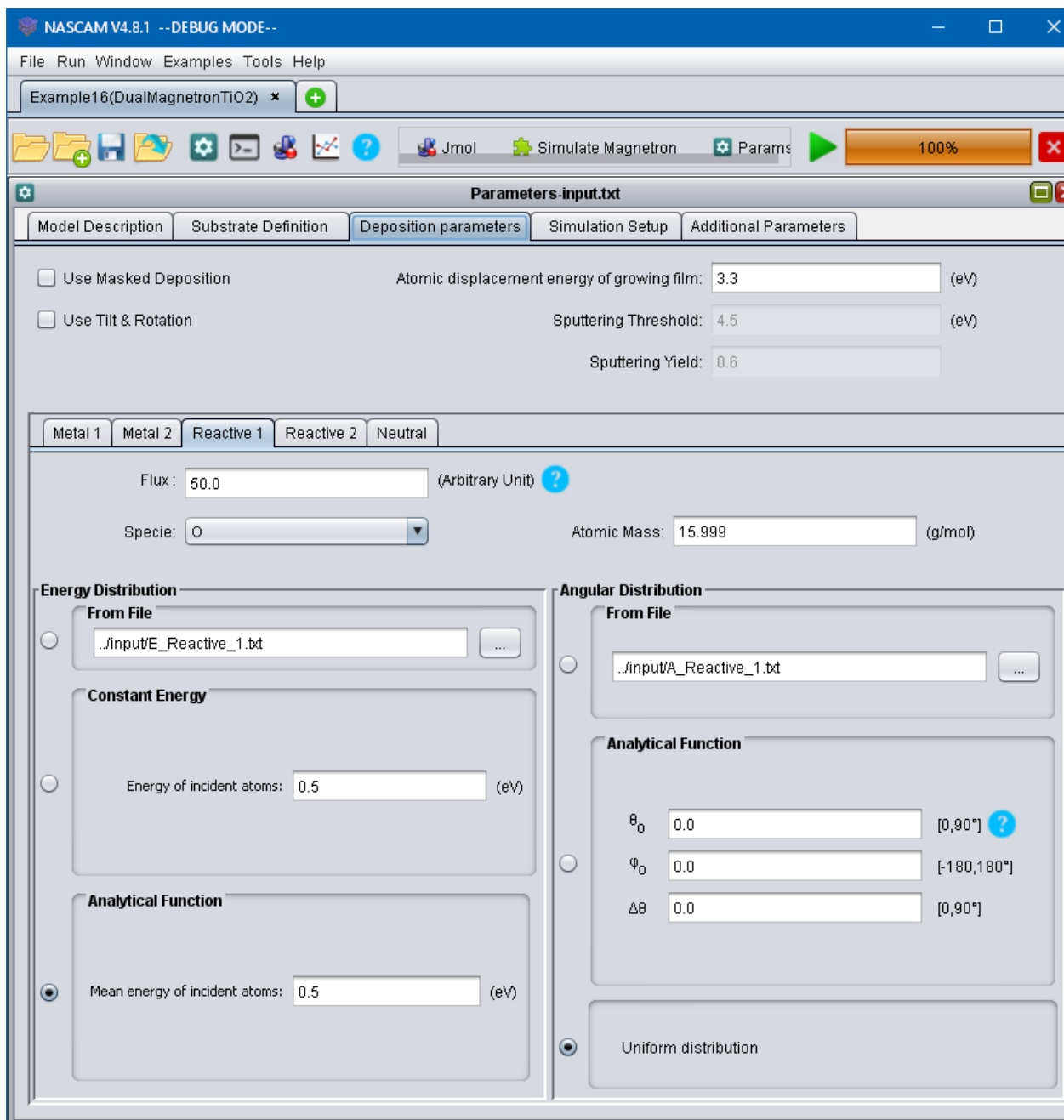


**Figure 69: Input parameters for the fluxes; top – for the left magnetron, middle – for the right magnetron, bottom – for Oxygen.**

The simulation results are shown in the Figure 70. In the figure one can see that the tilting of the substrate with respect to the magnetrons axes leads to the growth of the film with a tilted columnar structure. Note, that to see the film one should right click on a picture and choose “View → axis x”. The comparison to the experiment is also shown in the Figure 70.

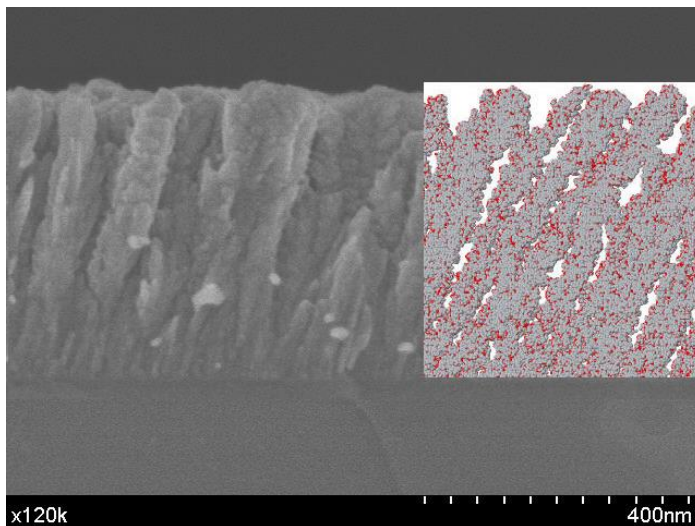


**Figure 70: Simulation results of a TiO<sub>2</sub> film growth in a poisoned mode.**

## 20 Example 18 Make Process

The aim of the next three examples is to demonstrate the usage of Make Process tool, its capabilities and flexibility for simulation of coating process with multiple sources and complex substrate motion.

### 20.1 Batchcoater

This example demonstrates Make Process capabilities of simulation deposition of a moving substrate in a coater with several magnetrons. General layout of the coater is shown in Figure 71.

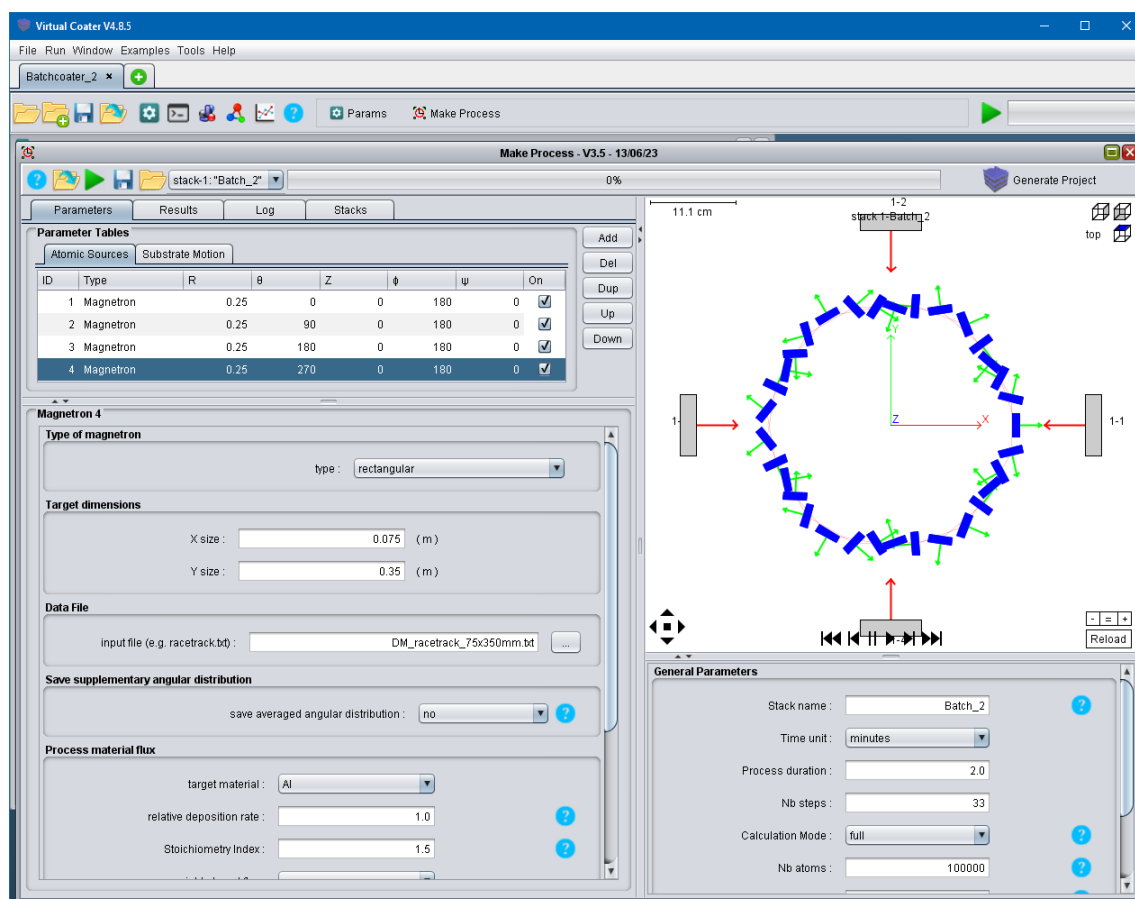


Figure 71: General layout of BatchCoater. There are 4 magnetrons in the chamber, movement of substrate is of double type rotations.

Sputtered materials are Zr, Cr, Ti, Al. Positions of magnetron and parameters of substrate movement are given in the tables below.

**Parameter Tables**

Atomic Sources    Substrate Motion

ID	Type	R	$\theta$	Z	$\phi$	$\psi$	On
1	Magnetron	0.25	0	0	180	0	<input checked="" type="checkbox"/>
2	Magnetron	0.25	90	0	180	0	<input checked="" type="checkbox"/>
3	Magnetron	0.25	180	0	180	0	<input checked="" type="checkbox"/>
4	Magnetron	0.25	270	0	180	0	<input checked="" type="checkbox"/>

**Parameter Tables**

Atomic Sources    Substrate Motion

ID	Type	Reference frame	On
1	Rotation	relative	<input checked="" type="checkbox"/>
2	Rotation	relative	<input checked="" type="checkbox"/>

	Main rotation	Second rotation
Radius, m	0.15	0.005
Angular speed, RPM	1.0	6
Starting angle, degrees	0	0

The output of Make Process are parameters of fluxes of sputtered material, energy and angular distribution each metal, as well as a relative amount of these materials deposited at each time step. Relative values of the fluxes are shown in Figure 72. One can see that due to the double rotation the fluxes are distributed uniformly in time. Still, there are several maximums, they can be explained by the fact, that at certain moments of time the substrate when the substrate passes near the source, the plane of the substrate is parallel to the plane of the source. Certainly, that results in a higher amount of deposited material.

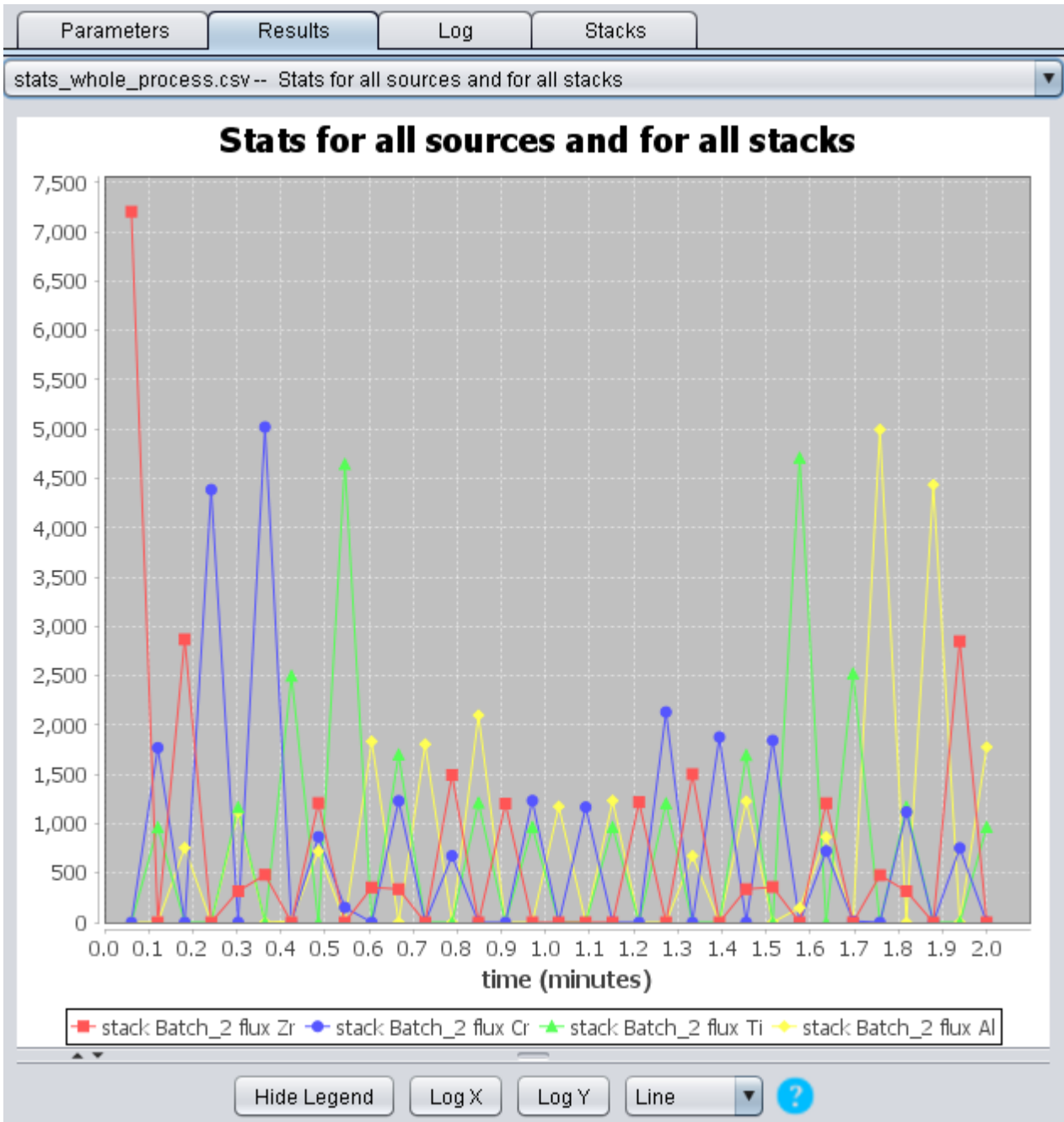


Figure 72: Relative amount of Zr (red), Cr (blue), Ti (green), and Al (yellow) deposited at each time step.

The concentration profile for each material and visualization of the coating are given in Figure 73. Certainly, the concentration profiles are in accordance with the deposition fluxes.

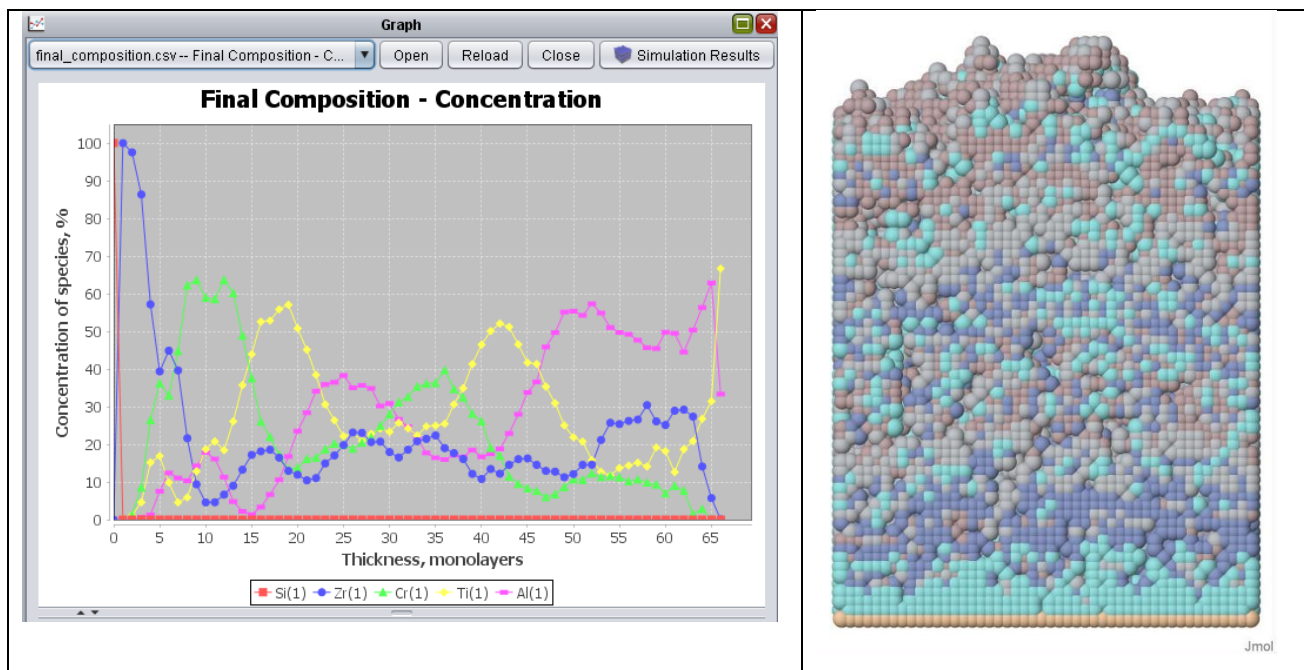


Figure 73: Concentration of each deposited material as a function of depth (left) and final coating (right)

## 20.2 Cluster

This example illustrates multilayer deposition in the configuration shown in Figure 74. Unlike the previous example, these magnetrons work not simultaneously, but in a sequence. Consequently, the final coating is not a mixture of different species but a multi-layer structure. That scheme of the simulation is possible due to the use of “stacks”. For each stack one can set up its sources and substrate motion. Thus, deposition at each stack forms a separate layer in the coating. Below are the parameters of the magnetrons for each of 5 stacks. Parameters K and Z determine the distance from the center and the height of sources,  $\theta$  determine the spatial position of the source,  $\phi$  and  $\psi$  determine source tilting, see Figure 74

Stack #	Element	R, m	$\theta$ , degree	Z, m	$\phi$ , , degree	$\psi$ , degree
1	Cu	0.3	0	0	0	232
2	Ag	0.3	72	0	0	232
3	Zn + O <sub>2</sub>	0.3	144	0	0	-128
4	Cr	0.3	216	0	0	-128
5	Zr	0.3	2880	0	0	232

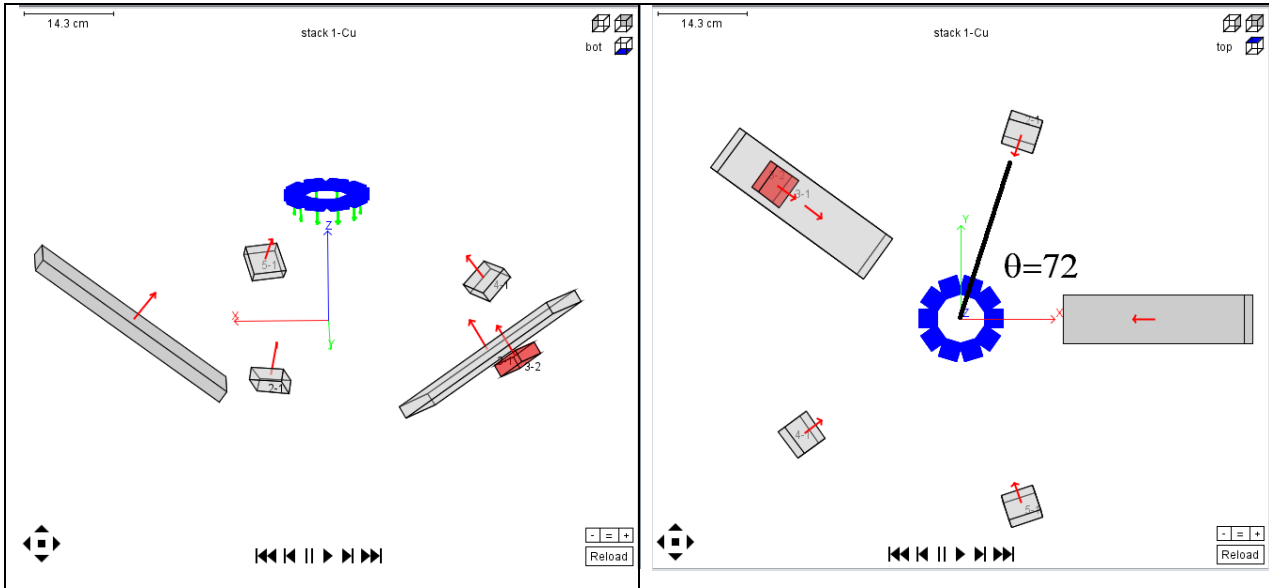


Figure 74: Coater configuration with 5 sources.

Substrate motion is a rotation along a circle with radius  $R = 0.2$  m at the height  $H = 0.2$  m, and additionally the substrate orientation is given by angles  $\alpha = 0, \beta = 90, \gamma = -90$ . The additional changing of the orientation is possible by using additional type of movement - substrate tilting.

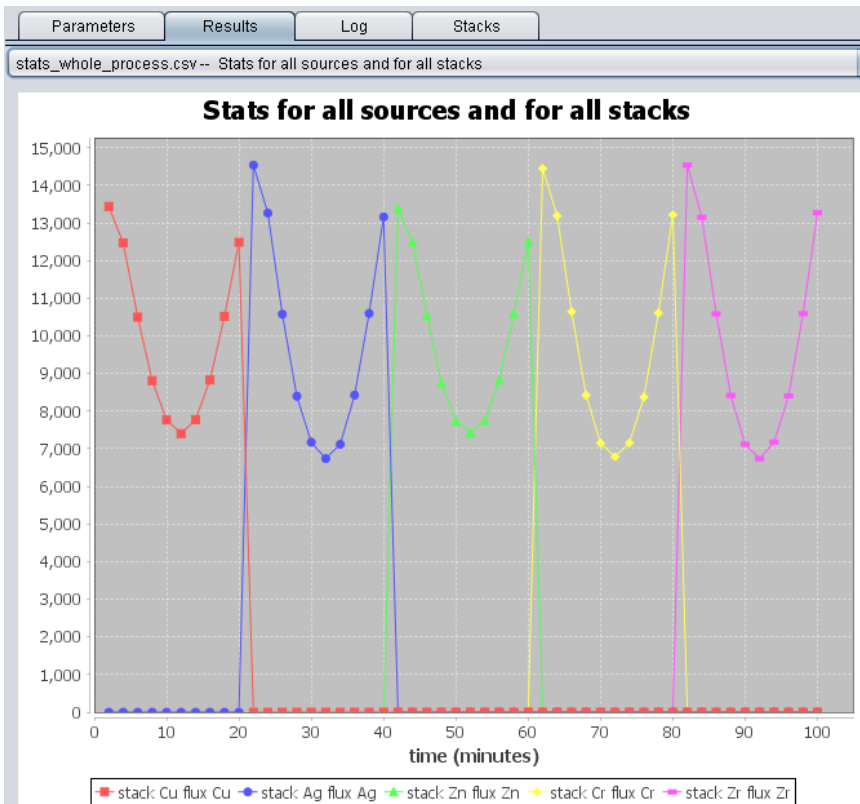


Figure 75: Fluxes to the substrate for all stacks.

Figure 75 represents the fluxes from all sources to the substrate as a function of time. One can see that the fluxes are well resolved in time. That leads to well-defined layers in the final coating structure, see Figure 76.

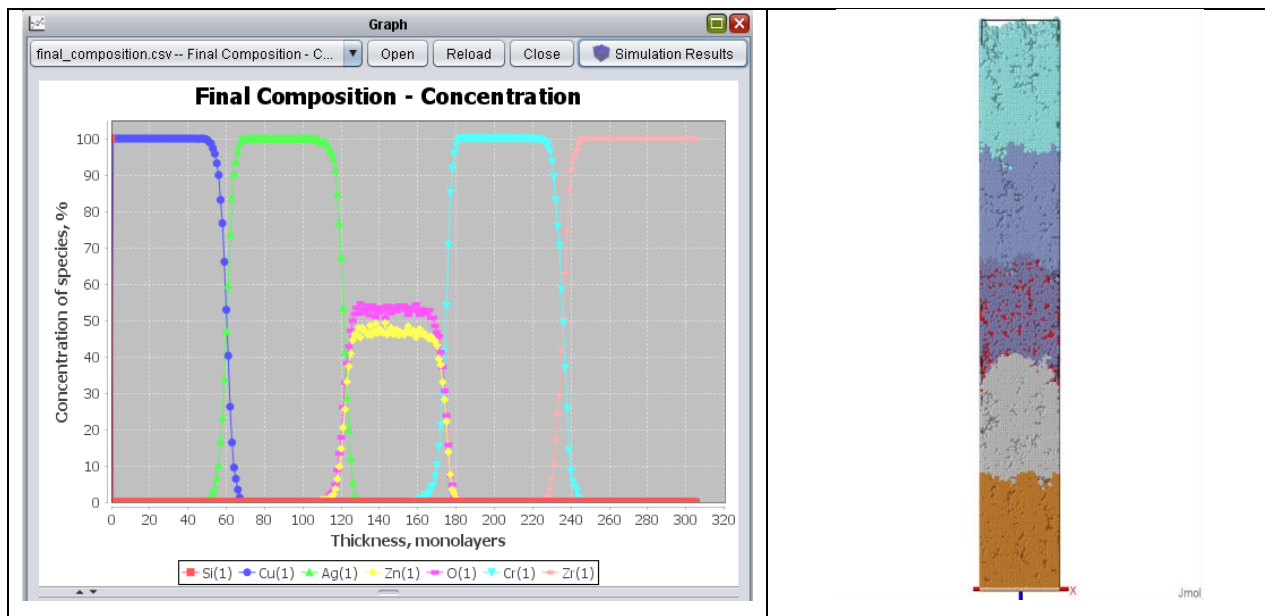


Figure 76: Concentration of each deposited material as a function of depth (left) and final coating (right)

### 20.3 Linear coater

This example also illustrates multi-stack capabilities of Make Process for optical applications. The arrangement of the sequence of deposition chambers is given in Figure 77.

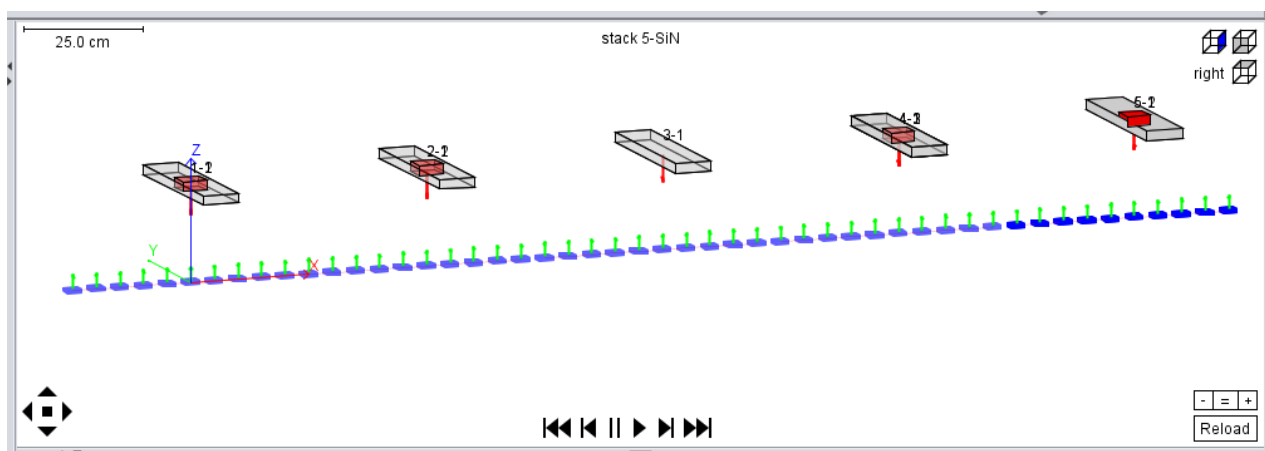


Figure 77: Model of a linear coater.

The coater consists of five compartments, as listed below.

Stack #	Element	R, m	θ, degree	Z, m	φ, degree	ψ, degree
1	Ti + O <sub>2</sub>	0	0	0.2	90	90
2	Zn + O	0.5	0	0.2	90	90
3	Ag	1.5	0	0.2	90	90
4	Al + Zn + O	2.0	0	0.2	90	90
5	Si + N	2.5	0	0.2	90	90

Movement of the substrate is linear, it is described by the equation  $X = X0 + A*t$ , parameters X0 and A for each stack are given below.

Stack #	X0, m	A, cm/min	α, degree	β, degree	γ, degree
1	-0.25	50		90	90
2	0.25	50		90	90
3	0.75	50		90 </td <td>90</td>	90
4	1.25	50		90	90
5	1.75	50		90	90

Next Figure 78 shows the material fluxes to the substrate. Like in the previous example, there is no mixing between the fluxes, thus the output of the deposition is a multi-layer coating. This is demonstrated by the next Figure 79 where the coating chemical composition and 3D view of the coating are shown.

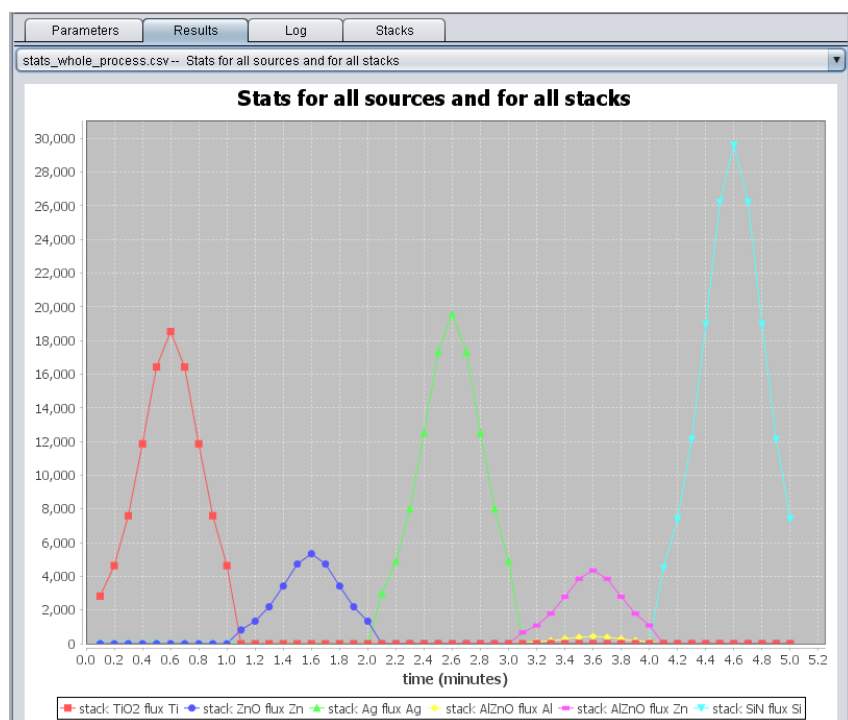


Figure 78: Fluxes of materials to the substrate in a linear coater.

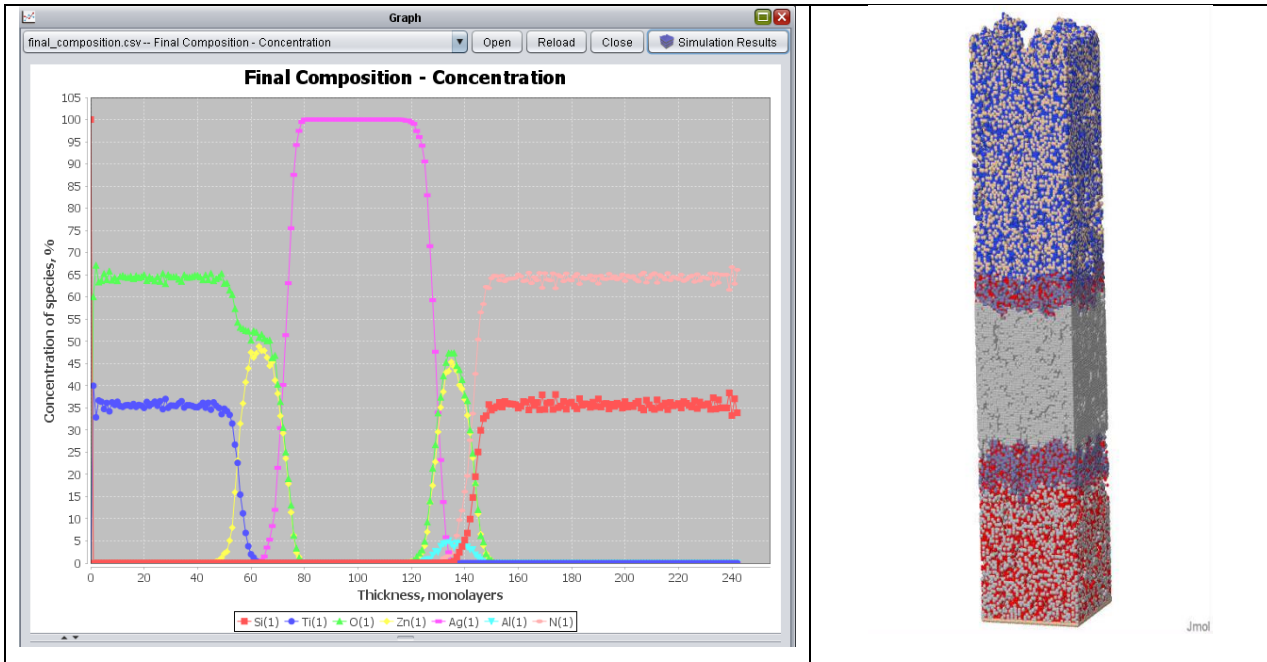


Figure 79: Concentration of each deposited material as a function of depth (left) and final coating (right).

Finally, one can examine optical properties of the coating by means of **Optics** tool. Figure 80 shows reflectance and transmittance of the coating for non-polarized light for normal incidence.

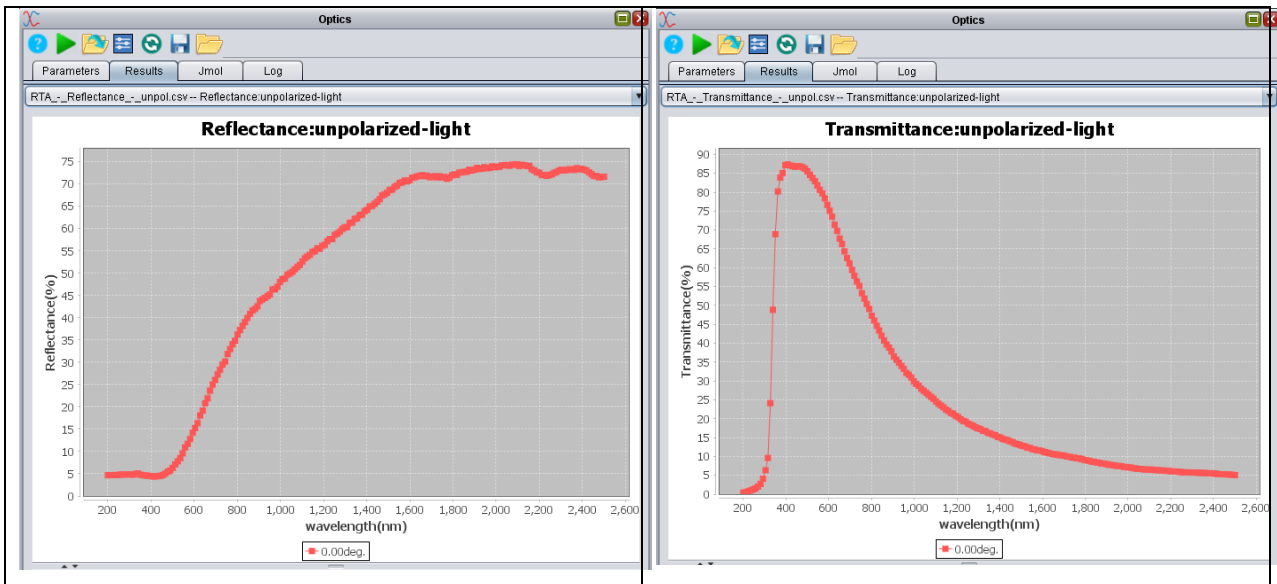


Figure 80: Reflectance (left) and Transmittance (right) of the coating.

## 21 Example 19. Columns

This example illustrates coating structure presented by data from “columns.xyz” file. Also, the influence of atomic surface diffusion on the size of the columns will be shown. Simulation parameters for three different cases, no surface diffusion, slow surface diffusion, and fast surface diffusion are given in the table below. **Note, that columns.xyz file is created only when the option “Save intermediate 3D structures” is ticked.**

	No diffusion	Slow diffusion	Fast diffusion
Simulation_options	6000 0 0	6000 1 1	6000 1 1
Dimensions	80 80 5 600000 0.0	80 80 5 600000 0.0	80 80 5 600000 0.0
Deposition_rate(ML/s)	0.01	0.01	0.01
Ea_diff(eV)	> 1.9	<b>0.95</b>	<b>0.75</b>
Ea_nn_inc(eV)	> 1.9	<b>0.99</b>	<b>0.99</b>
Ea_down(eV)	> 1.9	<b>1.0</b>	<b>1.0</b>
Ea_nn_dec(eV), Ea_detach(eV), Ea_up(eV), Ea_detrap(eV), Ea_sub_evap(eV), Ea_lay_evap(eV)	> 1.9	> 1.9	> 1.9
Temp (eV)	<b>0.04</b>	<b>0.04</b>	<b>0.04</b>

These three cases differ in the activation energy for the surface diffusion. The values of the energy barrier are Infinity, 0.95 eV, and 0.75 eV. Thus, the diffusion rates for these three cases are different. For the same deposition rate number of initially formed islands are different, the higher the diffusion rate, the lower the number of islands. That happens because at higher diffusion rate the mobility of adatoms is higher. Thus, they are more likely attached to already existing islands than form a new one. Islands are starting sites for growth of columns. Certainly, the number of columns also is smaller for the case of higher diffusion rate.

Simulation results for the cases of no surface diffusion, slow surface diffusion, and fast surface diffusion are shown in Figure 81.

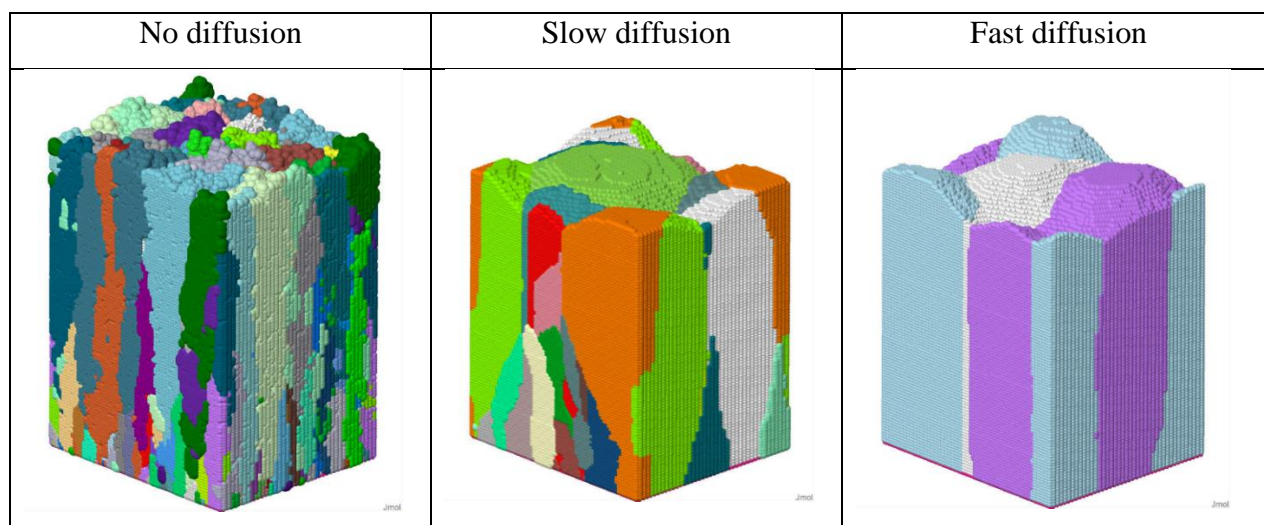


Figure 81: Columnar structure of the coating for different surface diffusion rates.



*VIRTUAL COATER™*

*Innovative Coating Solutions,  
Place Saint-Pierre, 11, B-5380 Forville., Belgium  
slu@incosol4u.com www.incosol4u.com*

## 22 Bibliography

1. P. Moskovkin and S. Lucas, *Thin Solids Film* 536 (2013) 313.
2. G. Vanda, P. Moskovkin, R. Alvarez, J. Caballero-Hernandez, R. Schierholz, B. Bera, J. Demarche, A. Palmero, A. Fernandez, S. Lucas, *Nanotechnology* 25 (2014) 355705.
3. Michael T. Taschuk, Matthew M. Hawkeye and Michael J. Brett - “*Glancing Angle Deposition*”, in “*Handbook of Deposition Technologies for Films and Coatings (Third Edition), Science, Applications and Technology*”, Edited by Peter M. Martin., 2011, ISBN: 978-0-8155-2031-3.
4. Stefan Braun, Hermann Mai, Matthew Moss, Roland Scholz and Andreas Leson, *Jpn. J. Appl. Phys.* 41 (2002) 4074.
5. Troparevsky, M. C. (2010). Transfer-matrix formalism for the calculation of optical response in multilayer systems: from coherent to incoherent interference. 18(24), pp. 24715-24721. doi:<https://doi.org/10.1364/OE.18.024715>